GEOLOGICAL SURVEY OF CANADA
· 1842 ·

GEOLOGICAL SURVEY OF CANADA

DEPARTMENT OF ENERGY, MINES AND RESOURCES

BULLETIN 217

THE GEOLOGY AND PETROLOGY OF THE ALKALINE CARBONATITE COMPLEX AT CALLANDER BAY, ONTARIO

John Ferguson and K.L. Currie

Ottawa, Canada
1972

Price, $2.00

THE GEOLOGY AND PETROLOGY OF THE
ALKALINE CARBONATITE COMPLEX
AT CALLANDER BAY, ONTARIO

GEOLOGICAL SURVEY
OF CANADA

THE GEOLOGY AND PETROLOGY OF THE ALKALINE CARBONATITE COMPLEX AT CALLANDER BAY, ONTARIO

By

John Ferguson and K. L. Currie

PREFACE

The origin of alkaline rocks remains one of the most interesting and controversial problems of igneous petrology. This report presents the results of a detailed examination of a small alkaline complex at Callander Bay which appears to contain clues to a number of problems of alkaline rock genesis. By means of control studies such as this, it is possible to determine relationships and test concepts that can be used by analogy elsewhere in correlating similar events and processes related to mineralization and emplacement. The authors re-emphasize the importance of dykes in determining the origin and development of igneous complexes. They put forward a novel, but experimentally supported, hypothesis for the origin of alkaline rocks by successive immiscibility, modified by fractionation in each of the resultant liquids, and apply this hypothesis to the Callander Bay complex. The mechanism of intrusion is considered in detail and related to this hypothesis, and the nature and conditions of alkaline metasomatism are also examined in detail.

Y.O. Fortier,
Director, Geological Survey of Canada.

OTTAWA, 29 March, 1971

BULLETIN 217 — Geologie und Petrologie des alkalinischen Karbonatit-Komplexes bei Callander Bay (Ontario)
Von John Ferguson und K. L. Currie

БЮЛЛЕТЕНЬ 217 — Геология и петрология щелочного карбонатитного комплекса в районе пролива Калландер, Онтарио
Дж. Фергюсон и К. Л. Кюрри

CONTENTS

Illustrations

THE GEOLOGY AND PETROLOGY OF THE ALKALINE
CARBONATITE COMPLEX AT CALLANDER BAY, ONTARIO

ABSTRACT

The Callander Bay complex, which is emplaced in north-northwest-trending, generally granitoid, Precambrian gneisses, is an almost circular body about 3 kilometres (about 2 miles) in diameter located in a crater-like depression at the east end of Lake Nipissing. The complex consists of a central core of interlaminated carbonatite and highly metasomatized country rocks, on the eastern side of which is a compound, crescentic mass of nepheline syenite, both being surrounded by a fenite aureole. All of these rocks are cut by a complex assemblage of dykes, consisting mainly of lamprophyre, carbonatite and potassium trachyte.

The complex originated from carbonated nephelinitic magma, which boiled off a CO_2-rich phase as it rose in the crust. The decarbonated magma then crystallized and separated olivine, eventually reaching a camptonitic composition at which further immiscibility occurred, resulting in the separation of a syenitic fraction. This fraction in turn followed a further course of differentiation. Each stage is well preserved in the dyke assemblages around the bay. The volatile, CO_2-rich phase gave rise to carbonates and the process of their formation caused extensive metasomatism (fenitization) of the country rocks with local anatexis.

The emplacement of the complex was controlled locally by its gas-charged nature which permitted a unique method of penetrating and opening fissures without significant loss of heat. On a regional scale the emplacement is controlled by the Nipissing graben system, along which an alkaline igneous province, 560 m.y. old, is well developed. The development of the graben system and the inception of alkaline igneous activity are both believed to be related to dehydration processes in the mantle.

RÉSUMÉ

Le complexe géologique de la baie Callander, situé dans des gneiss du Précambrien généralement granitoïdes, orienté en direction nord-nord-ouest, constitue un massif presque circulaire d'environ trois kilomètres (2 milles) de diamètre qui occupe une dépression cratériforme à l'extrémité est du lac Nipissing. Le complexe comprend un noyau central de carbonatite interfeuilletée et de roches encaissantes fortement métasomatisées, à l'est duquel se trouve une masse complexe en forme de croissant de syénite néphélinique; les deux sont entourés d'une auréole de fénite. Toutes ces roches sont coupées par un assemblage complexe de dykes composés principalement de lamprophyre, de carbonatite et de trachyte à potassium.

Le complexe tire son origine d'un magma néphélinique carbonaté à température suffisante pour éliminer une phase riche en CO_2 à mesure qu'il montait dans la croûte. Le magma décarbonaté s'est cristallisé et a séparé l'olivine pour parvenir éventuellement à une composition camptonitique, il s'est produit alors un autre état d'immiscibilité qui a entraîné la séparation d'une fraction syénitique. Cette fraction a ensuite fait l'objet d'une autre

différenciation. Chaque étape est bien conservée dans les assemblages de dykes autour de la baie. La phase volatile riche en CO_2 a donné lieu à la formation des carbonatites qui a entraîné une forte métasomatose des roches encaissantes avec anatexie locale.

L'emplacement du complexe a été contrôlé localement du fait qu'il était raturé de gaz ce qui a rendu possible une méthode unique de pénétration et d'ouverture des fissures sans qu'il y ait perte importante de chaleur. A l'échelle régionale, l'emplacement est contrôlé par le réseau de fossés Nipissing, le long duquel on trouve une province alcaline ignée bien développée, remontant à 560 millions d'années. On croit que la formation du réseau de fossés et le commencement de la formation de cette province se rattachent aux phénomènes de déshydratation qui se produisent dans le manteau.

CHAPTER I

INTRODUCTION

       The Callander Bay alkaline carbonatite complex, a nearly circular body roughly 3 kilometres (1.9 miles) in diameter, underlies Callander Bay at the eastern end of Lake Nipissing. The central core, now almost entirely covered by the waters of the bay, comprises interlaminated screens of carbonatite and intensely fenitized country rocks. At least two crescentic screens of nepheline syenite outcrop on the eastern edge of this core, along the shore of the bay, and the whole of the complex is surrounded by an elliptical aureole of fenitized country rocks. A varied assemblage of alkaline dykes cuts both the central complex and the surrounding Precambrian gneisses.

       Examination of the complex shows that due to natural and human causes the fenite zone and the dyke systems are exposed with an unusual degree of clarity and completeness. Because the fenite aureole is developed in rather uniform country rocks, the complex presents a favourable opportunity to study the chemical and mineralogical changes due to fenitization. The dykes appear to expose fundamental processes in the development of alkaline rocks arrested at various stages of development, in particular the relations among mafic, salic, and carbonatitic alkaline rocks. This study describes and interprets outcrop, petrographic, chemical and experimental data bearing on the origin of the alkaline rocks of the Callander Bay complex.

       The field work on which this study was based occupied parts of the field seasons of 1967, 1968, and 1969, about eight weeks in all. The field work was designed to produce a detailed map of the alkaline rocks, and to obtain as much information on the country rocks as was necessary to understand the fenitization process. Laboratory work included routine petrographic examination of over 200 thin sections, together with universal stage examination of all major minerals, and electron probe analysis of the genetically important minerals. Forty-eight complete chemical analyses were made. Some experiments aimed at elucidating the role of liquid immiscibility in alkaline rocks genesis are also reported.

ACKNOWLEDGMENTS

PHYSIOGRAPHY

Lake Nipissing lies within a sharply bounded east-west trench connecting Lake Huron with the upper Ottawa River. To the north and south the Precambrian rocks rise some 100 metres (330 feet) from the valley floor to rocky highlands sparsely covered by evergreen forest. The valley however, locally contains a deep fill of sand and clay mainly because it served as a temporary spillway for the Great Lakes during the Pleistocene period. This soil originally supported splendid stands of pine forest but is today largely farmland. In the immediate vicinity of Callander Bay the soil cover has been removed by erosion, exposing a drop of 30-50 metres (99-165 feet) into the bay through rock cliffs, and emphasizing the crater-like character of the bay. Outcrop is abundant along these cliffs, and wave-washed exposures are profuse around the shore of the bay but elsewhere outcrop is poor, particularly northwest of the bay. A very large road cut more than a kilometre (0. 6 mile) in length, crosses the fenite zone southeast of the bay, and other smaller cuts help alleviate the local lack of natural outcrop.

PREVIOUS WORK

The excellence of the trees and the soil early brought settlers to the Callander Bay region, and with them a number of pioneering geological investigators whose work was summarized and supplemented by Barlow (1897). Although these early investigators noticed the alkaline rocks, and 'crystalline limestone' (carbonatite) of the Manitou Islands complex 12 kilometres (7. 4 miles) northwest of Callander Bay, the Callander Bay complex was overlooked. After Barlow's work, no published geological work on this region appeared for more than 60 years, and the alkaline complex was unrecognized in the literature even though the town of Callander is built on the nepheline syenite. A station of a main line of the Canadian National Railways is built on the same rock, and Highway 11, the major north-south route in Ontario, passes across a magnificent fenite aureole. The complex was correctly identified by S. B. Lumbers (1968) who made a reconnaissance examination of it in 1964-65 in the course of regional mapping.

CHAPTER II

GEOLOGY OF THE COUNTRY ROCKS

INTRODUCTION

        The Callander Bay alkaline complex is emplaced within north-
northwesterly trending, generally granitoid, Precambrian gneisses. Although
these rocks are commonly assigned to the Grenville (Structural) Province of
the Precambrian Shield (Lumbers, 1968), they yield ages older than the
Grenville Orogeny (Krogh and Davis, 1969), and little resemble the Grenville
Group paragneisses to the southeast. Most of the gneisses in the region of
Callander Bay are granitoid or migmatitic in character and could as easily
have arisen from metamorphism of igneous rocks as from sedimentary rocks,
although the rocks to the east of the bay are notably more heterogeneous and
generally mesocratic. These latter may well be paragneisses.
        This crystalline complex, which forms a moderately rugged gla-
ciated upland to the north and south of Lake Nipissing, was dissected, begin-
ning in Cambrian time, by an east-west-trending graben system (Kumarapeli
and Saull, 1966). In the region of Callander Bay this subsidence produced
the broad depression now occupied by Lake Nipissing, but farther east, the
graben splits into an intricate series of narrow horsts and grabens (inset,
Fig. 1). Over a length of about 150 kilometres (93 miles) the graben system
was the site of alkaline igneous activity penecontemporaneous with the down-
faulting. Alkaline lamprophyre dykes were intruded over much of the graben
floor, and at least four central complexes, of which Callander Bay is one,
were emplaced. Beginning in latest Cambrian, or earliest Ordovician time,
the troughs became a site of sedimentary deposition now recorded only in
scattered outliers (Colqhoun, 1958).

DESCRIPTION OF COUNTRY ROCKS

Heterogeneous Paragneiss

Distribution and lithology

        Hetrogeneous mesocratic paragneisses outcrop east of Callander
Bay, and in a small lens north of the bay (Fig. 1). The unit has not
been studied in detail because it is intersected only by a small portion of the
outer fenite zone of the alkaline complex.
        These rocks are characterized by compositional and textural het-
erogeneity. Rock types are generally mesocratic, but massive quartz-rich
varieties occur, as well as dark diopside-bearing rocks. Segregation band-
ing is common, produced by strong fractionation of medium- to coarse-
grained mafic and felsic units. In all cases a foliation, caused by planar
orientation of mafic minerals, is present.
        Microscopically the rocks consist of varying amounts of potash
feldspar, plagioclase, quartz and biotite. Garnet and diopside are present
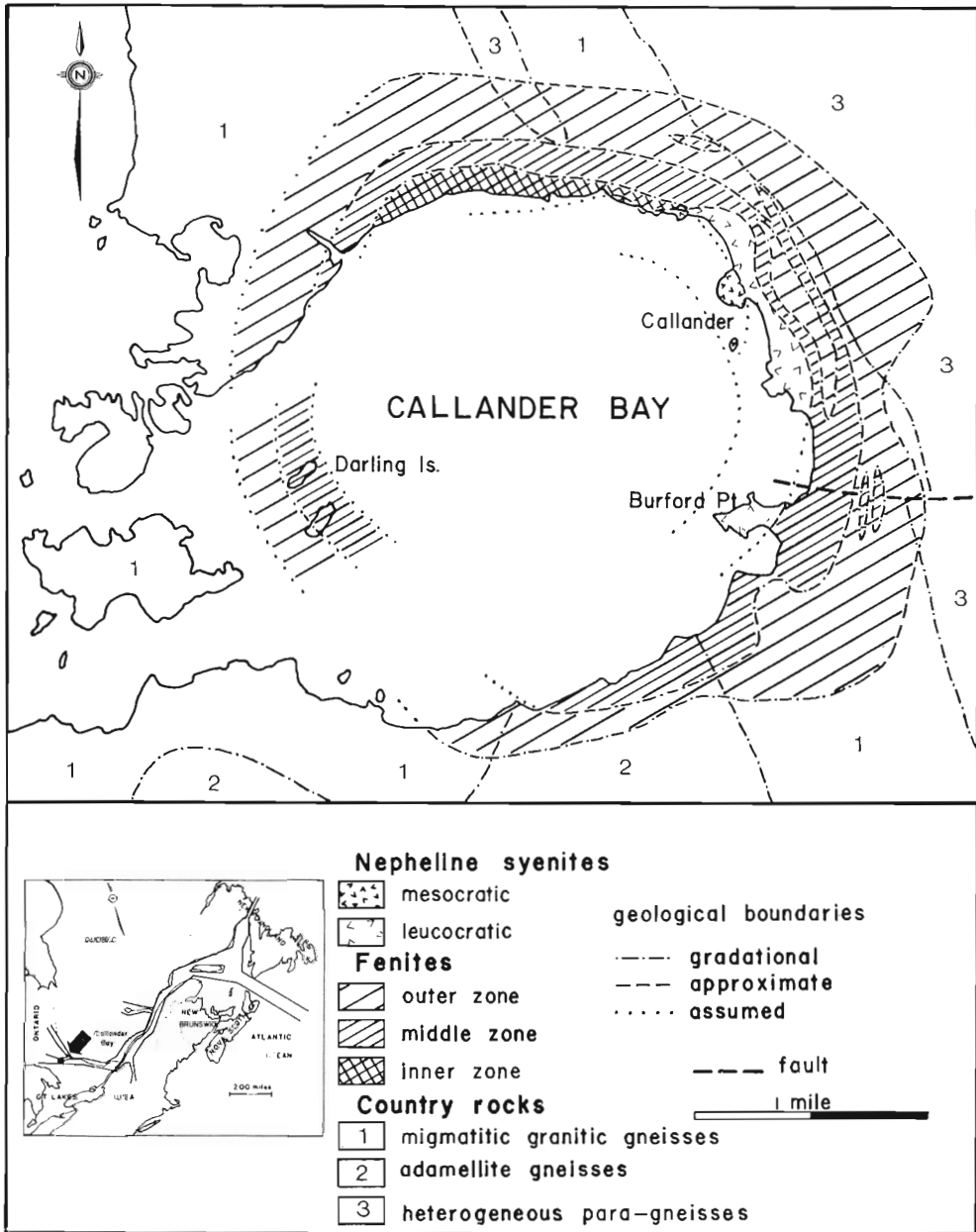
Figure 1. Geological map of the Callander Bay complex and inset showing
the St. Lawrence rift system.

in many specimens, and allanite and apatite are accessory minerals. Minor muscovite is present locally, and carbonate is abundant in one specimen. Modes of the rocks are presented in Table 1.

TABLE 1

Modes of Precambrian Rocks, Callander Bay Area.

Specimen number	2	19	39B	65	69	14	24	3	37	14B
quartz	33.8	23.6	30.8	22.0	21.9	20.4	18.4	28.3	27.7	--
plagioclase	36.1	35.1	13.6	29.4	31.8	39.4	31.9	38.5	38.3	21.4
K-feldspar + perthite	22.1	29.1	49.1	30.4	42.5	31.0	30.9	12.8	10.8	--
amphibole	1.8	6.5	--	9.2	--	5.3	10.0	2.1	--	50.6
biotite	4.8	3.7	--	8.4	2.4	0.8	5.1	14.3	17.5	20.7
garnet	--	--	--	--	--	2.8	2.1	--	3.6	1.5
opaque	0.4	--	4.6	0.4	1.4	--	0.4	1.8	0.3	5.5
apatite	0.5	0.1	--	0.1	--	--	--	--	0.5	0.3
other	--	1.4	1.9	--	--	--	0.8	1.4	0.7	--
sphene	0.5	0.5	--	0.1	--	0.3	0.4	0.8	0.6	--

Analyses 2, 19, 39B, 65, 69, are of migmatitic granitic gneiss. Analyses 14, 24, of adamellite gneiss, analyses 3, 37, of a heterogeneous paragneiss, and analysis 14B of an amphibolite schlier in adamellite. All point counts were made by counting 2000 points at 0.3 millimetre intervals.

In all specimens of this group except one the potash feldspar is orthoclase cryptoperthite (Fig. 4). In one specimen a single porphyroblast of antiperthite is developed in which the exsolved phase shows cross-hatched twinning. X-ray analysis shows this material to be dominantly orthoclase with a minor microcline component (Table 4; Fig. 3). In this specimen granules of microcline and lesser amounts of plagioclase are present in the ground-mass. All of the rocks contain polysynthetically twinned plagioclase (An 30±), frequently exhibiting slight bending and concentric zoning. Plagioclase commonly excedes potash feldspar in amount.

Quartz occurs as irregular grains showing undulose extinction. Myrmekitic texture is developed along the margin of the plagioclase grains. Biotite, commonly showing minor chlorite alteration, is by far the most abundant mafic mineral; garnet is present in half the specimens and occurs as deeply embayed, poikiloblastic grains. Diopside, when present, commonly forms an intimate mixture with biotite and garnet.

Chemical composition

Three analyses of heterogeneous paragneiss are shown in Table 2. These analyses show the expected diversity in composition, but suggest no startling chemical peculiarities in this unit.

Contact relations and origin

The contacts of this unit with the other Precambrian gneisses were not observed. The gneissosity appears to be sensibly identical to that in the migmatitic granitic gneiss, and the local presence of quartzitic bands within the latter suggests that a gradational contact is probable. The heterogeneity of the paragneiss, and the presence of quartzitic and calc-silicate bands within it suggests that it originated as a sedimentary sequence, now raised to amphibolite grade metamorphic rocks.

Migmatitic Granitic Gneiss

Distribution

A medium-grained banded gneiss, characterized by planar alternation of leuco- and melanocratic units outcrops around all the shore of Callander Bay, with the exception of a 1 kilometre (.62 mile) tract on the south shore (Fig. 1). These outcrops form part of a north-northwest trending belt of migmatitic gneisses that enclose a more homogeneous granite gneiss which outcrops on the south shore of the bay.

Lithology

In outcrop leucocratic, augen-like bands alternate with discoidal, occasionally nebulous, aggregates of dark minerals which parallel and define the gneissosity. Layers of aplite, pegmatite, amphibolite, feldspathic and quartzofeldspathic rocks grade imperceptibly into more normal medium-grained banded gneiss. Southwest of Callander Bay, immediately outside the map-area, a layer of coarse-grained massive red granite 100 metres (about 330 feet) thick grades into migmatitic gneiss.

Microscopically the rocks are composed of varying amounts of potash feldspar, plagioclase, quartz, biotite and hornblende. Garnet, sphene, opaque minerals and apatite are common accessory minerals. Modes are shown in Table 1.

The potash feldspars are commonly orthoclase cryptoperthites showing irregular extinction, which sometimes approaches a concentric pattern (Table 4; Fig. 3). Two specimens display cross-hatch twinning, but X-ray analysis shows these feldspars to be predominantly orthoclase with a minor microcline component. The plagioclase is polysynthetically twinned and usually displays bent twin lamellae and irregular extinction. A few of the plagioclase anhedra have an antiperthitic texture with the exsolved phase showing cross-hatch twinning. Quartz is present in very irregular anhedra displaying undulose extinction. In most specimens myrmekitic texture is developed in the marginal parts of feldspars. Interpenetrating biotite and hornblende make up the dominant mafic minerals. Biotite, which not uncommonly has rutile needles and minor opaques within the (001) cleavage planes, may show slight bending of the laths, whereas hornblende is undeformed but
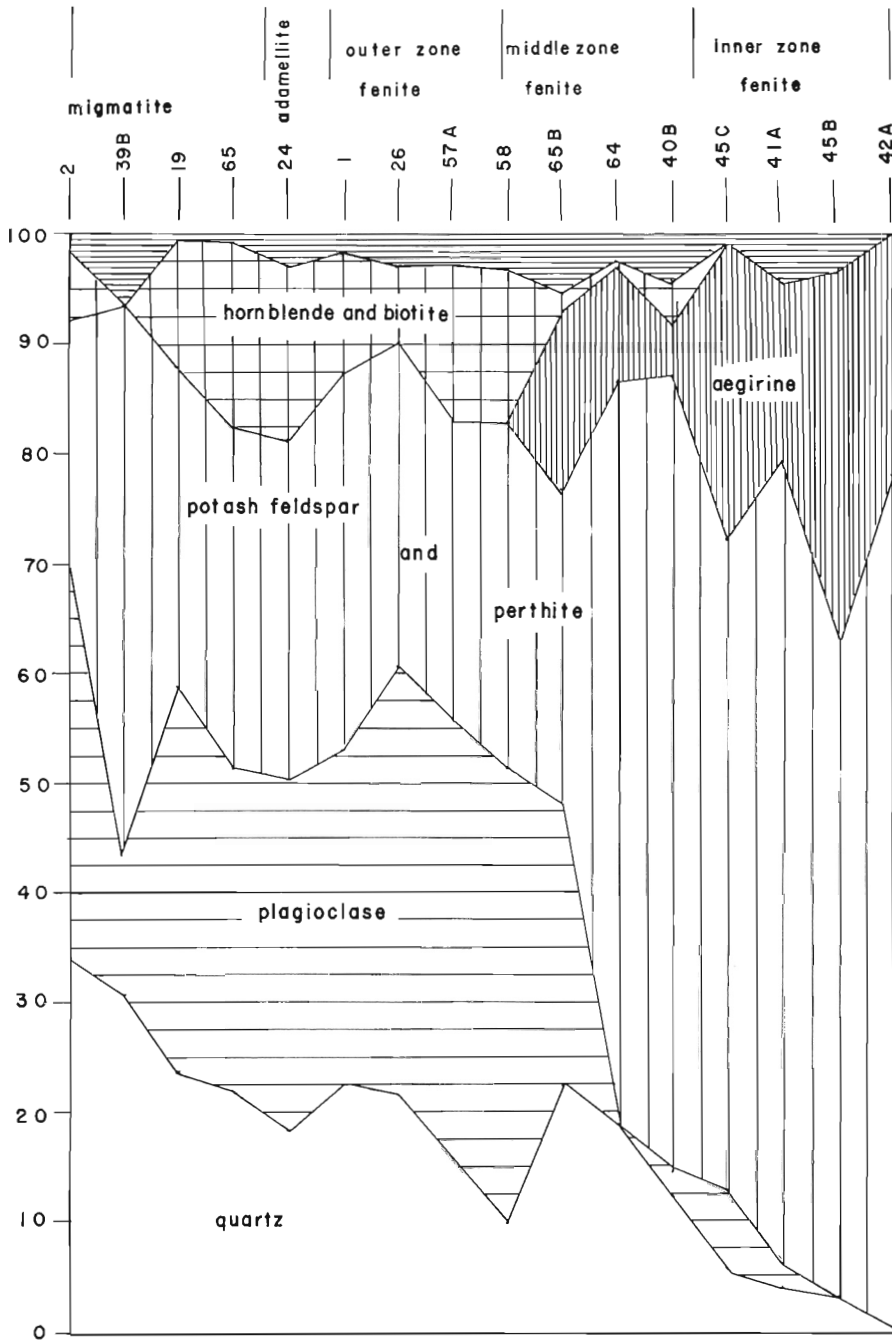
Figure 2. Changes in mode with progressive fenitization.
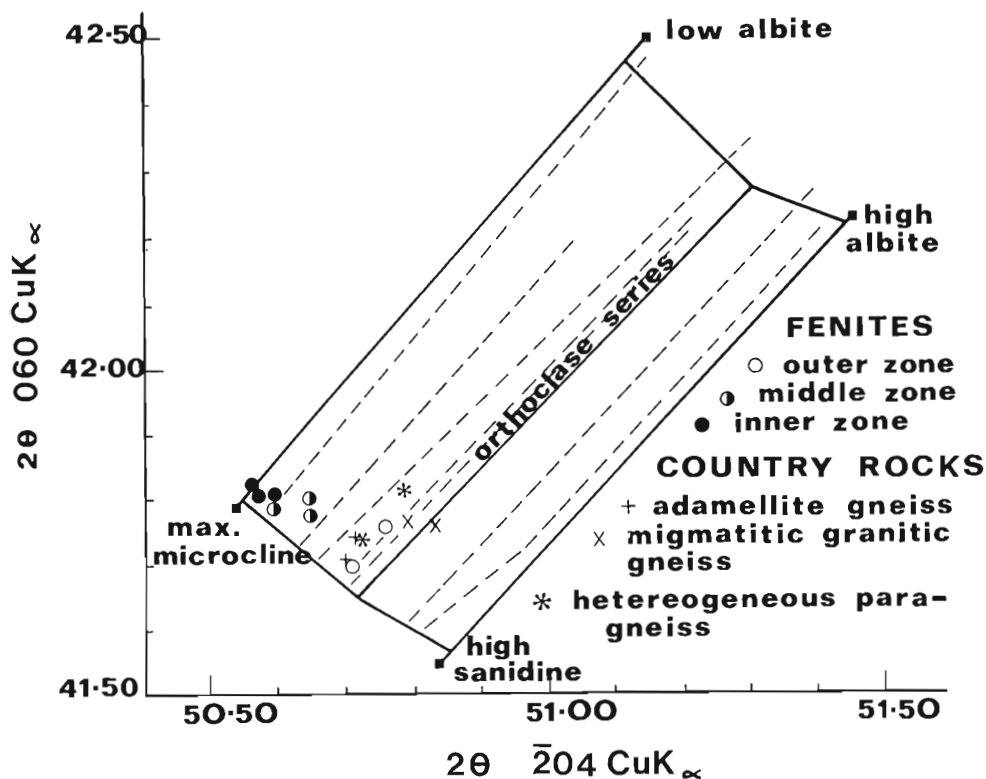
Figure 3. Structural state of feldspars in fenites and country rocks (diagram from Wright, 1968).

commonly shows partial alteration to a mildly pleochroic green or yellow-green chlorite, particularly along (110) cleavage planes. In extreme cases, a mixture of green chlorite and sericite pseudomorphically replaces horn-blende. Garnet and sphene normally occur associated with biotite and horn-blende, but may appear as isolated grains. Opaque minerals occur as inclu-sions or cores in sphene together with small, subhedral, partially metamict allanite grains. Very occasionally garnet shows minor chlorite alteration along cracks. Apatite, when present, occurs as water-clear euhedral grains included in other minerals.

The homogeneous granitic rocks, sometimes separating the mig-matitic gneiss from the adamellite gneiss and present as lits within the mig-matitic gneiss, differ from the migmatitic rocks in the type of potash feld-spar present, and the accessory minerals. In one specimen strongly devel-oped cross-hatched twinning is present in the potash feldspar, whereas in another, very finely veined cryptoperthite is found. In all cases potash feld-spar is much more common than the polysynthetically twinned plagioclase anhedra. One specimen contains biotite and minor muscovite as the only mafic minerals. Another contains accessory fluorite. Apatite is lacking in all the granitic rocks.
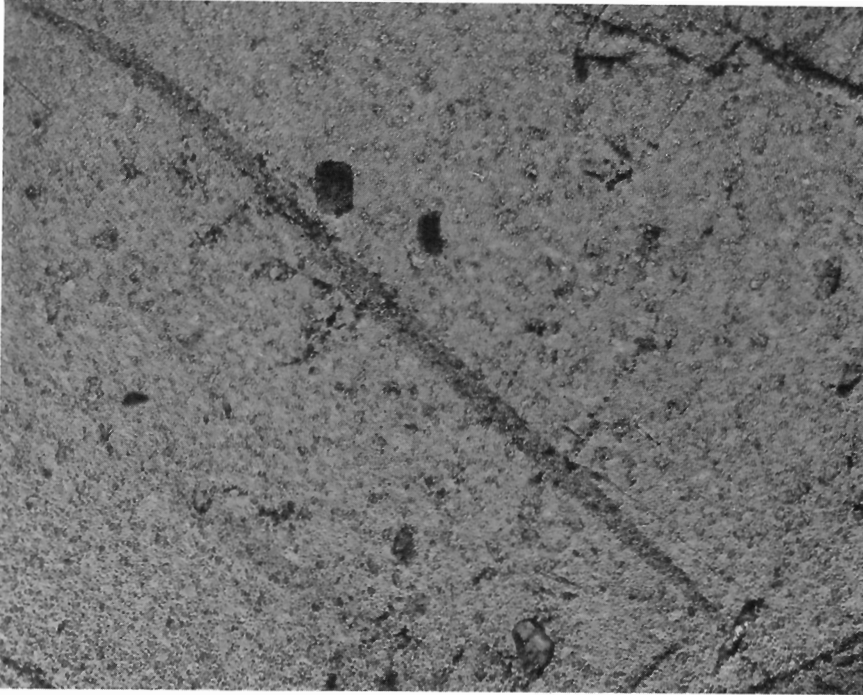
Figure 4. Cryptoperthite in unfenitized heterogeneous paragneiss. The scale in Figures 4-9 is identical, the width of field being about 1.5 millimetre. (x125, crossed nicols) (G.S.C. photo 201290-L)

Chemical composition

Four analyses of the migmatitic granitic gneisses are compiled in Table 2. These analyses show that if a sample sufficiently large to overcome the small scale heterogeneity of the unit is considered, the composition is quite uniform.

Contact relations and origin

The contact between the migmatitic gneiss and the heterogeneous paragneiss has not been observed. The concordance of gneissosity in the two units, their general similarity in style of gneissosity, and the inclusion of distinctive subunits (e.g. quartzite) in both of them, suggests that the contact is gradational. The contact relations with the adamellite gneiss are better exposed. Eight kilometres (5 miles) south of Callander Bay there is an abrupt but apparently concordant transition between these two rock types. Immediately southeast of Callander Bay, the contact is transitional, but the foliation of the migmatitic gneiss appears to truncate the foliation of the adamellite gneiss. In two small outcrops northeast and northwest of Callander Bay, the contact is marked by a 10-metre (33-foot) zone of fine-grained, gneissic

TABLE 2

Chemical Analyses of Precambrian Rocks

Specimen number	2	19	39B	65	69	14	24	3	37	14B
SiO_2	72.10	68.36	72.22	73.13	64.90	62.80	67.17	68.05	65.02	42.84
TiO_2	0.51	0.86	0.24	0.31	0.80	0.41	0.50	0.65	0.67	3.49
Al_2O_3	13.08	12.31	12.26	12.83	14.95	17.20	15.25	14.81	15.60	15.20
Fe_2O_3	1.52	1.21	2.53	1.06	0.91	1.10	1.43	1.10	0.36	3.44
FeO	1.40	5.60	0.20	1.80	5.50	3.20	3.00	2.40	5.00	13.21
MnO	0.06	0.12	0.05	0.03	0.14	0.09	0.11	0.07	0.11	0.12
MgO	0.62	0.71	0.46	0.43	1.25	0.60	0.47	1.27	1.72	6.32
CaO	1.76	1.88	1.54	0.46	2.33	2.20	1.69	2.17	3.27	6.34
Na_2O	2.98	3.40	3.10	2.71	3.21	5.38	4.01	3.22	3.20	3.70
K_2O	5.03	4.62	5.86	6.19	4.48	4.80	5.31	4.41	3.44	1.69
P_2O_5	0.21	0.18	0.08	0.05	0.30	0.08	0.12	0.22	0.23	0.31
H_2O	0.80	0.60	0.40	0.60	1.00	0.40	0.70	0.70	0.70	1.78
CO_2	<0.10	<0.10	0.80	<0.10	0.20	0.30	<0.10	0.40	0.30	0.19

Selected minor element data (ppm)

Rb	160	100	190	260	100	100	140	170	180	70
Sr	270	190	180	130	200	290	150	360	310	590
Ba	1300	1200	1100	960	1700	1800	1100	4300	780	<500
Zr	250	880	450	300	530	570	510	400	290	180
Nb	70	100	110	<30	<30	50	110	<30	nil	83

All analyses by Geological Survey of Canada rapid methods group, directed by S. Courville.
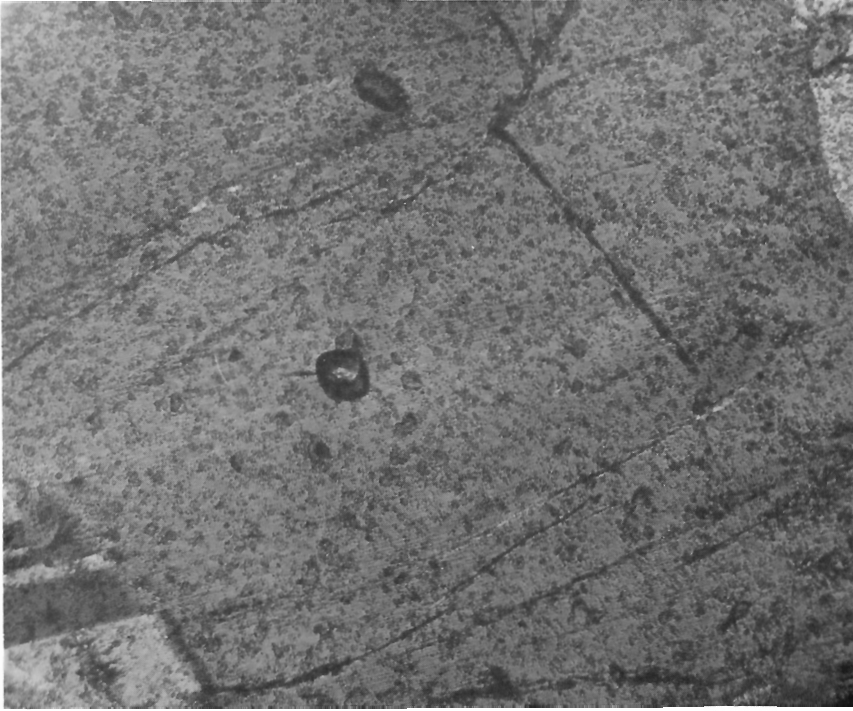
Figure 5. Cryptoperthite from unfenitized adamellite gneiss. (x125, crossed nicols) (G.S.C. photo 201290-J)

granite lacking segregation banding. Eleven kilometres (7 miles) to the north of Callander Bay, the contact is gradational over 25 metres (about 80 feet).

The presence of distinctive beds such as quartzite within the migmatitic gneiss strongly suggests that it developed in part at least from a sedimentary sequence. At present, however, it clearly forms part of a complex of granitoid rocks, and is a product of metamorphic, and possibly igneous, processes.

Adamellite Gneiss

Distribution

Medium- to coarse-grained gneissic rocks, composed dominantly of pink feldspar with lesser amounts of mafic minerals outcrop along the south shore of Callander Bay and to the southwest (Fig. 1). Beyond the map-area they form large nearly conformable massifs in the gneiss complex (Lumbers, 1968).

Lithology

In outcrop, the rocks display a near massive fabric of feldspar, in which the mafic minerals occur either as single anhedral grains, or more

commonly as lenticular or rod-like aggregates 0.5-1.0 centimetres in diameter which define a foliation and in many cases a lineation. Locally foliation is enhanced by layers of amphibolite, chains of mafic boudins, sporadic garnet concentrations, nebulous mafic schlieren, quartz lenses, biotite stringers and aplite. Amphibolite can occur as concordant sheets up to 20 metres (65 feet) long and 3 metres (10 feet) wide, and a sharply bounded amphibolite dyke 100 metres (about 330 feet) long was also observed. Zoned pegmatite lenses with alaskitic margins and granodioritic cores are found within the amphibolite.

Microscopically the rocks consist principally of potash feldspar and plagioclase, with subordinate amounts of quartz, hornblende, garnet and biotite. Sphene, allanite and apatite are present in accessory amounts. The modal compositions of these rocks are shown in Table 1.

The potash feldspars are dominantly anhedral orthoclase cryptoperthites (Fig. 5) with the rare presence of a minor microcline phase (Table 4). In all cases the feldspar displays irregular extinction.

Plagioclase anhedra show undulose extinction, and twin lamellae are commonly bent. Quartz is commonly present in the form of myrmekite, and the sporadic free quartz grains show undulose extinction.

Hornblende, commonly partially altered to chlorite, forms an interpenetrative structure with subordinate biotite. Deeply embayed garnet, rarely showing minor chloritic alteration along cracks, commonly occurs associated with the hornblende-biotite clumps, and also occurs as disseminated anhedra. Sphene and allanite form anhedral grains included in, or marginal to, the mafic clumps. Sericite and carbonate are occasionally present as alteration products of hornblende.

Chemical composition

The adamellite gneiss is relatively uniform, except for the various lits and schliers, and we have therefore made only one (listed in Table 2) analysis to determine its chemical composition.

Contact relations and origin

In the map-area the gneissic adamellite is in contact with only the migmatitic granitic gneisses. These contact relations have already been discussed. The adamellite gneiss in the map-area forms a small projection of a batholithic mass of granitoid rocks which has been metamorphosed and tectonically reconstituted since its original emplacement (Lumbers, 1968).

CHAPTER III

GEOLOGY OF THE CALLANDER BAY COMPLEX

INTRODUCTION

The Callander Bay complex consists of alkaline igneous rocks and associated alkaline metasomatic rocks. The largest exposures of igneous rocks are confined within an almost circular area about 3 kilometres (about 2 miles) in diameter, most of which is covered by the waters of Callander Bay. By no means all of the rocks within this boundary are igneous. Metasomatic rocks are exposed on Darling Island and in a drill core obtained off Burford Point. The metasomatic rocks also form an almost concentric aureole around this central core extending on the average about 500 metres (1,650 feet) beyond it. This aureole is shot through with many small occurrences of igneous rocks and it is indeed difficult in some instances to distinguish severely metasomatized country rocks from alkaline igneous rocks.

The complex has been divided, for ease of description, into seven units, three of which are fenites. This division, while it appears natural, is to some extent arbitrary, since there are many gradations from one unit to another, and many instances where the various units occur together with relationships so complex as to defy classification.

Fenites

Definition

The term fenite was introduced by Brogger (1921) to denote leucocratic metasomatic rocks around the Fen alkaline carbonatite complex. Brogger also introduced the term 'fenitize', referring to the metasomatic processes producing fenites, and this latter term has gradually been given the significance of encompassing every type of alkaline metasomatic alteration the products of which are therefore logically called fenites. As redefined by Von Eckermann (1948) a fenite designates a country rock altered in situ by alkaline metasomatism, but the term does not apply to mobilized and transported hybrid rocks. Fenitization is one of the most characteristic of all features associated with alkaline complexes.

Distribution

The fenite aureole around the Callander Bay complex forms an ellipse elongated in a northwest-southeast direction, extending a maximum of 1,000 metres (3,280 feet from the shore, and averaging 500 metres (1,640 feet) in width. Four independent areas of fenitization occur outside the aureole, at distances up to 13 kilometres (8 miles) from the complex, all associated with magnetic highs, and hematitized shatter zones. Fenitization haloes may also follow dykes extending beyond the main fenitization aureole.

The fenitization aureole may be divided, on petrographic criteria, into three gradational, roughly concentric zones. The outer fenite zone, characterized by narrow breccia veinlets, hematitization, and very rare development of soda pyroxene, forms a continuous shell around the complex,

varying from 400 to 1,000 metres (1,300 to 3,280 feet) in width. An isolated screen of outer zone fenite 1,000 metres long by 150 metres (3,280 by 490 feet) wide occurs within the middle zone fenite north of Burford Point. Inner zone fenite, characterized by recrystallized rocks with only nebulous remnants of the original texture occur in a narrow belt on the north shore of the bay. To the southeast their place appears to be taken by the nepheline syenite. Inner zone fenites are characteristically interspersed with middle zone fenites.

Lithology

Within the outer fenite zone the textures and structure of the original rock are essentially maintained. The boundary between fenitized and unfenitized rocks is determined by the degree of shattering and fenitization, but outlying patches of fenite are common. The outer fenite is characterized by shattering, and the presence of 0.5-2.0 millimetres wide veinlets. Locally breccia zones up to 2.5 centimetres wide are present. Hematite invariably is abundant along the shatter and breccia zones, commonly penetrating the surrounding rocks for several centimetres, giving the rock a distinctive red-veined appearance. Chloritization of mafics almost invariably accompanies hematitization

Middle zone fenites commonly show exaggerated foliation, compared to unfenitized rocks, due to development of sodic pyroxenes and amphiboles. Extensive areas where foliation is masked by intense development of hematite, giving the rock a fine-grained reddish appearance, are also common. These areas are commonly intensely shattered and mylonitized. In most of the rocks, the mineral grains appear to have undergone gentle brecciation of no fixed pattern. The zones are filled by a network of veinlets, commonly consisting of sodic pyroxene and/or hematite, but occasionally including veinlets of igneous-looking alkaline rocks, or carbonate, barite, fluorite, or soda amphibole veins. Pegmatoid patches of feldspar or aegirine are also present in these areas. Narrow mylonitized zones 5-10 centimetres wide may carry angular inclusions ranging from 0.5-8.0 millimetres diameter in a cryptocrystalline hematitized or carbonated quartz-rich matrix.

In large outcrops of inner zone fenites, a ghostly outline of gneissosity is discernable although there are many brecciated and disturbed areas. Contorted folded rocks mixed with massive rocks of igneous appearance are common. A red colour, with greenish highlights is pervasive due to the presence of hematite and sodic pyroxene. In hand specimen the original fabric of the rock appears entirely destroyed. In the brecciated areas, the angular fragments are drawn out into lenticular bodies. A marked feature of these rocks is the common presence of miarolitic cavities which appear to be arranged along planar features in the rock. The abundant sinuous veinlets in this rock, up to 1 centimetre in width, are normally monomineralic and consist of hematite, aegirine, carbonate, or K-feldspar. In the latter case, an inner veinlet, less than 1 millimetre wide, of aegirine is commonly present. Sulphides are occasionally associated with these veinlets. Intricate crosscutting relationships are common.

Microscopically the mineralogical changes occurring with fenitization are superimposed on country rocks mainly composed of anhedra of quartz and plagioclase feldspar in roughly equal amounts, with lesser amounts of quartz and mafic minerals. During fenitization alkali feldspar anhedra increase in amount and change in composition and structural state. Plagio-

Figure 6. Cryptoperthite from outer zone fenite. Note the develop-
ment of discrete strings compared to Figures 4 and 5.
(x125, crossed nicols) (G.S.C. photo 201290-H)

clase changes in composition and habit, quartz decreases drastically in
amount, and mafic minerals are replaced by other mafic minerals. Although
these changes are broadly correlated, they can be surveyed most easily by
considering each mineral separately. The sequence of mineral changes with
fenitization is whown in Table 3, and plotted in Figure 2.

Potash feldspars

The potash feldspars of the country rocks occur as orthoclase
crytoperthites, commonly with anomalous cell dimensions (Table 4; Fig. 3).
In the outer zone of fenitization the grain form and structural state of
the grains is similar, but the perthite is coarser, forming orthoclase
string microperthite commonly with minor sericitic alteration (Fig. 6). Pot-
ash feldspars of the middle zone of fenitization comprise microcline string
microperthites (Fig. 7), commonly with a minor orthoclase component
(Table 4). Grid twinning is restricted to the marginal parts of the anhedra,
which may show irregular or concentric zoning. Study of the structural state
suggests that there is a progressive change in this zone from orthoclase
through intermediate structural states toward maximum microcline usually
having normal cell dimensions. The grains of alkali feldspar are larger and
more numerous than in the country rocks and veinlets of very fine grained

TABLE 3

Mineralogical Changes With Fenitization

	Outer zone	Middle zone	Inner zone
quartz	strained, abundant	partly replaced	rare, unstrained
K-feldspar	orthoclase, cryptoperthite	Na-rich intermediate	maximum microcline
plagioclase	twinned	altered, replaced	albitic mantles on K-feldspar
biotite	abundant	altered, rare	absent
hornblende	chloritized	replaced	absent
garnet	chloritized	absent	absent
Na-pyroxene	rare in veins	common in veins	common disseminated
hematitization	on cracks	pervasive, strong on cracks	pervasive, strong
structural style	crackle-breccia	breccia with rotation	breccia with plastic distortion
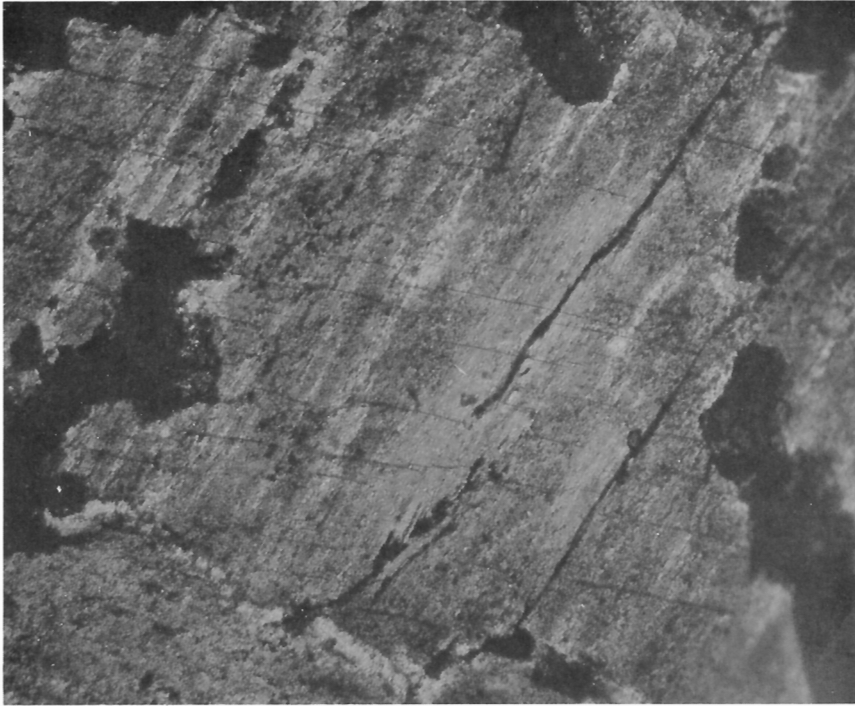
Figure 7. String cryptoperthite from middle zone fenite. (x125, crossed nicols) (G.S.C. photo 201290-C)

potash and/or soda-feldspar are present locally. The ratio of alkali to pla-gioclase feldspar anhedra is noticeably increased, even though mantles of albitic plagioclase commonly surround the alkali feldspar. Mild to intense sericitic alteration is ubiquitous. The inner zone fenites contain maximum microcline replacement perthite, heavily corroded and dissected by albite (Fig. 8). The microcline has normal cell dimensions.

To summarize, fenitization results in an ordering of the lattice of potash feldspar. Since maximum microcline can accommodate little sodium in the lattice (MacKenzie, 1954), this necessarily results in exsolution of sodic plagioclase.

Plagioclase feldspar

Plagioclase anhedra in the country rock display undulose extinc-tion and gentle flexuring of twin lamellae. This characteristic is preserved in the outer zone, but sericitic alteration becomes pronounced. Independent grains of plagioclase are not as abundant in main zone fenites, and where present are heavily sericitized. Virtually all plagioclase occurs as albitic mantles around alkali feldspar grains. In the inner zone fenites, the replace-ment albite comprises almost all of the plagioclase; separate albite anhedra are very scarce. These data show that calcium is steadily lost from plagio-clase during fenitization and that the remaining plagioclase is recrystallized around the alkali feldspar.
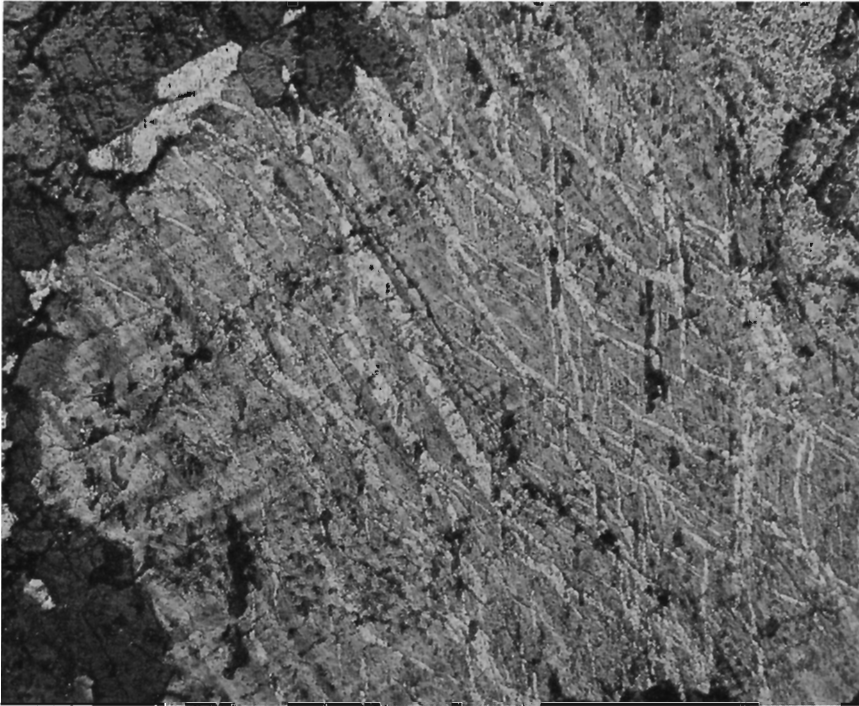
Figure 8. Microcline string perthite, replaced by albite (cutting
           obliquely across string structure), from inner zone
           fenite. (x125, crossed nicols) (G.S.C. photo 201290-D)

Data collected by X-ray and electron microprobe are compiled in
Figure 3 and Table 4. In the country rocks an orthoclase containing about
11 mol per cent of the albite molecule coexists with an oligoclase containing
about 2 mol per cent Or molecule. In the shatter zone of fenitization, although
the optical properties of the feldspars are very similar, a significant amount
of the Ab molecule has been transferred from plagioclase to the potash feld-
spar. In more strongly fenitized rocks, the tenor of Ab molecule in the pla-
gioclase steadily rises. Since the content of calcium (see below) is rising at
the same time as the An content of plagioclase is falling, a reaction involving
the An molecule is strongly suggested. In the potash feldspar, the content of
Ab reaches a maximum in the middle zone of fenitization and then declines
abruptly. This is presumably due to the presence of intermediate structural
state feldspar in the main zone which can accept relatively large amounts of
sodium in the lattice as compared to the low Ab content accepted by the highly
ordered K-feldspar of the inner zone fenite zone.

Quartz

Quartz occurs in the country rocks as very irregular grains with
undulose extinction and as myrmekite around the margins of plagioclase

Table 4

FELDSPARS

Composition and Structural Status

Rock type and specimen number	K-feldspars Composition	K-feldspars Structural state	Cell dimension	Type	Na-feldspars 2V	Na-feldspars Composition	Na-feldspars Structural state
COUNTRY ROCKS							
Migmatitic granitic gneiss							
2	$Or_{87.0}Ab_{11.8}An_{0.3}$	Or	Anomalous	Orthoclase cryptoperthite	65°	$Or_{2.5}Ab_{79.2}An_{19.2}$	Low
19	$Or_{88.2}Ab_{12.2}An_{0.2}$	Or	Anomalous	Orthoclase cryptoperthite	66°	$Or_{2.1}Ab_{89.7}An_{6.7}$	Low
Adamellitic gneiss							
14A	$Or_{88.9}Ab_{11.5}An_{0.2}$	Or	Anomalous	Orthoclase cryptoperthite	62°	$Or_{2.1}Ab_{87.3}An_{11.9}$	Low
24	$Or_{90.2}Ab_{11.0}An_{0.2}$	Or	Normal	Orthoclase cryptoperthite	53°	$Or_{1.5}Ab_{87.9}An_{10.6}$	Low
Heterogeneous paragneiss							
3	$Or_{90.7}Ab_{8.4}An_{0.2}$	Or + Mi	Anomalous	Orthoclase antimicroperthite	58°	$Or_{2.1}Ab_{77.2}An_{18.1}$	Low
37A	$Or_{88.8}Ab_{9.1}An_{0.3}$	Or	Anomalous	Orthoclase cryptoperthite	60°	n.d.	Low
Average	$Or_{88.5}Ab_{10.7}An_{0.2}$					$Or_{2.1}Ab_{84.2}An_{13.3}$	
FENITES							
Outer							
26	$Or_{71.8}Ab_{27.8}An_{0.8}$	Or	Anomalous	Stringlet orthoclase microperthite	59°	$Or_{1.1}Ab_{78.8}An_{17.9}$	Low
58	$Or_{86.4}Ab_{1.8}An_{0.3}$	Or	Normal	Stringlet orthoclase microperthite	56°	$Or_{2.1}Ab_{83.7}An_{12.7}$	Low
Average	$Or_{79.1}Ab_{19.8}An_{0.6}$					$Or_{1.6}Ab_{81.3}An_{15.3}$	
Middle							
40B margin	$Or_{53.6}Ab_{47.8}An_{0.2}$	Mi + Or	Normal	String microcline microperthite	70°	$Or_{1.1}Ab_{92.1}An_{7.7}$ (unzoned)	Low
40B core	$Or_{72.8}Ab_{20.0}An_{0.2}$	Mi + Or-			76°		
68B	$Or_{87.1}Ab_{10.4}An_{0.2}$	Max. Mi	Anomalous	String microcline microperthite	57°	$Or_{2.5}Ab_{93.7}An_{1.1}$	Low
64B	n.d.		Normal	String microcline microperthite	62°	n.d.	
margin	$Or_{53.6}Ab_{47.8}An_{0.2}$					$Or_{1.8}Ab_{92.2}An_{4.4}$ (unzoned)	
Average core	$Or_{80.4}Ab_{19.7}An_{0.2}$						
Inner							
41A	$Or_{93.9}Ab_{6.5}An_{0.1}$	Max. Mi	Normal	Replacement microcline microperthite	n.d.	$Or_{2.1}Ab_{95.7}An_{0.2}$	Low
42A	n.d.	Max. Mi + Or	Normal	Replacement microcline microperthite	56°	n.d.	Low
45B	$Or_{92.9}Ab_{6.8}An_{0.1}$	Max. Mi + Or	Normal	Replacement microcline microperthite	66°	$Or_{2.4}Ab_{94.4}An_{0.2}$	Low
Average	$Or_{93.4}Ab_{6.7}An_{0.1}$					$Or_{2.3}Ab_{95.3}An_{0.2}$	

Or = Orthoclase   Max. = Maximum

Mi = Microcline   n.d. = Not determined

feldspars. No change is observed in this characteristic in the outer zone but in the main zone strained quartz is surrounded by a selvage of soda-pyroxene and myrmekite is rare. Rare lentils 1 to 2 centimetres long, can occur in the inner zone fenites which are unstrained and strongly replaced by soda-pyroxene. The unstrained character suggests recrystallization during fenitization.

Mafic minerals

In the country rocks the major mafic mineral is green hornblende intergrown with subordinate biotite. Garnet is sporadically present either intergrown with hornblende and biotite or independently. In the outer zone, all these minerals are heavily chloritized, and in the middle zone they are almost entirely pseudomorphed by green pleochroic aegirine, and by lesser amounts of bluish soda-amphibole. In the outer zone these minerals are rarely found as veinlets, but in the middle and inner fenite zones they replace all other mafic minerals and parts of some leucocratic minerals until the percentage of mafic minerals becomes roughly twice that of the country rocks. The properties of the sodic mafic minerals are compiled in Table 5. In the ultrafenite zone, extreme hematitization has locally replaced soda-pyroxene and soda-amphibole by a semiopaque brown aggregate containing rutile and carbonates as well as hematite.

TABLE 5

Optical Properites of Sodic Mafic Minerals in Fenites

		Middle zone fenite	Inner zone fenite
Na-pyroxene	$2V_\alpha$	61 - 68°	68 - 75°
	$\alpha \wedge Z$	7°	8 - 12°
	α	green	deep grass green
	β	pale green	green
	γ	pale brown - green	pale brown
Na-amphibole	$2V_\alpha$		62°
	$\alpha \wedge Z$		30°
	α	not present	very pale lavender
	β		pale lavender
	γ		pale blue - green

Accessory minerals

Sphene, zircon, allanite, apatite, and rare fluorite occur in accessory amounts in the country rocks. The latter four minerals appear little affected by fenitization, but sphene is converted to anatase. As already noted,
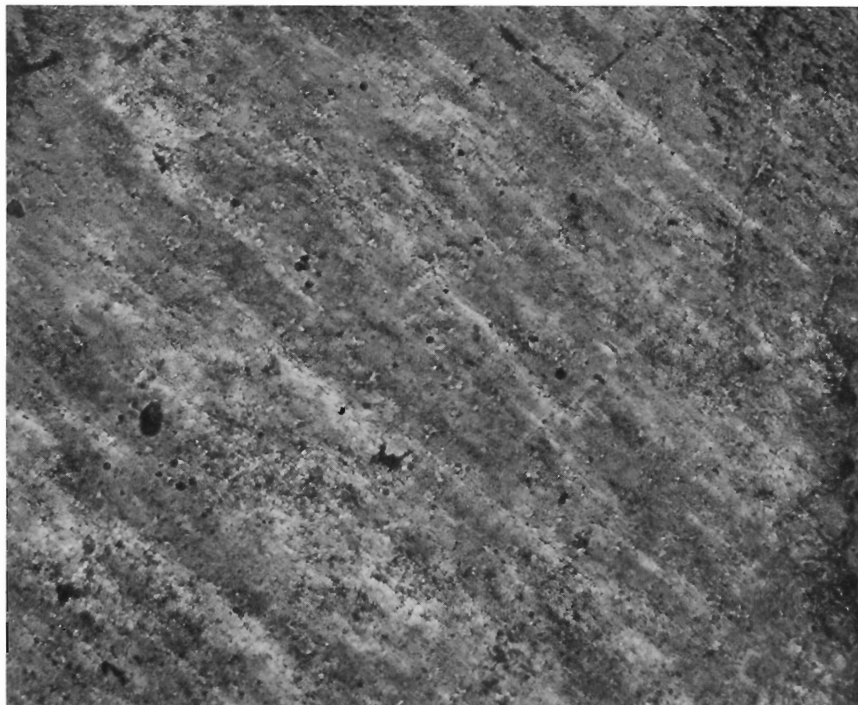
Figure 9. Cryptoperthite from nepheline syenite dyke. (x125, crossed nicols) (G.S.C. photo 201290-N)

rutile is occasionally found in inner zone fenites. Apatite and fluorite are locally concentrated in fenites, but whether this is due to introduction or redistribution of material is uncertain.

The fenites contain trace amounts of a large number of minerals not found in the country rocks, including pyrite, chalcopyrite, molybdenite and probably radioactive rare-earth minerals (thorite?). Barite veinlets are widespread. Chemical analyses suggest that the elements forming these minerals are extremely erratically distributed.

Calcite

Calcite is sparingly present in country rocks but consistently accompanies fenitized rocks. In the less altered zones it appears as veinlets, but in many middle zone rocks it forms discrete pegmatoid patches, either separately or intergrown with aegirine and potash feldspar. In some inner zone fenites it is finely dispersed throughout the rock.

Chemical composition (major elements)

Sixteen chemical analyses of country rocks and their fenitized equivalents are listed in Table 6. Some aspects of the variation of bulk

Table 6

Chemical composition of country rocks and fenites.

Specimen number	Country rocks						Outer zone fenite				Middle zone fenite			Inner zone fenite		
	2	19	39B	65	24	1	26	57A	58	68B	40B	64B	41A	42A	45B	45C
SiO_2	72.10	68.36	72.22	73.13	67.17	69.53	70.69	67.71	64.91	62.99	69.60	60.27	61.70	58.70	59.37	57.30
TiO_2	0.51	0.86	0.24	0.31	0.50	0.56	0.46	0.39	0.40	0.51	0.37	0.35	0.25	0.47	0.36	0.62
Al_2O_3	13.08	12.31	12.26	12.83	15.25	13.90	13.91	15.25	16.43	14.85	14.90	12.64	15.20	15.00	12.27	11.70
Fe_2O_3	1.52	1.21	2.53	1.06	1.43	0.82	0.88	1.32	1.69	3.20	2.30	2.81	5.00	5.80	4.29	9.80
FeO	1.40	5.60	0.20	1.80	3.00	1.70	1.50	2.20	1.90	2.30	1.00	1.70	0.60	1.90	2.90	1.80
MnO	0.06	0.12	0.05	0.03	0.11	0.04	0.04	0.06	0.09	0.09	0.04	0.10	0.05	0.23	0.08	0.38
MgO	0.62	0.71	0.46	0.43	0.47	0.91	0.93	0.48	0.41	1.29	0.50	1.32	1.80	0.50	1.77	1.40
CaO	1.76	1.88	1.54	0.46	1.69	1.64	1.10	1.62	2.25	1.87	1.00	5.76	1.30	1.70	5.92	3.80
Na_2O	2.98	3.40	3.10	2.71	4.01	3.76	3.80	4.62	5.24	4.97	5.19	4.13	5.00	6.33	5.78	7.08
K_2O	5.03	4.62	5.86	6.19	5.31	5.31	5.30	5.10	4.94	4.61	5.26	4.65	6.62	6.99	4.59	3.87
P_2O_5	0.21	0.18	0.08	0.05	0.12	0.24	0.16	0.10	0.12	0.25	0.08	0.14	0.11	- -	0.51	0.10
H_2O	0.80	0.60	0.40	0.60	0.70	0.70	0.60	0.60	1.20	1.70	0.20	1.50	0.70	0.20	0.40	0.40
CO_2	0.10	0.10	0.80	0.10	0.10	0.30	0.10	0.30	0.50	1.10	0.10	4.40	1.40	0.10	0.90	1.20
Sr	0.027	0.019	0.018	0.013	0.015	0.027	0.020	0.033	0.034	0.033	0.028	0.028	0.018	0.064	0.190	0.044
Ba	0.130	0.120	0.110	0.096	0.110	0.150	0.110	0.130	0.170	0.095	0.110	0.074	0.028	0.140	0.130	0.190
Zr	0.025	0.088	0.045	0.030	0.051	0.035	0.041	0.073	0.058	0.031	0.060	0.027	0.030	0.030	0.044	0.110
Rb(ppm)	160	100	190	260	140	170	220	110	120	120	195	120	190	160	190	90
Nb(ppm)	70	100	110	30	110	70	80	50	40	30	50	- -	50	275	30	50
Total	100.25	100.07	99.91	99.75	99.94	99.62	99.64	99.99	100.34	99.89	100.74	99.90	99.80	98.15	99.50	99.79

All analyses by Rapid Methods Group, Geological Survey of Canada, directed by S. Courville.
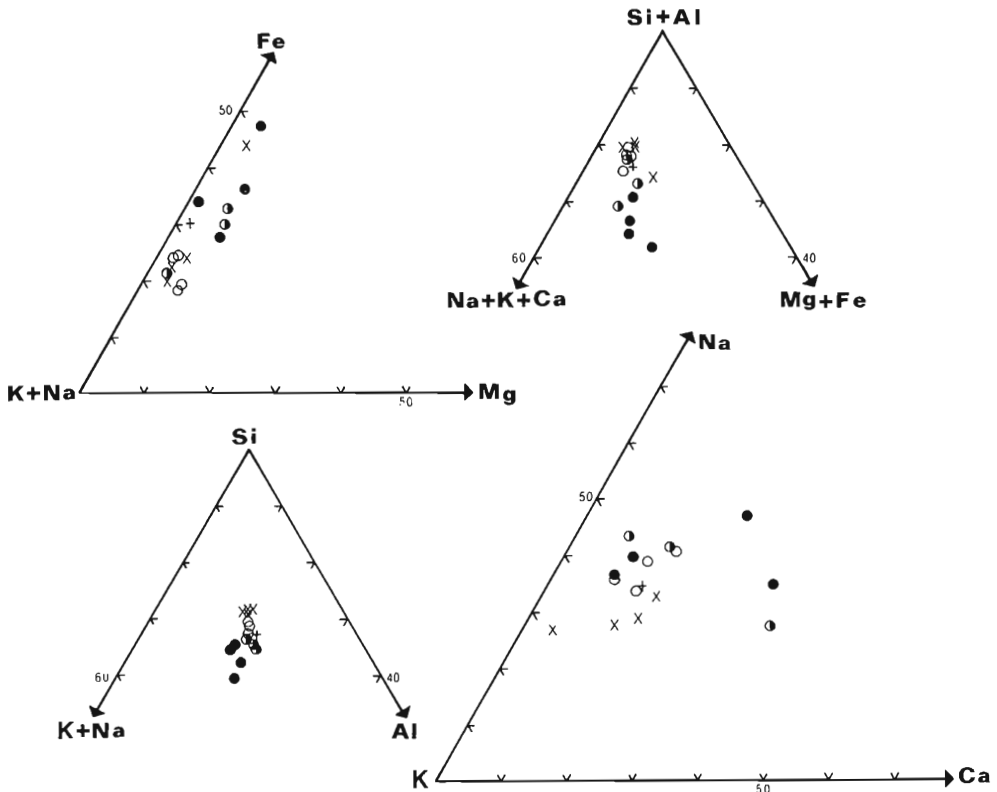
Figure 10. Ternary diagrams representing the chemistry of progressive
fenitization (symbols same as Fig. 12, values in cation per cent).

chemistry with fenitization are summarized in the ternary diagrams of
Figure 10. The AMF diagram shows but slight changes with fenitization. A
slight enrichment of iron relative to alkalis and magnesium appears at the
highest grades. The K-Na-Ca diagram shows an erratic but unequivocal
trend away from the K corner with increasing fenitization, suggesting enrich-
ment in both sodium and calcium relative to potassium during fenitization.
More pronounced effects appear in diagrams including SiO_2 as a variable.
The fenitization trend runs directly away from the silica corner suggesting
that desilication is a major factor in the process. A particularly striking
representation of this trend is obtained by projecting the analyses into the
system quartz-nepheline-kalsilite (Fig. 11); this plot shows the fenitization
trend crossing the albite-orthoclase join almost at right angles. Even allow-
ing for errors due to neglect of plagioclase in the projection this behaviour
contrasts sharply with melt-crystal equilibria since the compositions run
toward a thermal barrier and possibly cross it. Note that the fenitization
trend does not run directly toward the minimum melt composition in the under-
saturated part of the diagram, although it passes fairly close to it.

A quantitative representation of fenitization is rendered difficult
by the ambiguity between material added and material removed. For exam-
ple, if sufficient SiO_2 is removed to lower the SiO_2 content from 70 to 60 per
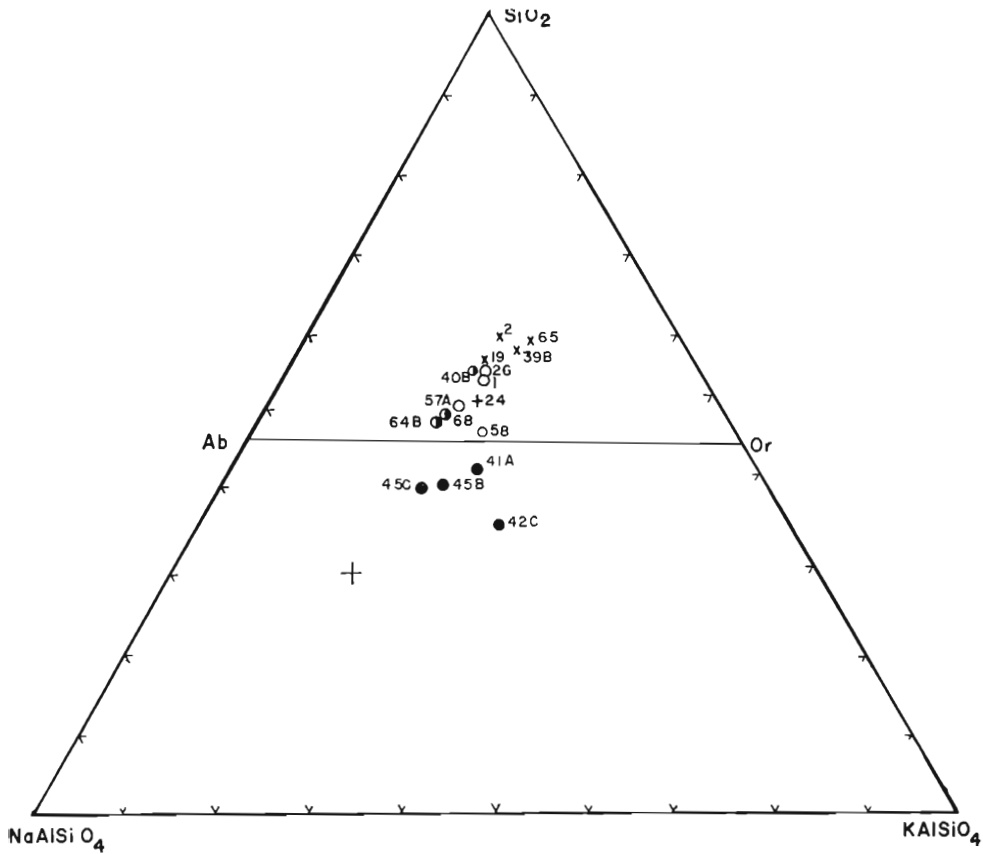
Figure 11. Projection of chemical analyses of fenitized rocks into the system quartz-nepheline-kalsilite. Cross marks position of ternary undersaturated minimum at atmospheric pressure. (Numerical values in mol per cent.)

cent, then in the absence of other factors, the apparent content of all other oxides would rise by one-third in order to make the chemical analysis of the residue total 100 per cent. This ambiguity can be avoided by selecting a suitable parameter invariant during fenitization, and comparing other variables with it. McKie (1966) selected a standard cell containing 100 oxygen atoms for this purpose. Although violations of this standard can easily be envisaged, it seems much superior to any other standard which has been suggested, and in Table 7, the chemical analyses have been recomputed to this standard cell.

Recomputed to a standard cell, the analyses show a steady increase in number of cations per standard cell with grade of fenitization. McKie's (1966) data show a similar increase for all fenite aureoles considered by him. According to the rationale of the standard cell method, in which the volume of the oxygen framework is assumed to remain constant, this must correspond to an increase in density with fenitization. In fact, an increase in

Table 7

Chemical Composition of Country Rocks and Fenites Computed as Cations per 100 Oxygens.

Specimen number	Country rocks						Outer zone fenites			Middle zone fenites			Inner zone fenites			
	2	19	39B	65	24	1	26	57A	58	68B	40B	64B	41A	42A	45B	45C
Si	39.39	38.48	40.19	47.79	37.71	38.66	39.04	37.88	36.66	35.69	38.53	35.77	35.75	35.34	35.29	34.48
Ti	0.21	0.37	0.10	0.13	0.21	0.23	0.19	0.16	0.17	0.22	0.17	0.16	0.11	0.21	0.16	0.28
Al	8.42	8.17	8.02	8.31	9.30	9.11	9.05	10.06	10.84	9.91	9.72	8.84	10.38	10.64	8.59	8.30
Fe^{3+}	0.62	0.51	1.05	0.44	0.41	0.34	0.37	0.56	0.71	1.36	0.96	1.26	2.18	2.63	1.92	4.44
Fe^{2+}	0.64	2.64	0.09	0.83	1.41	0.79	0.69	1.03	0.89	1.09	0.46	0.85	0.29	0.96	1.44	0.91
Mn	0.03	0.06	0.02	0.01	0.05	0.02	0.02	0.03	0.04	0.04	- -	0.05	0.02	0.12	0.04	0.20
Mg	0.51	0.60	0.38	0.35	0.40	0.76	0.77	0.04	0.34	1.09	0.41	1.17	1.56	0.45	1.57	1.27
Ca	1.03	1.13	0.92	0.27	1.02	0.98	0.65	0.97	1.35	1.13	0.59	3.66	0.81	1.10	3.77	2.45
Na	3.15	3.71	3.33	2.89	4.37	4.05	4.07	5.01	5.69	5.46	5.57	4.75	5.62	7.39	6.66	8.25
K	3.50	3.31	4.15	4.34	3.81	3.76	3.73	3.63	3.53	3.33	3.71	3.52	4.89	5.37	3.47	2.97
P	0.10	0.09	0.04	0.03	0.05	0.11	0.11	0.05	0.05	0.12	0.04	0.07	0.06	- -	0.26	0.05
H	2.91	2.25	1.48	2.20	2.63	2.60	2.21	2.25	4.49	6.43	0.73	5.94	2.71	0.80	1.59	1.61
C	0.08	0.08	0.55	0.08	0.08	0.23	0.08	0.23	0.38	0.77	0.08	3.33	1.08	0.08	0.72	0.97
Total	60.59	61.40	60.32	60.07	61.45	61.64	61.08	61.90	65.14	66.64	60.97	69.37	65.46	65.09	65.48	66.18
K/Rb	261	384	256	198	315	259	200	385	342	319	224	322	289	363	201	357
Fe^{3+}/Fe^{2+}	0.97	0.20	11.06	0.53	0.43	0.43	0.53	0.54	0.80	1.25	2.00	1.49	7.00	2.73	1.33	4.93
Sr/Ba$(\times 10^3)$	21.4	14.1	16.2	39.4	12.4	22.9	25.3	28.4	21.0	29.6	38.9	68	194	525	447	161
Ba/Sr	4.81	6.32	6.11	7.38	7.33	5.56	5.50	3.94	5.00	2.88	3.93	2.64	1.56	2.19	0.68	4.32
Ba/K$(\times 10^3)$	31	31	23	19	25	34	25	31	41	25	25	19	5	24	34	59

Chemical analyses by Rapid Methods Group, Geological Survey of Canada, directed by S. Courville.
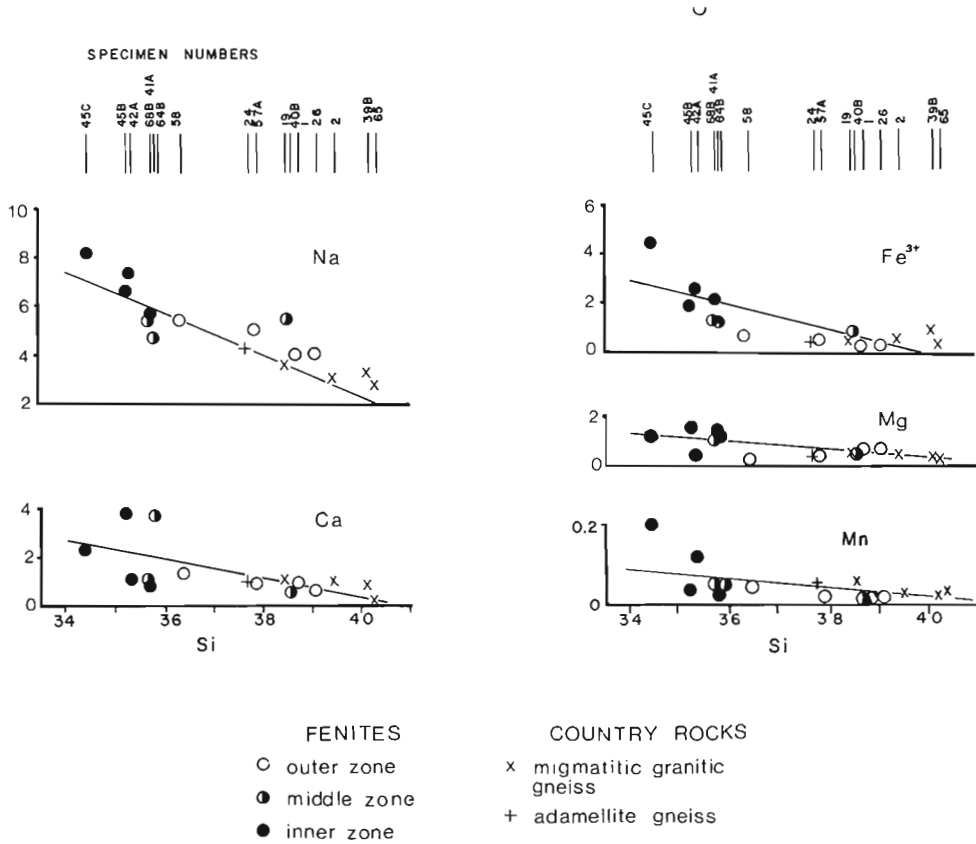
Figure 12. Graphical representation of regression lines of cations against Si in fenitized rocks, for a unit cell containing 100 oxygen ions.

density with fenitization has been found around the Khibinskii massif (Borodin, 1967), suggesting that the standard cell method at least qualitatively represents the fenitization process.

McKie manipulated his data by computing the correlation coefficient between Si and other cations, presumably on the grounds that Si shows a monotonic decrease with grade of fenitization. These computations showed rather small correlation coefficients, except for Mg and Ti. McKie therefore computed the slopes of the regression lines of various cations against Si, and compared the value of the slope with the standard deviation to reach a decision about its significance. We have followed a different procedure. We compute the correlation coefficients between Si and other cations (Table 8), and then compute the probability that the value of the correlation coefficient is zero, using the students "t" test. If this probability is less than 0.01, we compute the regression line. The results are shown in Figure 12. There are significant negative correlations between Si and Na, Fe^{3+}, Mg, Ca, and Mn.

TABLE 8

Variation of Cation Content of Standard Cell With Si

Element	Correlation coefficient with Si	Significant	Slope of regression line on Si
Ti	-0.0394	No	
Al	-0.2315	No	
Fe^{3+}	-0.7856	Yes	-0.528
Fe^{2+}	-0.0834	No	
Mn	-0.6288	Yes	-0.032
Mg	-0.6145	Yes	-0.159
Ca	-0.6146	Yes	-0.385
Na	-0.8440	Yes	-0.703
K	+0.0806	No	
P	-0.1056	No	
H	-0.2138	No	
C	-0.4881	No	

(For the 16 analyses quoted, the correlation coefficient is significant at the
1 per cent level if it exceeds 0.567 and significant at the 0.1 per cent level
if it exceeds 0.756.)

An examination of the content of the cations makes it clear that
they are not all independent. The sum of Na + Si remains constant through
fenitization within 1 per cent, while the sum of Si + (Al+Mg+Ca+Fe) increases
by less than 2 per cent. These data make it clear that fenitization is a replace-
ment of an Si atom by an alkali plus a cafemic atom. Heuristically it is obvi-
ous that linked substitution of this kind is necessary to maintain charge bal-
ance within the crystals. According to this view fenitization can be explained
as a series of desilication reactions of the type

$$Na^+ + Fe^{3+} + 3\ SiO_2 = NaFeSi_2O_6 + Si^{4+}$$

$$Na^+ + Al^{3+} + 4\ SiO_2 = NaAlSi_3O_8 + Si^{4+}$$

$$6Na^+ + 8Mg^{2+} + 2Fe^{3+} + 2H_2O + 23\ SiO_2 = 2Na_3Mg_4Fe(OH)_2Si_8O_{22} + 7\ Si^{4+}$$
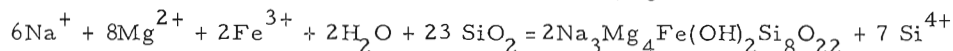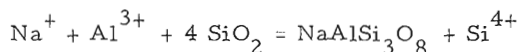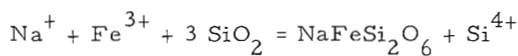
(eckermannite)

where the ions are assumed to be carried in the fenitizing solutions. Note that where hydration reactions are involved, as in the formation of eckermannite, the number of Si ions removed need not be half that of the cations added. Reactions of this kind explain both the success and limitations of plotting degree of fenitization against Si content of a standard cell. The content of Si is, according to this hypothesis, a correct measure of the extent of fenitization, but the atoms substituted for it vary. Plotting of Si against Na (or against total alkalis where K-metasomatism is significant) yields good correlation. Na appears in almost all the new minerals, but plots of Si against Al, Fe, Mg and Ca yield poorer correlation because these atoms may substitute one for another due to local variations in composition, or conditions in the fenitizing fluid. Correlation of Si against the sum of Al + Fe + Mg + Ca is much superior to correlation against any one of them, as shown in Figure 13.

Plotting the data of McKie (1966) for Spiktskop, and Oldonyo Dili in the same way (Fig. 13) gives very similar results. The sum of Si + alkalis is virtually constant, and the plot of Si against (Al+Fe+Mg+Ca) yields a smooth curve with little scatter. McKie's data for Alno, however, do not fit these generalizations. The situation is complicated by the presence of rather heterogeneous rocks which obviously will not fall on a single curve, but examining the original work of Von Eckermann (1966 and references therein), it appears the major reason for the discrepancies is the inclusion of numerous melted rocks ('rheomorphic fenites') in his description of fenites. The presence of melted equivalents of fenite rocks at Alno, at Khibini (Borodin, 1967) and at other complexes is well documented.

Although these rocks may arise as an end product of fenitization, their chemistry must be quite different from that of fenites proper, since it was shown (Fig. 11) that the metasomatic processes do not tend toward thermal minima as do crystal-melt equilibria. This confounding of two different phenomena may be partially responsible for the confusion over fenite chemistry evident in the literature.

Thus far we have confined ourselves to consideration of generally granitoid compositions. It was noticed in the field however that amphibolitic schlieren in the granitoid rocks appeared to have fairly uniform compositions consisting of roughly equal amounts of amphibole and biotite and plagioclase commonly with subordinate garnet. Schliers of similar, but more diffuse character are found up to the highest grade of fenitization. Table 9 contains four analyses showing the results of fenitization on amphibolite, assuming the initial composition of the amphibolite to have been uniform.

Manipulation of these analyses shows that the net effect of fenitization was to add potash feldspar to the amphibolite. This accords well with petrographic observations. There is a lesser increase in the components of albite.

The literature on fenitization of basic rocks is scanty (Verwoerd, 1966), but the above observation seems to accord well with other data. It shows that desilication will not be effective in rocks already strongly undersaturated, especially if these rocks are surrounded by saturated, or nearly saturated rocks. Further, the relatively rapid increase of potash with respect to soda in the basic fenites suggests that the K:Na ratio of fenites is in some way related to their composition. One possibility may be that potassium is mobilized in the surrounding rocks, and that for reasons previously discussed is soon dropped out of solution. In such a case the undersaturated basic rocks
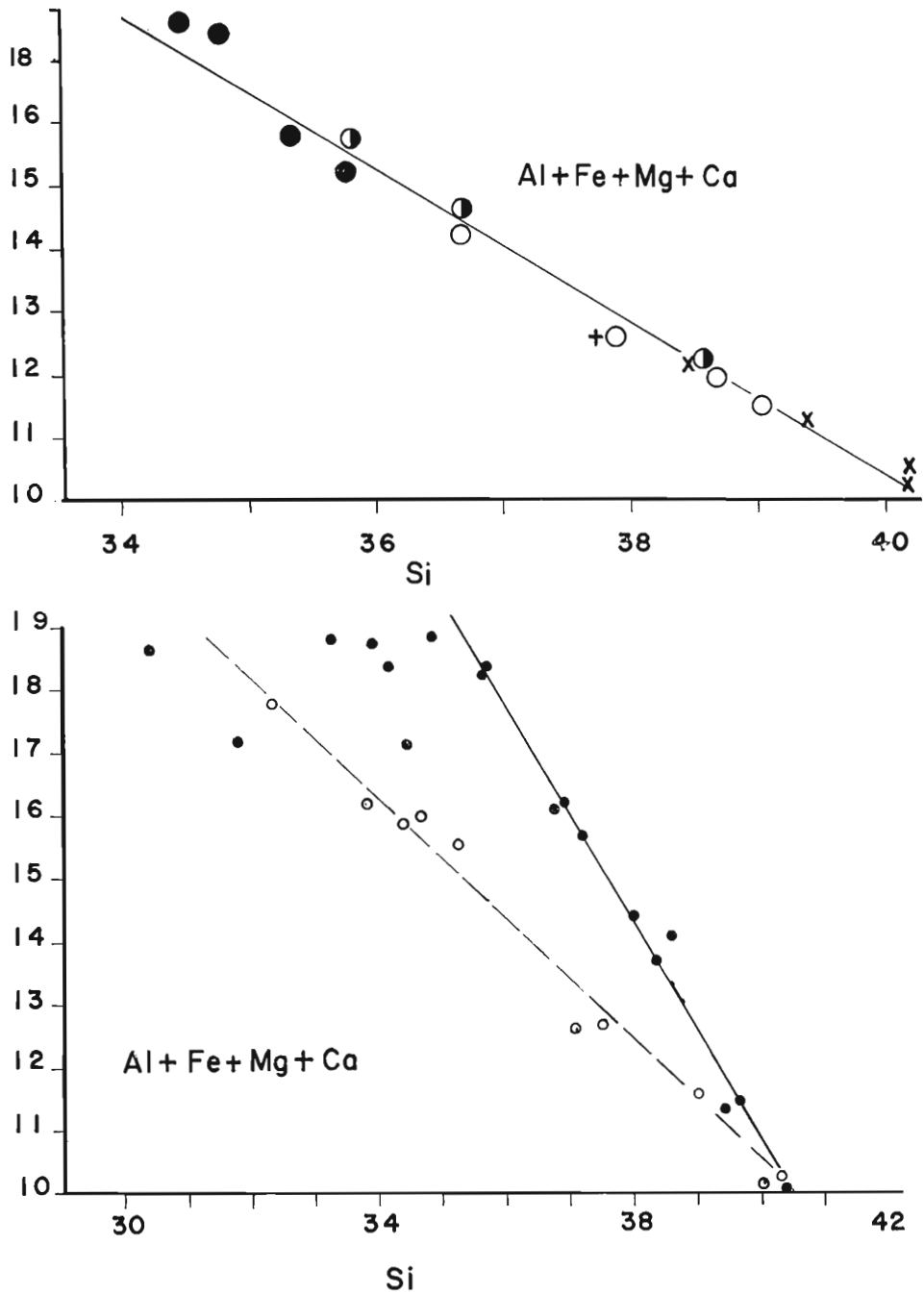
Figure 13. Variation of the sum of Al, Fe, Mg, and Ca against Si in a unit
cell containing 100 oxygens for rocks around Callander Bay (top)
and for other alkaline complexes (bottom). Open circles and
dashed lines are McKie's (1966) data for Spitskop and Oldonyo
Dili respectively. Solid circles are data from Alno Island (Von
Eckermann, 1948). Lines are least squares fits, but for Alno
Island only data with more than 35 Si per standard cell were used
in the computation.

may well have a higher chemical potential for potash than the relatively potash-rich surroundings. Indeed, the results suggest that a major aspect of fenitization may be homogenization by supplying a mobilizing and transporting medium to smooth inhomogeneities.

TABLE 9

Chemical Composition of Amphibolite and Fenitized Equivalents

Analysis	1326	1328	1327	1329
SiO_2	42.84	44.92	47.78	50.32
TiO_2	3.49	2.05	1.89	2.17
Al_2O_3	15.20	15.41	14.27	19.34
Fe_2O_3	3.44	3.03	4.59	2.38
FeO	13.21	9.11	9.11	4.52
MgO	6.32	7.51	6.18	3.33
MnO	0.12	0.16	0.16	0.06
CaO	6.34	8.60	8.51	3.59
Na_2O	3.70	3.13	2.15	4.59
K_2O	1.69	2.62	2.12	3.91
P_2O_5	0.31	0.34	0.37	0.24
H_2O	1.78	1.64	1.84	3.06
CO_2	0.19	0.26	0.38	0.36
Sr	0.06	n.d.	0.01	0.30
Ba	0.05	n.d.	0.05	0.66
Zr	0.018	n.d.	0.072	0.10
Nb	0.0083	n.d.	0.0099	0.028
Total	98.96	98.78	99.49	99.30

Analysis 1326 is of an amphibolite from unaltered granitoid gneiss, 1328 is an amphibolite from the outer zone of fenitization, 1327 from the main zone, and 1329 from the inner zone. Although these analyses were all made and repeated by classical methods, the totals are anomalously low. The reason for this is unknown.

Chemical composition (minor elements)

With five exceptions all the fenites and country specimens display
a consistent depletion in Rb relative to K in terms of the crustal average
K:Rb value of 230 given by Ahrens et al. (1952) (Table 7). Seven specimens
also fall outside of the normal limits of scatter, having K:Rb values in excess
of 300. There is no regularity or progression in the K:Rb values of the fen-
ites relative to the country rocks.

There is no strong covariance between Sr and Ca in the country
rocks and fenites although there is a tendency for the rocks that are high in
Ca to be correspondingly high in Sr. Isomorphous replacement of Sr by K
has also been postulated (Gerasimovskii and Lebedev, 1958). However, a
plot of these two elements showed no strong covariance although a general
negative slope is evident. Siedner (1965) and Ferguson (1970) have shown
that there can be a strong correlation between Ba and Sr; however, in the
present case no interdependence was noted.

No covariance is present between Ba and Rb or Ba and K for the
country rocks and fenites. Furthermore, there is no significant difference
between the average values for the Ba:Rb and Ba:K ratios for these two rock
groups (Table 7). Outer zone fenite specimen 58 has an anomalously high Ba:Rb
value of 14.17 resulting from a high Ba content, this in turn probably reflects
the high K-feldspar content of this rock. The abnormally low Ba:K ratio of
5 in outer zone fenite specimen 41A is produced by the low Ba content and
normal K content. The low amount of Ba present in this specimen is puzzling
as the K-feldspar content of the rock displays no abnormality. The some-
times erratic distribution of Ba could be a result of the presence of barite as
an accessory mineral particularly in the inner fenite zone where veins of this
mineral are not uncommon.

Ti shows enrichment relative to Zr but their ratio shows very lit-
tle variation within the country rocks and fenites. The Ti:Nb ratio is far
more erratic resulting from marked fluctuation in Nb. Nb is presumably
substituting for Ti^{4+} and Zr^{4+} in the Ti-Zr silicates, sphene and zircon,
which have erratic accessory distribution in these rock groups.

Structure and contact relations

Shattering and brecciation are highly characteristic features of
the fenites. In addition to being characteristic of the fenite aureole as a
whole, various degrees of shattering demarcate zones within the fenites.
Thus the main zone fenites are more shattered than the outer zone, and unusu-
ally severely shattered lenses within the outer zone commonly show petro-
graphy typical of the middle zone. The inner zone fenites show a very strong
disruption of the fabric, but plastic deformation plays some part here also,
and distorted lenticles and small scale folding are as common as mechanical
shattering. Since there is a continuous spectrum of deformation, the bound-
aries between the various fenite zones are gradational and somewhat arbi-
trary. Transitions from one to another are rapid, commonly occurring within
a few metres, or even within a few centimetres. Intercalation of one zone of
fenite with another is common, on both large and small scales.

Contacts with the country rocks are also gradational. Beyond the
well defined outer zone of fenitization, rare hematitized cracks and joints
accompanied by minor chloritization and development of hematite, extend at

least another 1,000 metres (3,280 feet) in some areas, passing imperceptibly into normal country rocks. Fenite aureoles surrounding igneous dykes, likewise pass gradationally but more rapidly into country rocks.

Contact relations of fenites with the alkaline igneous rocks are more cryptic. There is no doubt that they are intruded but not hornfelsed by lamprophyre. Locally they appear to grade into potassium trachyte and nepheline syenite. The gradation to trachyte is well exposed at several localities on the south shore of the bay, but the high Al_2O_3 content of trachyte suggests it is not melted fenite. The relations with the nepheline syenite are more doubtful. In the large road-cut on Highway 11, nepheline syenite dykes clearly cut sharply across fenite. However, at Callander railway station, the margin of the nepheline syenite is intensely altered, and there seems to be a gradation from nepheline syenite through fenite riddled with pegmatitic patches, to normal middle zone fenite.

Origin

The petrographic character of low-grade fenite zones, notably the intensification of fenitization along natural channels such as joints, and breccia zones, and the zoned character of some minerals, suggest that the fenitizing fluid flowed along definite channels, rather than diffusing through a passive medium. If the latter alternative were correct, the presence of unmetamorphosed remnants close to the igneous complex, and local screens of high-grade fenitization at a considerable distance, would be particularly hard to explain. In the standard cell computation the rapid increase of H and C up to the middle zone of fenitization suggests that not only was the fluid aqueous, but that it was saturated with CO_2. Both these concentrations fall off in the inner fenite zone, but this can be accounted for by the higher temperatures prevailing in this zone. McKie (1966) pointed out that the high concentrations of water and carbon dioxide ensure the highly oxidizing character of the fenitization medium.

Some data on the composition of the fenitizing solutions can be deduced from experimental evidence. The chemistry of the fenitization process shows that: (1) the solutions are very undersaturated in silica and oversaturated in sodium relative to solutions in equilibrium with granitic rocks; and (2) Fe, Ca, and Mg are relatively mobile in the fenitizing solutions.

We will consider the second point first. Leaching experiments on natural rocks (Ermanovics et al., 1967; Burnham, 1967) show that Fe, Ca, and Mg are very nearly immobile in distilled water brought into equilibrium with rocks at elevated temperature and pressure. These elements are reasonably mobile only in the presence of moderate to high concentrations of cations such as Cl^- (Burnham, 1967). From consideration of the alternatives it seems very probable that Cl^- is the ion involved. Burnham (1967) shows that F^- would be ineffective. If SO_4^{2-} were present in any significant amount the mobility of barite in the fenite zone is very difficult to understand; NO_3^- is unstable at the temperatures (400-600°C) involved in fenitization. We shall proceed on the tentative assumption that a high concentration of Cl ion is present in the fenitizing solutions.

Since the data of Burnham (1967) show that solutions, chloride-rich or not, in equilibrium with rocks or magmas saturated with SiO_2 are also saturated with SiO_2, it is clear that the fenitizing solutions can never have been in equilibrium with a rock or melt saturated in SiO_2. Further the

Na:K ratio of solutions must have been much higher than that of the country rocks. Otherwise significant amounts of potassium would have been added to the fenites (Burnham, 1967; Orville, 1963). The solutions are clearly highly concentrated in alkalis relative to those in equilibrium with feldspar. In fact, allowing for the increase in Si:alkalis ratio caused by the presence of CO_2 in solution (Burnham, 1967), it seems unlikely that the solutions could ever have been in equilibrium with an alkali feldspar-bearing rock and yet arrived at the site of fenitization so poor in silica.

  The pressure conditions of fenitization can be estimated from data on nearby alkaline complexes with fenite aureoles. The Manitou Islands alkaline complex, 6 kilometres (3.75 miles) northwest of Callander Bay retains part of a sedimentary infilling in the crater. The Brent complex, 65 kilometres (41 miles) to the east retains most of the sedimentary infilling. From these data it seems probable that the present erosion level at Callander Bay is not more than a few hundred metres below the surface at the time of emplacement. Hence the pressures cannot have been more than a few hundred bars. The temperature during fenitization can be estimated from experimental data on some typical fenitization reactions. Particularly characteristic is the reaction

$$Na^+ + Fe^{3+} + 3\ SiO_2 \quad NaFeSi_2O_6 + Si^{4+}$$
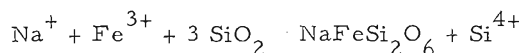
This reaction has been studied by Sieber and Tiemann (1968) in connection with silica leaching by Na(OH) from taconite iron ores. At about 50 bars fluid pressure, the equilibrium temperature is near 485°C. In the fenitization aureole, acmitic pyroxenes are very rare or absent in the outermost part, occur along veinlets in the middle zone, and throughout the rock in the inner zone fenites. This can be interpreted as suggesting that in the outer zone the temperatures were below 485°C, in the middle zone the temperature of the solutions was above 485°C but only a narrow fringe of the wall-rocks was heated to this temperature, and in the inner zone the whole rock was above this temperature.

  Corroboration of this temperature can be obtained by considering the hypothetical reaction

$$CaAl_2Si_2O_8 + Na_2CO_3 + 4\ SiO_2 = 2\ NaAlSi_3O_8 + CaCO_3$$
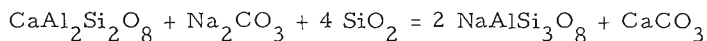
In the middle and inner fenite zones, the right-hand side of this equation is stable, whereas in the outer zone, the left-hand side is stable, with the exception that the sodium carbonate is in solution. The equilibrium of this reaction can be evaluated from thermodynamic data in Robie and Waldbaum (1968) and the JANAF tables (1966). These data are compiled in Table 10. They suggest an equilibrium temperature of slightly over 500°C for stabilization of the right hand side of the equation.

  An independent estimate of temperature in the outer part of the fenite aureole can be obtained by applying the Barth feldspar thermometer to the feldspar of the outer zone fenites in which redistribution of sodium has clearly taken place. This zone shows a plagioclase (An_{16} on average) in equilibrium with a potash feldspar containing 20 per cent albite (Table 4). According to the tables of Davidenko (1966) this indicates a temperature of formation of 490°C. The inner zone fenites, in which albite and microcline coexist, show that the temperature did not exceed the homogenization temperature of alkali feldspar, roughly 750°C.

TABLE 10

Free energy $\left(\dfrac{-(G_T-H_{298})}{T}\right)$ data for the equation

$$CaAl_2Si_2O_8 + Na_2CO_3 + 4\ SiO_2 \rightleftharpoons 2\ NaAlSi_3O_8 + CaCO_3$$
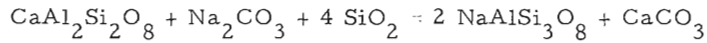
All data in kilocal $mol^{-1}\ deg^{-1}$

T(°K)	Anorthite	Na_2CO_3	4 Quartz	ΔG	Albite	Calcite	ΔG
600	59.69	38.98	49.28	147.95	122.20	26.58	148.78
700	64.86	41.75	53.84	160.45	132.26	28.59	160.85
800	70.01	44.59	58.44	173.04	142.26	30.59	172.85
900	75.01	47.32	63.04	185.37	152.00	32.54	184.54
1000	79.85	49.95	67.52	197.32	161.44	34.42	195.86
1100	84.50	52.48	71.76	208.74	170.48	36.23	206.71

Thermodynamic data from Robie and Waldbaum (1968) and JANAF tables (1966).

The agreement for the temperature of the lowest grade fenites is very satisfactory. It can be concluded that fenitization takes place essentially at temperatures above 450°C, and that extensive fenitization occurs only above 500°C. The maximum temperature at which fenitization can take place is limited by the melting temperature of the rocks. At the Alno Island complex (Von Eckermann, 1948) it seems clear that fenitization and anatexis (rheomorphism) form a continuous spectrum. Fenitization may therefore take place up to temperatures of 700°C or more.

The sericitic alteration of the feldspars within the fenites suggests that the fenitizing agent was somewhat acidic. According to the plots of Meyer and Hemley (1967) the ratio of molality of alkali chlorides to hydrochloric acid at which alkali feldspar is in equilibrium with mica is of the order of 100, if the total pressure is 1 kilobar, while the total acidity suggested by the same equilibrium under the same conditions is of the order 0.01 molal. Hence alkali chlorides in the fenitizing solution are of the general order of 1 molal concentration. Comparison with the sulphide assemblages erected by Holland (1965) shows that Callander Bay approximates the assemblage chalcopyrite-molybdenite-hematite-magnetite-K-feldspar-sericite, characterized at 500°C by oxygen fugacity near 10^{-17} bars and sulphur fugacity near 10^{-3} bars.

Potassium Trachyte

Distribution

Potassium trachyte intrusives are widely distributed in the imme-
diate environs of Callander Bay, particularly in the more strongly fenitized
and mylonitized zones. A compound trachyte-carbonatite dyke was also noted
4 kilometres (2.5 miles) south of Powassan.

Lithology

These rocks are all fine grained to aphanitic, but otherwise are
variable in appearance. The colour is most commonly brick-red varying to
dull brown, but mottling produced by lens-shaped leucocratic areas 1-3 cen-
timetres long is common. Phenocrysts are commonly, but not invariably
present. Potash feldspar phenocrysts up to 12 millimetres long may define
trachytic texture. Biotite phenocrysts up to 3 millimetres long occur rarely.
Carbonate ocelli are very rare. Altered and resorbed lenses or fragments
of country rocks are rather common, particularly in the marginal parts of
the intrusions. Where the intrusions are more than 2 metres wide, they are
invariably associated with carbonatite.

Microscopically, the trachyte consists mainly of sericitized pot-
ash feldspar, with subordinate plagioclase, altered biotite and carbonate.
Sphene and opaque minerals are usually present in accessory amounts.

For the most part the potash feldspars are string microperthites
composed either of microcline or orthoclase, with either anomalous or nor-
mal cell dimensions. In one sample both phases are present. Potash feld-
spar phenocrysts are seldom seen in the very fine grained and cryptocrystal-
line varieties, in which plagioclase laths 1-2 millimetres long, locally aggre-
gated with carbonate, are plentiful. The prominent mottled appearance of
some of these rocks results from aggregations of fine-grained feldspar sur-
rounded by a hematitic matrix containing minor plagioclase and chlorite.

Biotite usually occurs as very fine laths, rarely as phenocrysts.
In some cases the biotite is entirely hematitized or chloritized. Sericite is
distributed generally through the matrix, and also pseudomorphically replaces
part of the potash feldspar.

Carbonate is a minor matrix mineral in most of the rocks. The
rare 0.5-1.5 millimetre carbonate ocelli also contain chlorite rosettes and
muscovite laths.

Chemical composition

Five analyses of potassium trachytes are presented in Table 11.
Two of the analyses approach pure feldspar rocks (35B, 70A) while the others
appear to be more akin to the nepheline syenites (see Table 15) particularly
the more mafic varieties. None of the analyses appears to approach very
closely the fenite analyses (Table 6) mainly because of the low content of
alumina in the latter. Since aluminum appears to be relatively inert during
fenitization this evidence appears to be a strong argument against develop-
ment of the trachyte by way of the fenitization process.

TABLE 11

Chemical Composition of Potassium Trachyte

Specimen number	35B	50A	70A	119	107
SiO_2	57.00	52.90	60.40	55.40	57.53
TiO_2	0.39	0.57	0.05	0.80	0.52
Al_2O_3	20.00	20.80	19.40	21.64	21.04
Fe_2O_3	5.90	2.50	0.20	3.16	2.06
FeO	0.50	2.00	0.20	1.34	1.01
MnO	0.06	0.14	0.06	0.03	0.07
MgO	3.00	2.90	0.80	1.34	1.86
CaO	0.50	2.00	1.10	0.09	1.32
Na_2O	0.40	2.72	1.49	1.97	4.29
K_2O	11.27	9.80	12.83	9.91	7.57
P_2O_5	0.02	0.04	0.24	0.28	0.08
H_2O	2.30	2.30	0.50	3.92	2.04
CO_2	0.40	1.70	1.70	0.04	0.20
Total	100.74	100.37	99.97	99.72	99.79

Selected trace element data (ppm)

Rb	230	265	410	n.d.	n.d.
Nb	270	170	100	130	183

n.d. = not determined

Structure and contact relations

The potassium trachyte is mainly present in the form of dykes and sheets ranging in width from 0.5 millimetre to 2.5 millimetres. They tend to follow the same regional joint sets occupied by the carbonatite and lamprophyre intrusives (see Fig. 27), but in some cases are found in 25 centimetre-wide fracture zones in the country rocks. A sheet seldom retains the same width for more than 2-3 metres. In addition to pinch and swell, discrete off-sets along planar elements occur, but the characteristic thin 'horn-like' appendages, universal in the offset lamprophyres, were not seen. Contacts with the country rocks tend to be sharp, although some fragment-charged dykes appear to have gradational margins with fenite. Aphanitic chilled margins 2-3 centimetres wide occur on some dykes, commonly displaying a fine fissility and marked by hematite staining in the margin and the surrounding country rock. Rheomorphic veining of the trachyte by the country rock occurs at one place, where 1 to 2 centimetre-wide veinlets of mobilized country rock penetrate the trachyte for distances of up to 60 centimetres.

Despite the back-veining, the trachytes are clearly younger than the country rocks. Their relationships to the other rocks of the intrusion, however, are complex. Although they generally cut the fenites, and send apophyses 2-3 centimetres wide, and a metre long into middle zone fenites, in one case a sinuous 3-4 millimetre-zoned vein of potash feldspar with a margin of radial soda pyroxene cuts the trachyte. This veinlet appears typical of those developed during fenitization. This suggests that the development of the fenites and emplacement of the potassium trachytes may have been simultaneous, or at least partly overlapping.

Potassic trachytes have been found to cut lamprophyre dykes and vice versa. The latter relation is much more common and it appears that most of the trachyte is older than most of the lamprophyre.

The trachyte is older than the carbonatite, by which it is consistently brecciated. On the island south of Darling Island there is an intrusive sheet consisting of an upper zone of 25-40 centimetres, of potassium trachyte, and a lower brecciated zone more than 1 metre thick of carbonatite containing angular inclusions of trachyte. Southeast of Burford Point there are repeated occurrences of carbonatite dykes 5-10 centimetres wide brecciating potassium trachytes. Four miles south of Powassan a series of en échelon veins, each 2-8 centimetres wide occur over a zone 3-4 metres wide. In the widest vein five carbonate zones alternate with potassium trachyte zones which bifurcate and anastamose over distances of a few centimetres.

Origin

The origin of the potassium trachyte will be considered in Chapter IV.

Nepheline Syenite

Distribution

The largest area of nepheline syenite occurs along the north and east shores of Callander Bay. Discontinuous outcrop is found in a crescent extending about 2,000 metres (6,500 feet) from the Old Mill site on the north shore of the bay, to Burford Point, on the east side of the bay. This zone

appears to have a maximum width of 300 metres (1,000 feet) exposed above water. Nepheline syenite dykes occur southeast of Callander Bay, mainly within the fenite aureole. Four dykes have been identified with widths from 10 to 20 metres (33 to 66 feet) and maximum strike lengths of 1,500 metres (4,900 feet), part of which is soil covered.

Lithology

Three varieties of nepheline syenite are recognized on textural and mineralogical grounds. Along the north and northeast shores of Callander Bay, including the island immediately south of the dock at Callander, an inhomogeneous coarse-grained mesocratic variety outcrops, characterized by ellipsoidal aggregates of fine-grained mafic minerals 0.5-1.0 centimetre in diameter. Here and there these aggregates are as large as 8 centimetres in diameter. To the east and southeast of this belt, an outer crescent of leucocratic, coarse-grained, locally trachytic syenite outcrops, a rock which lacks the discoidal mafic aggregates. In contrast to the grey shades of the mesocratic rock, this variety has pink colours.

The nepheline syenite dykes tend to be homogeneous, coarse-grained and markedly trachytoid. Small discoidal mafic aggregates, 2-4 millimetres diameter, occur in the 1 metre-wide central zone of one 10 metre (33-foot) dyke. Chalky white, pitted, "nepheline weathering" is characteristic of all varieties. Highly irregular pegmatitic patches, locally very nepheline-rich, are present in all three nepheline syenite varieties. Locally the feldspar and nepheline crystals are up to 4 centimetres long. Aegirine veins 1-4 millimetres wide are also present in all varieties of nepheline syenite.

TABLE 12

Modal Composition of Nepheline Syenite

Specimen number	13	31	53	63	72	74
plagioclase	--	--	--	--	--	--
K-feldspar/perthite	51.8	80.6	60.1	55.7	20.6	2.9
biotite	1.1	0.3	2.9	0.1	3.5	38.6
aegirine	1.8	0.4	--	8.8	26.1	34.3
Na-amphibole	--	--	--	--	--	1.0
nepheline	43.2	18.2	34.4	34.1	45.1	19.2
calcite	--	--	--	0.1	--	--
apatite	--	--	--	--	1.0	0.2
sphene	--	--	0.5	--	3.6	3.8
opaque(s)	2.1	0.5	2.1	1.2	0.1	--

TABLE 13

K-FELDSPARS

Composition and Structural States in the Nepheline Syenite

Rock variety and specimen number	Composition of K-phase	Bulk composition	Structural state	Cell dimension	Perthite type	2V
Mesocratic						
50A	n.d.	n.d.	Mi + Or	Normal	Microcline string microperthite	54°
74	n.d.	n.d.	Or	Anomalous	Orthoclase string microperthite	54°
Leucocratic						
53	n.d.	n.d.	Mi + Or	Anomalous	Microcline microperthite	n.d.
63A	$Or_{61.2}Ab_{38.9}An_{0.3}$	n.d.	Mi + Or	Anomalous	String microperthite	56°
Narrow dykes						
10A	n.d.	$Or_{69.9}Ab_{27.8}An_{0.1}$	n.d	n.d	String microperthite	56°
13	$Or_{65.4}Ab_{33.5}An_{0.2}$	$Or_{62.1}Ab_{34.1}An_{0.1}$	Or + Mi	Anomalous	String microperthite	56°
31	n.d.	n.d.	Or + Mi	Anomalous	String microperthite	58°
60A	n.d.	$Or_{65.1}Ab_{36.1}An_{0.4}$	n.d	n.d	String microperthite	58°

Microscopically, the rocks consist of varying proportions of potash feldspar, altered nepheline, biotite, and aegirine, with minor amounts of sphene and opaques. Some modal compositions are tabulated in Table 12.

The potash feldspars (Table 13) are string cryptoperthites of either orthoclase or microcline with anomalous cell dimensions (Fig. 9). In leucocratic and dyke varieties, they are commonly rimmed by thin discontinuous mantles of albitic plagioclase. The feldspar laths are commonly 0.5-1.0 centimetre long, but may reach 3 centimetres. Nepheline and mafics fill the interstitial areas. A characteristic feature of the perthitic feldspars is the presence of twinning in almost every lath, most commonly on (010), but also commonly after the Baveno law.

In the mesocratic nepheline syenite, the nepheline is almost always entirely pseudomorphed, except in the mafic clots. The replacement products may be either cancrinite or 'gieseckite' (an intimate mixture of sericite and minor analcite), with the former commonly restricted to the margins of the nepheline. In two cases veins of cancrinite less than 0.5 millimetre wide traverse the rock. In the more leucocratic varieties of syenite the nepheline is frequently fresh, or preserved as cores surrounded by alteration products. Soda-pyroxenes, opaques and rarely carbonates are found as inclusions within nepheline or its pseudomorphs. Analyses of nepheline (Table 14) show it to fall in the range of nephelines from plutonic or hypabyssal nepheline syenites (Deer et al., 1963, p. 243).

TABLE 14

Chemical Composition of Nepheline From Nepheline Syenite

Sample	52	10A
SiO_2	41.1	43.6
Al_2O_3	35.0	33.5
CaO	0.1	0.1
K_2O	7.3	6.6
Na_2O	16.2	17.2
Total	100.2	100.9

Electron microprobe analysis by G.R. Lachance. Sample 52 is of a homogeneous, mesocratic nepheline syenite; Sample 10A is of a pink, coarse to pegmatitic, leucocratic nepheline syenite.

Mafic minerals are commonly concentrated along the margins of nepheline. Sodic pyroxene (-2V = 78-80°, z∧c = 8-10°, pleochroism, a = deep green, b = grass green, c = yellow green) is commonly intergrown with biotite, opaque minerals, and sphene. Both biotite and pyroxene show strong zoning in the mesocratic variety, but not in the leucocratic rocks. Within the fine-grained mat of mafic minerals, small amounts of unaltered nepheline, cancrinite and feldspar occur as inclusions. The mafic clots previously noted in the syenite dykes, appear identical to those in the mesocratic syenite,

Figure 14. Pseudoleucite(?) phenocrysts from a fine-grained,
green nepheline syenite dyke. (G.S.C. photo 201305-F)

Figure 15. Photomicrograph of intergrown nepheline (dark grey) and
microcline in pseudoleucite phenocrysts. (x125, crossed
nicols) (G.S.C. photo 201290-G)

TABLE 15

Chemical Composition of Nepheline Syenite

Specimen number	13	31	53	63	72	74	5B
SiO_2	53.00	58.68	55.34	53.70	48.20	50.87	50.76
TiO_2	0.46	0.37	0.47	0.45	1.02	1.21	1.34
Al_2O_3	23.50	19.80	21.04	22.60	20.20	18.92	20.80
Fe_2O_3	2.10	1.84	2.26	1.90	3.50	3.55	1.05
FeO	1.80	1.40	1.40	1.60	2.70	2.50	4.20
MnO	0.15	0.11	0.08	0.15	0.29	0.22	0.11
MgO	1.00	0.24	1.90	2.30	4.30	2.05	2.93
CaO	1.00	0.74	1.36	1.70	4.40	3.81	3.18
Na_2O	4.13	5.07	2.16	3.47	3.08	6.81	3.49
K_2O	8.73	9.47	9.86	9.25	8.20	7.88	7.52
P_2O_5	0.00	0.14	0.08	0.06	0.28	0.25	0.33
H_2O	2.80	0.90	2.80	3.00	3.10	0.80	4.60
CO_2	0.20	0.60	0.80	0.80	1.00	0.40	n.d.
Total	98.87	99.36	99.94	100.98	100.27	99.27	100.31

Selected trace element data.

Rb	205	270	270	225	160	140	n.d.
Sr	1400	1900	1200	1500	3000	2100	1300
Ba	1100	920	1000	1200	2400	2500	3800
Zr	440	250	490	630	1600	630	1200
Nb	50	140	250	200	225	220	130

n.d. = not determined

All analyses by Rapid Methods Group, Geological Survey of Canada, directed by S. Courville. Analyses 13, 31, 53, 63, are leucocratic nepheline syenite; analyses 72, 74, mesocratic nepheline syenite; analyses 5B, is a nepheline syenite dyke.

except that the nepheline is replaced by sericite. The opaque mineralogy of
the nepheline syenites is distinctive. Magnetite containing oriented blades of
hematite forms ameoboid blebs of skeletal habit associated with biotite, or
spindle-shaped grains found as inclusions in all mafic minerals. The specu-
larite blades appear to be oriented along (111) planes, and commonly form
10-20 per cent of the grain.

       An unusual nepheline syenite dyke appears to contain pseudoleucite.
The matrix is a dense, fine-grained, deep green rock with dark phenocrysts
1-2 millimetres long, containing white or pale pink masses 1-2 centimetres
across which form perfect dodecahedra, giving hexagonal cross sections when
broken (Fig. 14). Microscopically the matrix consists of a fine-grained inter-
growth of potash feldspar laths, aegirine needles, and subordinate amounts
of subhedral nepheline. The 'phenocrysts' are intergrown biotite and soda-
pyroxene stained by hematite, forming a loose aggregate enclosing matrix
material. Their subhedral outline strongly suggests pseudomorphed sphene.
The hexagonal leucocratic areas are composed of blocky to lath-like poikilitic
aggregates of potash feldspar and nepheline (Fig. 15). A distinct fine-grained
rim occurs around the edge of the areas, which show a very sharp, clean
boundary. Aegirine-biotite intergrowths, similar to those in the coarse-
grained syenites occur in the hexagonal areas, but not in the matrix. The
composition of these hexagonal, pseudoleucite-like areas was examined by
electron microprobe.

Chemical composition

       The compositions of seven nepheline syenites are presented in
Table 15. The analyses fall into the same three groups as were defined pet-
rographically. The mesocratic rocks are low in silica and rubidium, and
high in titania, total iron, magnesia, and manganese. The dyke rocks differ
from the leucocratic syenite belt in a lower content of magnesia and calcium,
and a higher content of sodium. All of the analyses are rather high in potas-
sium, and display markedly high K:Na ratios.

TABLE 16

Chemical composition of pseudoleucite

Specimen	W. R.	P. L.
SiO_2	50.53	55.86
Al_2O_3	20.10	24.43
Na_2O	1.59	7.51
K_2O	13.98	8.10
CaO	1.58	1.58
Total	87.87	97.48

Analyst, J.L. Bouvier. W.R. is a partial analysis of the matrix containing
pseudoleucite; P.L., partial analysis of pseudoleucite phenocryst.
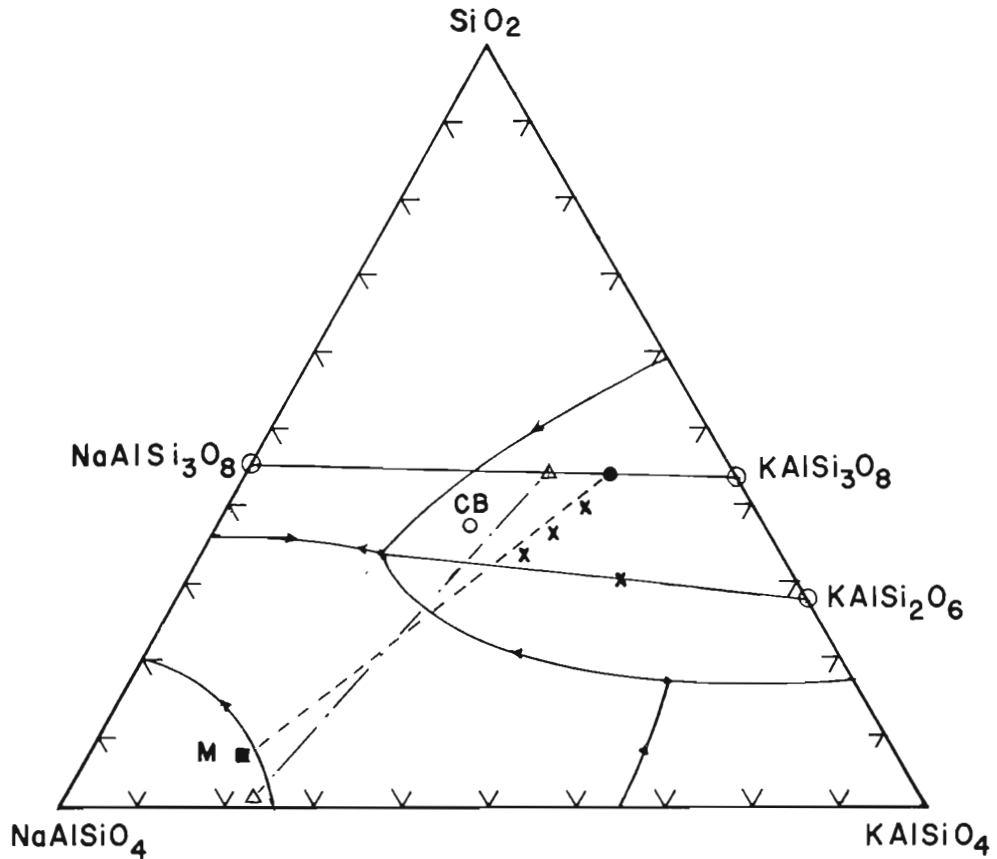
Figure 16. Position of pseudoleucite analyses in the system quartz-nepheline
kalsilite (diagram after Deer, Howie and Zussman, 1963), CB =
Callander Bay intergrowth, x = analyses quoted by Deer et al.
Triangles show composition of coexisting nepheline and feldspar
in Callander Bay syenite, M = Morozewica nepheline composi-
tion. Diagram in mol per cent.

        Analyses of the components of the pseudoleucite are tabulated in
Table 16, and plotted in Figure 16. The bulk analyses fall in the leucite field
in this projection, but are somewhat more sodic than most analyzed pseudo-
leucites (Deer et al., 1963, vol. 4, p. 281).

Contact relations

        The various varieties of nepheline syenite were nowhere seen in
direct contact. However on the island just south of the government dock in
Callander, an angular block, 0.5 metre (1.5 feet) in greatest dimension is
enclosed in mesocratic nepheline syenite (Fig. 17), together with a rounded
inclusion of adamellite gneiss. The dykes appear to cut cleanly, and with
locally sharp, fine-grained margins, across the enclosing fenites. Four
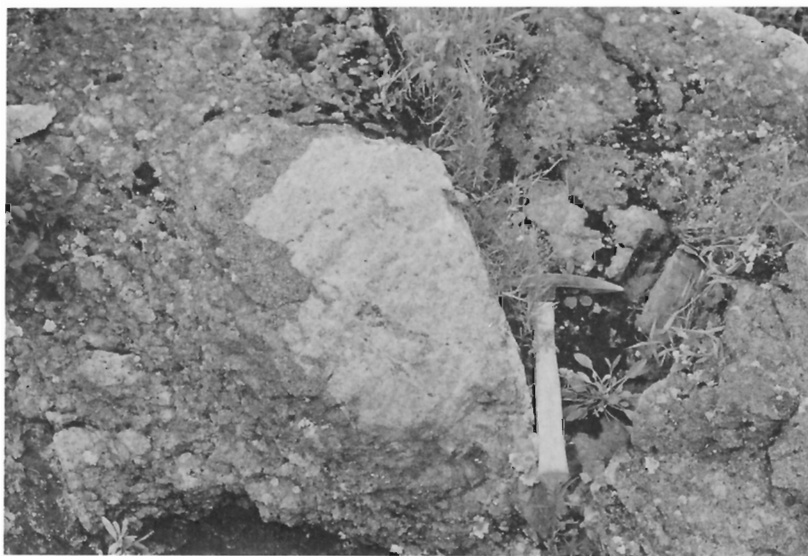
Figure 17. Inclusion of leucocratic nepheline syenite in meso-
            cratic nepheline syenite on the island south of govern-
            ment dock, Callander. (G.S.C. photo 201305-I)

hundred metres west of the old mill site on the north shore of Callander Bay,
and immediately east of Burford Point syenite blocks up to 50 centimetres
diameter appear to be enclosed in fenite. However it is uncertain that these
blocks are part of the main nepheline syenite mass and are not merely
extremely fenitized country rocks. In the town of Callander the contact
between the fenites and the leucocratic nepheline syenite can be defined within
2 metres.

        Nepheline syenite is cut by lamprophyre dykes in numerous out-
crops along the shore of the bay. A dense fine-grained nepheline syenite dyke
10-15 centimetres wide cuts leucocratic nepheline syenite in a boulder observed
southeast of the bay.

        The exact attitude of the screens of nepheline syenite is uncertain.
Where present, trachytoid texture appears to roughly parallel the shore of
the bay, and to dip steeply suggesting a form somewhat like a ring dyke.

Origin

        The coarse grain size of the nepheline syenite, together with the
composition of the nepheline strongly suggest emplacement at considerable
depth where cooling was slow thus permitting the growth of large crystals,
and the attainment of equilibrium between crystals. A plentiful supply of
water would greatly assist the development of both features and the locally
intense hydrous alteration of the nepheline syenite suggests that considerable
water was, in fact, present during the emplacement of this rock type.

This conclusion leads to difficulties in explaining the origin of the dyke containing the intergrowth of nepheline and potash feldspar if this intergrowth is "pseudoleucite". The composition of the intergrowth (Table 16) exceeds the 40 weight per cent $Na_2AlSi_2O_6$ soluble in dry leucite, and this solubility is substantially reduced by the presence of water (Fudali, 1963). In addition, the composition of the intergrowth is richer in sodium than that of the matrix, whereas Fudali's experiments show clearly that leucite is always richer in potassium than is the coexisting liquid (Fudali, 1963, compare particularly Figs. 3 and 7 of Fudali's paper with Fig. 16). These considerations clearly indicate that the intergrowth could not form by breakdown of leucite. However the striking geometric form and intimate texture of the material suggest that the intergrowth is a breakdown product of a pre-existing mineral. Another possible parent is analcite. The most potash-rich natural analcite known contains 4.48 per cent K_2O, substantially below the K_2O content of the intergrowth, but Barrer and Baynham (1956) have prepared a synthetic potash analcite in which potash substitutes for all the soda. Pearce (1967) described a trachyte containing 58.1 per cent SiO_2, 10.10 per cent K_2O, and 2.26 per cent Na_2O containing 30 per cent modal analcite phenocrysts. While the composition of this analcite is not known, the amounts and nominal composition of other modal minerals strongly suggests that its potash content must be high. If the intergrowth does result from the breakdown of analcite, this suggests high water pressures during part of the crystallization history. Peters et al. (1966) found that the presence of potash stabilizes analcite at high temperature but that at least 2.3 kilobars water pressure are required to stabilize analcite on the melting curve. If the water pressure were this high during part of the crystallization history it strongly suggests that the intergrowth-bearing rock has risen from a considerable depth (7-8 kilometres (4.3 to 4.9 miles) minimum).

Chemical analyses of the dyke-forming nepheline syenites show strong similarities to those of the mesocratic, coarse-grained varieties. It is not unreasonable to suppose that they represent the same magma emplaced under different conditions. On the other hand there is a marked difference in composition between these rocks and the leucocratic nepheline syenite, which in at least one instance is intruded by the mesocratic variety. These relations can be explained by identifying the mesocratic nepheline syenite with the material separated by immiscibility from the lamprophyres (see below), while the leucocratic material was generated at shallow depths by anatexis of undersaturated fenites.

The variations in composition of the nepheline syenite could also be due to magmatic differentiation. The composition of the potassium trachytes (Table 11) shows marked similarities to that of the nepheline syenite, and it is possible that the sequence mesocratic nepheline syenite-leucocratic nepheline syenite-potassium trachyte represents a line of magmatic liquid descent. The strongly potassic character of the nepheline syenite is noteworthy. All of the igneous rocks from this complex appear to be unusually high in potash. This could well represent an original characteristic, but their emplacement in a highly potassic granitoid terrane inevitably suggests the possibility of acquisition of potassium from the country rocks.

Carbonatite

Distribution

Carbonatite layers were repeatedly intersected in a borehole drilled to intersect a magnetic anomaly 0.7 kilometre (0.4 mile) west-northwest of Burford Point. Dykes and sheets of carbonatite are found on Darling Island, and in the fenite aureole southwest of Callander Bay. Carbonatitic selvages on lamprophyre dykes are common and ocelli of carbonatite occur within these dykes.

Lithology

The occurrences of carbonatite are uniformly rather thin. The maximum single intersection of carbonatite in the borehole was 10 metres (33 feet). Many of these intersections were texturally and mineralogically heterogeneous with irregular carbonatite bodies as veins and breccia patches, in many cases containing major amounts of magnetite, biotite, apatite, aegirine and sulphides. A 2.5 metre (8.2 feet) wide dyke on Darling Island consists of coarse-grained carbonate, magnetite, biotite and aegirine with a marginal biotite-rich zone 5-8 centimetre wide containing books of biotite to 1 centimetre diameter. As with all the other carbonate intrusives, veinlets of pure carbonate occur within the mass, and country rock inclusions up to 40 centimetres diameter are locally abundant. Adjacent to this body the wall-rock is shattered for 2 metres (6.5 feet) and filled with aegirine veins containing rounded feldspar inclusions. Sulphides vein the rocks and fill interstitial areas.

The veinlets within the fenite zone are commonly less than 30 centimetres wide, and display markedly sinuous and irregular form, commonly pinching out, and reappearing on the same fracture. In general the carbonatites weather to brownish shades, less commonly grey. On a fresh surface many of the bodies have a characteristic salmon pink colour but pale grey or white shades are not rare.

Microscopically the rocks consist mainly of a complex mixture of calcite and dolomite with varying but commonly accessory or major amounts of biotite, aegirine, potash feldspar, apatite, barite and opaques.

From staining techniques, supplemented by X-ray diffraction identification, it is evident that the distribution of calcite and dolomite is complex, and that they usually occur in close association. These distributions range from nearly pure calcite, with minor en echelon veins of dolomite less than 1 millimetre wide, to nearly pure calcite with minor veining of mixed calcite and dolomite. Elsewhere dolomite and calcite have patchy or homogeneous granular distribution. Commonly border zones of veins comprise a mixture of calcite and dolomite which grades into pure dolomite in the central part of the vein.

Potash feldspar may make up as much as 40 per cent by volume of the carbonatite, either as large porphyroblasts, or as a fine, intimate intermixture with calcite and dolomite. The potash feldspar is a microcline microperthite. Minor plagioclase is occasionally present in the feldspar carbonate intergrowths.

Biotite commonly occurs as subhedral grains which may show weak concentric zoning. The grains are pleochroic in deep red-browns. Those

sectioned perpendicular to (001) commonly show gentle bending. Inclusions are commonly euhedral apatite, less commonly bladed magnetite, while biotite in turn is included in aegirine and magnetite. Carbonate, chlorite and magnetite penetrate along cleavage planes, and in some cases form an aggregate replacing the biotite.

Apatite generally occurs as clear grains, locally euhedral, which tend to aggregate into irregular patches up to 1.5 centimetre diameter. Individual grains may be present as inclusions in other major minerals, and occasionally a veinlet of carbonate cuts an apatite aggregate.

Barite forms irregular aggregates or separate anhedra surrounded by carbonate. Veinlets of barite up to 3 centimetres wide are a common feature of breccia fillings. Aegirine occurs as stumpy subhedral prisms containing minor apatite and biotite inclusions.

The opaque minerals encountered in the carbonatite are magnetite, specularite, pyrite, and rarely chalcopyrite and pyrrhotite. Magnetite occurs as subhedral grains or blebs, commonly embayed by, and containing inclusions of, silicates. Oriented blades of specularite are commonly present on (111), and patchy alteration of the host to specularite is common. Spindles or blades of magnetite are common within silicates and often aligned on particular crystallographic directions. Skeletal magnetite occasionally forms an open intergrowth with pyrite and silicates.

Pyrite occurs in two distinct forms. The older appears to be euhedral to subhedral corroded grains, riddled with inclusions, which are invariably mantled by, or mantle magnetite. Intergrowths with stubby magnetite blades are common. The second variety occurs in single subhedral cubes, or chains of cubes with small, infrequent inclusions. The cubes may rarely show rounding or embayment. The pyrite of this type contains rare exsolution blades of pyrrhotite and/or chalcopyrite.

The assemblage of opaque minerals gives unique information on the temperature, and oxygen and sulphur fugacities during emplacement of the carbonatite (Holland, 1959). This will be discussed in Chapter IV.

Chemical composition

Two analyses of carbonatites are given in Table 17. Note the relatively high potassium contents, and the extreme Na:K ratios.

Contact relations

Carbonatite intrudes and brecciates country rocks (rarely), fenites and potassium trachytes. Commonly carbonatite dykes have sharply dfeined margins surrounded by a rather intense fenitization halo up to five times the width of the dyke. Local areas of brecciation with carbonatite breccia fillings occur along almost every well exposed carbonatite dyke.

No contact between nepheline syenite and carbonatite was seen. The relations of the carbonatite to the lamprophyre dykes is complex. Carbonatite dykes cut some lamprophyres, and lamprophyres cut some carbonatites. In addition, substantial amounts of carbonatite occur as selvages and as ocelli in the lamprophyres. These data clearly suggest contemporaneous, and closely related intrusive mechanisms. Since the lamprophyre is younger than the nepheline syenite, the carbonatite is also thought to be younger than the nepheline syenite.

TABLE 17

Chemical Composition of Carbonatites

Specimen number	60B	BH1-533
SiO_2	18.00	19.30
TiO_2	0.99	1.06
Al_2O_3	4.00	4.20
Fe_2O_3	2.20	0.14
FeO	4.50	5.30
MnO	0.83	0.96
MgO	11.00	6.83
CaO	26.00	26.00
Na_2O	0.42	0.52
K_2O	4.40	2.58
P_2O_5	2.00	1.65
H_2O	0.40	0.30
CO_2	29.30	29.90
Total	102.04	98.74

	60B	BH1-533
Rb(ppm)	50	50
Sr	0.14	0.097
Ba	0.10	0.58
Zr	0.006	0.016
Nb(ppm)	330	150

Modes

	60B	BH1-533
calcite	46.1	18.7
dolomite	20.2	18.7
opaque	7.9	0.1
feldspar		51.1
sphene		2.5
zeolite		0.5
chlorite + alteration	25.8	--

Chemical analyses by Rapid Methods Group, Geological Survey of Canada, directed by S. Courville.

Origin

The origin of the carbonatite, and its relation to the rest of the Callander Bay complex are discussed in Chapter IV.

Lamprophyres

Distribution

Lamprophyre dykes are concentrated within the fenite aureole and nepheline syenite zone of the Callander Bay complex although they are by no means confined to it. Concentrations of dykes are found associated with at

- 50 -
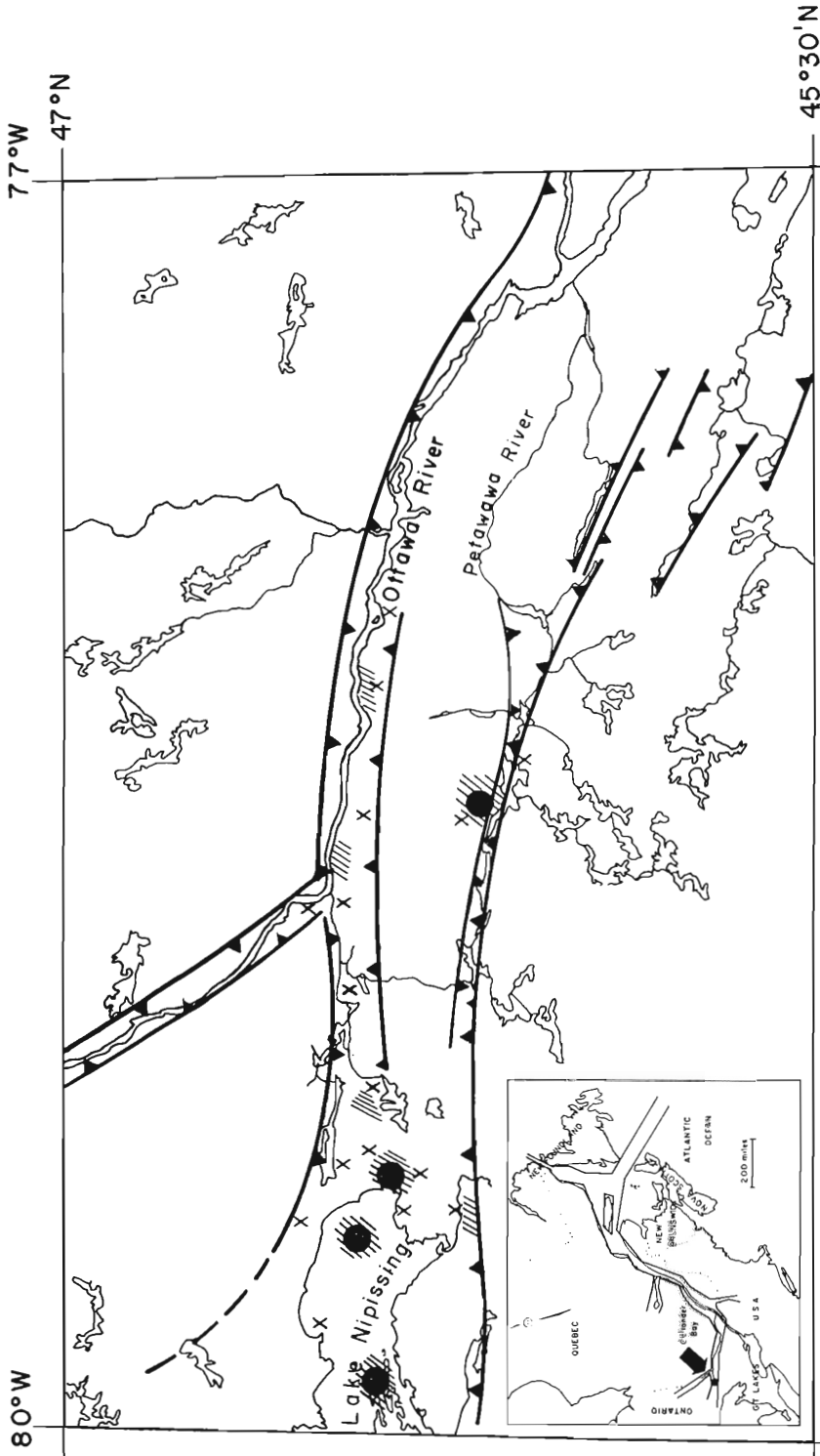
Figure 18. The Ottawa-Bonnechere graben system (teeth on down thrown fault block). Solid circles = alkaline complexes (Callander Bay) at east end of Lake Nipissing, hachure = fenitized areas, x = lamprophyre dykes. Inset shows relation to St. Lawrence rift system defined by Kumarapeli and Saull (1964).

least five independent areas within 20 kilometres (12.5 miles) of Callander Bay, and very similar dykes occur sporadically over the floor of the Paleozoic rift system with which Callander Bay is associated (Fig. 18).

Lithology

The lamprophyres occur as tabular bodies ranging from a fraction of a centimetre to 1.6 metre (5.25 feet) in width, with a large majority between 0.3 and 1.0 metre (1 and 3 feet) thick. All are fine grained melanocratic rocks with porphyritic texture. By far the most common variety, comprising 85 per cent of the lamprophyres, consists of phenocrysts up to 1 centimetre diameter of altered olivine, clinopyroxene, and commonly biotite, set in a dark, fine-grained greenish black matrix. The remaining lamprophyres lack olivine and contain kaersutite, and in most cases clinopyroxene phenocrysts, set in a fine-grained brownish black matrix. A few dykes appear to be transitional between lamprophyre and more trachytic types.

Natural outcrops of the lamprophyres are very poor, and, except for wave-washed outcrops along the shore of the bay, almost useless in determining the internal structure of the lamprophyres. The useful outcrops are found in blasted road-cuts.

Spherical to ellipsoidal, sharply bounded, leucocratic masses are ubiquitous in the lamprophyres of the Callander Bay area (Fig. 19). These ocelli range from 0.05 to 2.50 centimetres in diameter, averaging 1-3 millimetres, and form 7-16 per cent of the rock volume. There is an almost imperceptible decrease in grain size towards the margin of some lamprophyres, occurring over a width of 1-4 millimetres. Ocelli are absent from these chill margins. Infrequent country rock inclusions and screens tend to parallel the margins of the sheets (Fig. 20), although small definitely rotated inclusions are not rare (Fig. 21).

Microscopically the dykes consist of two distinct portions, the matrix and the ocelli. The major minerals in these portions are identical, with the exception of olivine, which is not found in the ocelli. The major minerals are clinopyroxene, olivine, biotite, kaersutite (in kaersutite-bearing varieties), calcite, dolomite, analcite, and lesser amounts of sericite, potash feldspar, albite and natrolite. Apatite, sphene, chlorite and fluorite are commonly present in accessory amounts. A considerable number of other minerals occur in the ocelli locally, or in minute amount, including celestite, siderite, and quartz. Detailed descriptions of the more important rock-forming minerals follow.

Olivine

Subhedral to euhedral pseudomorphs after olivine are very common in dykes reaching diameters up to 1 centimetre. Replacement minerals include various mixtures of carbonate, chlorite, sericite and opaques. Unaltered olivine was found in only three rocks. Determinations of its composition by the X-ray powder diffraction technique of Yoder and Sahama (1957) gave values of Fo_{77} to Fo_{78}.

Neither olivine nor its pseudomorphs was found in the ocelli. Pseudomorphs are present touching the ocelli but they never straddle the boundary in the manner of the other minerals.
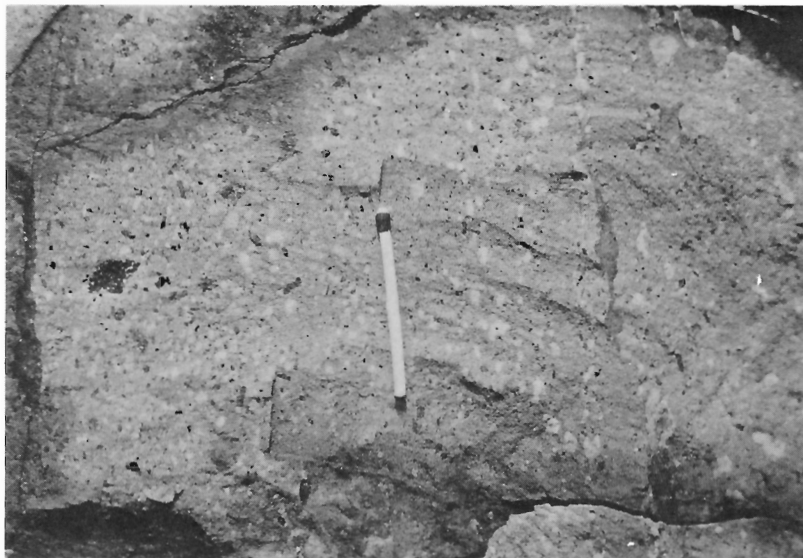
Figure 19. Typical occurrence of ocelli in a 1.8 metre wide
            lamprophyre dyke. (G.S.C. photo 201305-G)

Figure 20. Screen of partially assimilated country rock paral-
            leling margin of lamprophyre. Note rounded edges
            of screen, and curved shape. (G.S.C. photo 201305-J)

Figure 21. Small rotated inclusion of country rock in lamprophyre. Note
reaction rim on inclusions, and strong zonation in the dyke.
(G.S.C. photo 201305-E)

Clinopyroxene

Phenocrysts of zoned clinopyroxene are ubiquitous in the lampro-
phyres. Exceptionally they reach 1 centimetre in length but more commonly
are 2-3 millimetres. In addition to these phenocrysts, nonpleochroic pris-
matic clinopyroxenes, seldom measuring more than 1 millimetre long are
the most common mineral of the matrix. A further variety may be present
as deep green granules in both matrix and ocelli. In the matrix these deep
green clinopyroxenes occur either as discrete interstitial grains or as incom-
plete mantles on pyroxene and biotite phenocrysts. In the ocelli, the green
clinopyroxenes occur as prisms less than 1 millimetre long or less commonly
as very narrow but complete mantles on biotite.

The phenocryst pyroxene is commonly zoned, either normally
from augitic centre to aegirine-augite rim, or irregularly from pale green
pleochroic centres through nonpleochroic zones, to pleochroic green margins.
The phenocrysts occasionally contain inclusions of biotite and, rarely, apa-
tite. In some cases the phenocrysts are partially or completely replaced by

carbonate, chlorite, sericite, and minor amounts of opaque minerals. The properties of the fine-grained nonpleochroic matrix pyroxene were found to be identical to those of the nonpleochroic portion of the phenocrysts, and the pleochroic green prisms are identical to the pleochroic green margins of some of the phenocrysts. The optical properties of these varieties are summarized in Table 18.

 Partial analyses of each of these types of clinopyroxene were made by electron microprobe. These analyses are tabulated in Table 18. Two of the phenocrysts selected for analysis straddled the boundary of the ocellus and matrix, and from textural evidence appeared to be in equilibrium in both environments. The pyroxenes range from diopsidic in the nonpleochroic varieties, to almost pure aegirine. From the textural evidence, it appears that the order of formation of the pyroxenes was a pale green aegirine-augite, followed by diopsidic augite and finally aegirine. The earliest pyroxene is not present in the ocelli but the latter two are present in both ocelli and matrix and have identical compositions in both. Since the green aegirine is present as independent grains in the ocelli and mantling biotite, it must be concluded that at least this pyroxene crystallized from the contents of the ocellus. It is identical in composition to the green pyroxene of the matrix.

Biotite

 Biotite occurs in anhedral to euhedral grains poikilitic with pyroxene, opaques and rarely apatite. Rutile needles commonly occur on (001) planes. Strong concentric colour zoning is commonly present, particularly in the better formed crystals. The centres range from nearly colourless to pale reddish brown, and the margins are pleochroic in intense shades of reddish brown. In some specimens bent biotite flakes are common in the ocelli but do not occur in the matrix. Some grains of biotite are partially or completely altered to sericite and chlorite. As previously noted, biotite in the ocelli commonly has a very thin continuous rim of aegirine; in the matrix the rim is discontinuous. Like pyroxene, biotite is fairly commonly found straddling the boundary between ocellus and matrix. In a few cases, however, biotite grains in the ocelli appear to be truncated at the boundary of the ocellus.

 In a number of specimens the biotite grains show three distinct zones, but in others only two are apparent. All of these zones were analyzed by microprobe for Fe, Mg, and Ti. The results are compiled in Table 19. All examples show strong iron enrichment from the centres toward the margins. With one exception (specimen D56) the compositions of the biotites in the matrix are virtually identical to those in the ocelli. The lath straddling the boundary between the ocellus and the matrix has the same zoning, and the same composition in both parts.

Kaersutite

 Kaersutite occurs as phenocrysts up to 6 millimetres long, and may also be present as 1 millimetre long prisms in the same rocks, both in the matrix and in the ocelli. The smaller prisms are more euhedral than the larger, but both appear very similar optically. A strong concentric zoning from dark pleochroic brown centres to much paler brown at the margin is displayed by all examples. Despite colour variations optical properties vary only slightly as shown in Table 20. Like pyroxene (Fig. 25) and biotite,

TABLE 18

Optical Properties and Composition of Pyroxenes from Lamprophyres

Specimen	Type	2V	Pleochrism			MgO	CaO	FeO	Na₂O
			α	β	γ				
125A	Nonpleochroic small prisms (matrix)	50	colourless	colourless	colourless	12.9	23.7	8.5	0.8
D56	Pleochroic green mantle on biotite (ocellus)	63	green	pale green	yellow green	2.0	5.5	26.2	n. d.
D56	Pleochroic green grains (matrix)	63	pale green	very pale green	pale yellow green	tr.	3.0	30.0	n. d.
D56	Pleochroic green grains (ocellus)	63	green	pale green	yellow green	0.3	2.8	31.7	n. d.
125A	Pleochroic green grains (matrix)	63	green	pale green	yellow green	2.6	1.6	29.2	11.3
125A	Pleochroic green grains (ocellus)	63	green	pale green	yellow green	0.8	3.6	28.0	9.2
D56	Nonpleochroic phenocryst (matrix)	52	colourless	pale green	yellow green	13.5	24.2	8.0	n. d.
D56	Same phenocryst (ocellus)	52	colourless	colourless	colourless	13.5	24.7	6.9	n. d.
604	Nonpleochroic phenocryst (matrix)	50	colourless	colourless	colourless	12.0	23.9	7.4	n. d.
604	Same phenocryst (ocellus)	50	colourless	colourless	colourless	11.9	23.5	8.9	n. d.
604	Same phenocryst, rim in ocellus	n. d.	pale green	very pale green	pale yellow green	0.3	1.8	27.9	n. d.
125A	Zoned phenocryst, core (matrix)	61	pale green	very pale green	pale yellow green	7.7	22.7	12.0	1.4
125A	Same crystal, centre (matrix)	52	colourless	colourless	colourless	12.5	23.7	8.5	1.0
125A	Same crystal, rim (matrix)	63	green	pale green	yellow green	1.7	5.0	26.2	8.4

n. d. = not determined

tr. = trace

Microprobe analyses by A. G. Plant.

TABLE 19

Composition of Biotite From Lamprophyres

Specimen	Type	Matrix									Ocelli								
		Core			Centre			Margin			Core			Centre			Margin		
		TiO_2	MgO	FeO	TiO_2	MgO	FeO	TiO_2	MgO	FeO	TiO_2	MgO	FeO	TiO_2	MgO	FeO	TiO_2	MgO	FeO
34C	Zoned phenocryst	4.3	23.3	8.6	absent			2.0	6.9	29.5	3.1	22.9	10.6	3.4	14.9	17.5	4.4	5.9	30.7
76A	Zoned phenocryst	6.5	15.3	10.8	6.8	12.1	16.0	n.d.	5.5	32.2	6.4	14.7	10.2	6.5	11.3	16.1	5.6	1.8	30.2
D57	Zoned phenocryst	3.0	22.1	9.2	2.6	11.1	24.0	3.8	7.8	27.4	3.0	21.9	8.9	3.5	10.6	23.4	3.0	8.0	27.6
D56	Zoned phenocryst	5.2	20.1	9.5	absent			n.d.	19.4	12.2	5.8	19.1	9.9	absent			2.2	3.4	25.8
CP41	Phenocryst crossing Ocelli boundary	3.9	25.7	7.8	absent			4.6	9.0	25.4	4.2	23.9	8.1	absent			2.0	10.0	29.2

n. d. = not determined

Microprobe analyses by A. G. Plant.

TABLE 20

Optical Properties and Composition of Kaersutite From Lamprophyres

Specimen	Type	2r	Pleochroism			Y:Z	Na_2O	CaO	FeO
			α	β	γ				
125	Matrix phenocryst (core)	65	brown	red-brown	very dark brown	14°	3.0	12.4	14.7
125	Same crystal (intermediate zone)	n.d.	brown	red-brown	dark brown	14°	2.8	12.4	13.9
125	Same crystal (margin)	73	light brown	pale red-brown	yellow brown	14°	2.9	13.2	13.6
125	Matrix euhedra (core)	n.d.	brown	red-brown	very dark brown	14°	2.8	11.4	13.5
125	Matrix euhedra (rim)	n.d.	light brown	pale red-brown	yellow-brown	14°	3.2	11.7	13.7
125	Ocellus euhedra (core)	65	brown	red-brown	very dark brown	14°	3.5	12.1	15.1
125	Ocellus euhedra (rim)	73	light brown	pale red-brown	yellow-brown	14°	3.4	11.9	20.5

n. d. = not determined

Microprobe analyses by A.G. Plant.

kaersutite phenocrysts have been observed to straddle the boundary between matrix and ocellus. Commonly no change can be seen in the mineral on opposing sides of the boundary, but in one example the part of the mineral in the ocellus is replaced by carbonate and chlorite.

Microprobe analysis of the kaersutites shows that despite strong optical zoning the margins are virtually identical to the core in iron, magnesium and sodium content (Table 20). In the ocelli the rims of the kaersutite are noticeably enriched in iron compared to the matrix kaersutite, but the compositions of the cores are remarkably similar.

Potash feldspar

Potash feldspar is found both in matrix and ocelli in the form of small laths and as minute patches of very fine grained to cryptocrystalline material. Both of these types of feldspar were analyzed by microprobe. The results, given in Table 21, show that the composition of both types of feldspar is very similar, and that the potash feldspar of the ocelli has a similar composition to that of the matrix.

Calcite

The matrix contains tabular crystals of carbonate which appear to be of primary origin. Many of the ocelli in the olivine-bearing lamprophyres are composed mainly of carbonate. Both these types of carbonate were tested by microprobe. The results in Table 21 show that all the carbonate is essentially calcite. However, there is a significantly higher content of magnesium in the ocelli.

Carbonates are found sparingly in the more felsic ocelli, most commonly as a central rounded core of carbonate in the ocellus.

Analcite

Major amounts of analcite are present in both matrix and ocelli of many rocks. However, the analcite occurs in colourless to pale buff masses of very fine grained material riddled with minute grains of contaminants. This habit prevented finding material suitable for probe analyses.

Opaque minerals

There is a strong differentiation of opaque minerals between matrix and ocelli. In the matrix the usual opaque mineral is titano-magnetite, with blades of ilmenite along octahedral planes. This mineral is commonly present in euhedral to subhedral forms, but a considerable amount of fine rodlike material is also present. Small amounts of pyrite are in the matrix, commonly in the form of anhedral interstitial growths. Within the ocelli pyrite is the dominant mineral, forming cubes concentrated in marginal zones of the ocellus. A small amount of magnetite is commonly present, displaying lamellae of ilmenite, in a much more irregular pattern than the matrix material.

Other minerals

Apatite is consistently present in both matrix and ocelli, occasionally forming small veinlets. Plagioclase is exceedingly rare in the matrix.

TABLE 21

Composition of Calcite and Potash Feldspar from Lamprophyres

Specimen	Mineral	Matrix						Ocellus					
		Na$_2$O	K$_2$O	CaO	Ab	Or	An	Na$_2$O	K$_2$O	CaO	Ab	Or	An
125A	Feldspar lath	2.5	11.9	<0.1	21.2	70.5	--	2.2	12.0	0.2	18.7	72.3	1.0
125A	Cryptocrystalline feldspar	3.1	12.3	0.1	26.3	72.7	0.5	2.6	11.0	0.3	22.1	65.3	1.4

Specimen	Mineral	CaO	MgO	CaCO$_3$	MgCO$_3$	CaO	MgO	CaCO$_3$	MgCO$_3$
76A	Tabular calcite	55.9	<0.1	99.6	0.2	54.0	1.2	96.3	2.5
34C	Tabular calcite	52.8	0.3	94.3	0.6	50.3	1.3	89.9	2.7

Microprobe analyses by A. G. Plant.

Figure 22. Fractionated ocellus. Light upper portion is rich in pot-
ash feldspar, the lower portion is rich in kaersutite (grey)
and biotite (dark) which are concentrated along the lower
border. (x5, crossed nicols) (G.S.C. photo 201290-R)

Albite is occasionally found in feldspar-rich ocelli. Celestite and quartz were
seen in the ocelli, one specimen concentrated in a small central core.
Fractionated ocelli are common. In the kaersutite lamprophyre
density layering is shown by a concentration of kaersutite and biotite set in a
cryptocrystalline mixture of K-feldspar in the lower half, grading into a roof
zone of pure K-feldspar (Fig. 22). At times the minerals in the ocelli dis-
play a concentric pattern (Fig. 23), usually involving a combination of no more
than three of the minerals calcite, dolomite, analcite, plagioclase and
K-feldspar. There is no overall pattern to the concentric distribution of the
minerals in these ocelli, although within any one rock the pattern is constant.
Opaque minerals are usually concentrated in the margins. Within one rock
the individual ocelli generally have the same minerals but the relative quan-
tities show marked variations from ocellus to ocellus. This variation may,
in part, be due to the thin section having been cut obliquely to segregated ocelli.
The clinopyroxenes, biotite, and kaersutite in the ocelli and in
juxtaposed parts of the matrix are usually arranged concentrically, becoming
tangential towards the sides of the ocelli though frequently straddling the bound-
ary. Both the phenocrystal variety of clinopyroxene and the small nonpleo-
chroic prisms transgress this boundary and are not wholly contained within
the ocelli (Fig. 25). At times the biotite flakes in the ocelli appear to be trun-
cated at the contact with the matrix material. The coloured minerals are

Figure 23. Concentrically zoned ocellus, with calcite core, and
dolomite + K-spar rim. (x10, crossed nicols)
(G.S.C. photo 201290-B)

absent from the central parts of the analcite- and carbonate-rich ocelli and
have only limited distribution in the marginal parts. However, within the
same rock those ocelli that are poor in analcite and carbonate display a regu-
lar distribution of the coloured minerals throughout the ocelli. A prismatic
kaersutite that straddles the boundary between matrix and an analcite-rich
ocellus is pseudomorphed within the ocellus by a mixture of calcite, analcite
and opaque(s) (Fig. 36). The biotite in the matrix has developed a poikilitic
texture due to pyroxene inclusions contrasting with those in the ocelli which
are free of these inclusions. Furthermore, the biotites in the ocelli of sev-
eral lamprophyres show bending and fracturing in contrast to the underformed
flakes in the matrix.

Where ocelli coalesce, mineralogical differences are usually pres-
ent in the juxtaposed ocelli. In specimen 76A, two ocelli have an interpene-
trative structure; this has resulted in a narrow, discontinuous double-walled
ellipsoidal body. The outer or earlier ocellus contrasts with the inner or
later one in that, besides the calcite which is common to both, the former has
biotite and the latter quartz plus minor celestite. A concentration of opaque(s)
delimits the boundary between the two ocelli. In specimen D56, five ocelli
appear to have coalesced (Fig. 24). The outer four are only partially pre-
served, contrasting with the latest ocellus which is nearly spherical and trun-
cates the others. The outer four produce cuspate margins where they inter-
sect. In addition to the analcite and minor carbonate and K-feldspar common
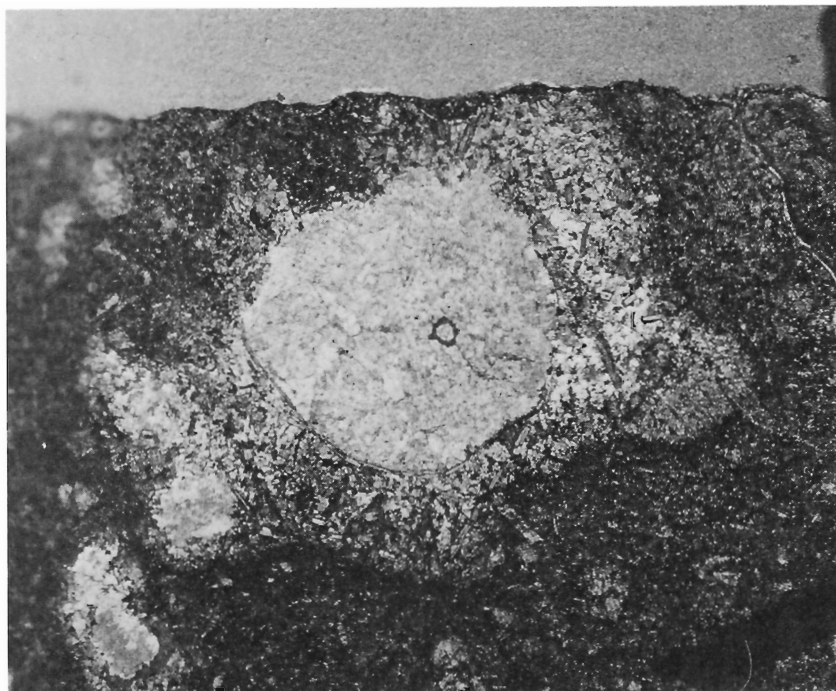
Figure 24. Five or six ocelli coalesced around a central, younger
          ocellus. Note septa separating parts. (x10, crossed
          nicols) (G.S.C. photo 201290-P)

to all of the ocelli, the outer four contain abundant clinopyroxene, biotite and
sericite; these minerals are absent in the later spherical ocellus other than
where they define the boundary. A striking aspect of the lamprophyres that
contain coalescing ocelli is the frequent presence of veins and lenses of pot-
ash feldspar and carbonates ranging in width from 1 to 5 millimetres and up
to 5 centimetres long. These veins and lenses reflect the identical composi-
tion of the ocelli in the rock and, where the ocelli are fractionated, display
the identical zonation.

          In most of the lamprophyres, ocelli are accompanied by pseudo-
morphs of olivine and/or clinopyroxene. The euhedral to subhedral outlines
of the pseudomorphs clearly distinguish them from the near spherical to glob-
ular ocelli. Opaques are dominant in the pseudomorphs whereas the presence
of biotite, kaersutite and fine clinopyroxene needles characterize the ocelli.
In addition, the ocelli can be fractionated. Contrasting further with the ocelli,
the pseudomorphs offer no textural disparity with juxtaposed matrix minerals.

Chemical composition

          Seven analyses of lamprophyres are compiled in Table 22. It can
readily be seen that their chemistry is as unusual as their petrography. The
olivine-bearing types all contain relatively large amounts of CO_2 and water,
whereas the content of these elements in the kaersutite-bearing lamprophyres

- 63 -

TABLE 22

Chemical Composition of Lamprophyres and Coexisting Ocelli From the Callander Bay Complex

	1(a)	1( )	1(c)	2(a)	2(b)	2(c)	3(a)	3(b)	3(c)	37B	56D	BHI-542	6A
SiO_2	37.71	39.40	17.43	34.86	36.34	25.00	40.26	53.6	38.96	50.35	37.85	39.46	37.71
TiO_2	4.10	4.35	1.12	4.62	5.11	0.11	3.95	0.7	4.27	--	3.54	3.84	3.90
Al_2O_3	7.69	8.91	nil	7.61	7.62	7.60	15.48	21.6	14	17.12	10.26	11.57	11.02
Fe_2O_3	4.83	5.84}	9.49	1.84	2.71}	1.61	6.23}	4.1}	13.46	2.07	6.77	4.76	5.39
FeO	7.67	8.05}		9.76	10.06}		6.56}			5.96	7.38	7.38	6.52
MgO	8.63	8.81	6.12	8.13	8.92	0.92	5.29	2.2	5.60	2.62	10.35	8.31	8.46
CaO	14.20	12.72	31.20	14.41	14.08	20.62	10.28	1.3	11.66	4.76	12.77	12.16	13.51
MnO	0.13	0.15	nil	0.17	0.17	0.17	0.23	n.d.	--	0.15	0.15	0.18	0.26
Na_2O	0.81	0.93	nil	0.42	0.52	nil	2.52	2.1	2.58	5.73	1.69	2.51	1.83
K_2O	2.86	3.08	0.62	3.51	3.13	8.15	3.69	10.2	3.05	3.43	2.97	3.75	3.31
H_2O	4.63	4.61	4.60	2.73	2.71	2.70	3.68			1.47	4.16	2.47	3.07
CO_2	4.86	2.88	27.81	10.16	8.10	32.20	1.20}	4.1*}	5.66	2.94	3.07	3.86	4.02
P_2O_5	1.61	1.61	1.61	1.09	1.12	0.92	0.63			1.10	0.91	0.96	1.08
Total	99.69	101.42	100.00	99.33	100.69	100.00	100.00	99.8	100.00	99.74	101.21	101.17	100.02

n.d. = not determined
* - loss on ignition
1(a) – olivine lamprophyre, 76A
1(b) – olivine lamprophyre, 76A, less ocelli constituting 7.9 per cent of volume
1(c) – computed composition of ocelli in specimen 76A (total iron computed as FeO)
2(a) – olivine lamprophyre, 34C
2(b) – olivine lamprophyre, 34C, less ocelli constituting 9.8 per cent of volume
2(c) – computed composition of ocelli in specimen 34C
3(a) – kaersutite lamprophyre, 125A
3(b) – ocelli from specimen 125A (electron microprobe analysis by G.R. Lachance)
3(c) – matrix of specimen 125A (rock analysis less 8.9 per cent of ocelli)
37B – dark, coloured, fine grained ocellar dyke
56D – olivine lamprophyre
BHI-542 – olivine and kaersutite free lamprophyre
6A – olivine lamprophyre

Analyses by Rapid Methods Group, Geological Survey of Canada, directed by S. Courville.
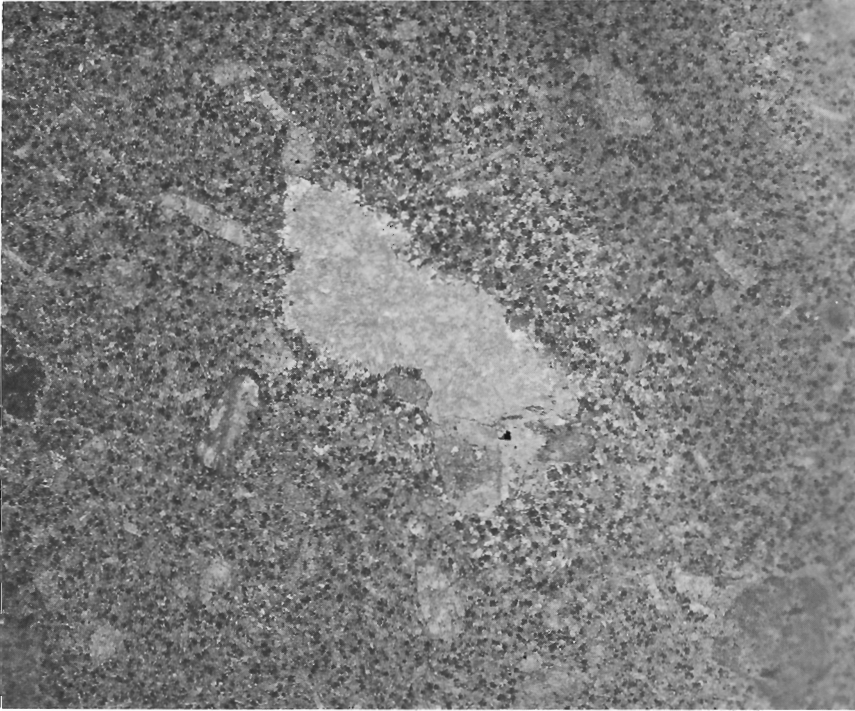
Figure 25. Irregular ocellus with three stubby clinopyroxene crys-
            tals straddling the boundary. (x10, crossed nicols)
            (G.S.C. photo 201290-K)

is very much smaller. All have high to extreme titania contents, high total
iron content, and very high iron to magnesium ratios for such ultrabasic rocks.
The content of alkalis is extreme for ultrabasic rocks.

Structure and contact relations

          Both the phenocrysts and ocelli tend to define a planarism in the
rock which parallels the margins of the intrusives. The prismatic pheno-
crysts indicate planarism by their elongate alignment whereas the more equant
olivine pseudomorphs and ocelli tend to concentrate in zones that parallel the
margins. Furthermore the planarism defined by the ocelli is exaggerated by
their progressive size increase towards the centre of the intrusive. In intru-
sives less than 30 centimetres wide the range in diameter of the ocelli is 0.5
to 2.0 millimetres whereas across a 1.6-metre-wide lamprophyre this range
is 0.05 to 2.50 centimetres. A further planarism is also produced by tex-
tural changes in zones 0.5 to 1.0 centimetre-wide, involving a fine- and
coarse-grained facies. These zones normally parallel the margins of the
intrusives but in very limited cases appear in random swirls. Commonly
this zonation produced a very strong lamination in the dyke (Fig. 20). The
fine-grained zones offer further textural contrasts in that there is a general
absence of ocelli within these zones and a concentration of them marginal to
these zones. The phenocrysts also offer a marked contrast by varying from

Figure 26. Zoned lamprophyre dyke, with a thin carbonate margin (white).
(G.S.C. photo 201305-H)

1.0 to 10.0 millimetres in diameter in the coarser grained facies and from 0.3 to 1.0 millimetre in the finer grained facies. Very infrequently the clinopyroxene phenocrysts are aligned at right angles to the margins of the internally occurring finer grained zones. There is an imperceptible decrease in grain size towards the margins of some lamprophyres occurring over a width of 1 to 4 millimetres. Ocelli are absent from these chill margins. The infrequent country rock inclusions and screens in the lamprophyres also produce a planar fabric as in most cases they parallel the margins of the intrusives (Fig. 20).

The contacts of the dykes are extremely sharp. A common feature of the lamprophyres is the presence of hematite-stained, lensoid carbonate margins 1 to 12 centimetres (commonly 1 to 3 cm) in width (Fig. 26). In some instances the carbonate is confined to one margin only, in others the margin can be traced as a transgressive vein into the country rock or lamprophyre. Brecciation is frequently associated with these carbonate margins. In three separate occurrences lamprophyre intrusives gradational into carbonatite were observed. In addition to these massive carbonates associated with the lamprophyres carbonatization has also taken place, commonly along
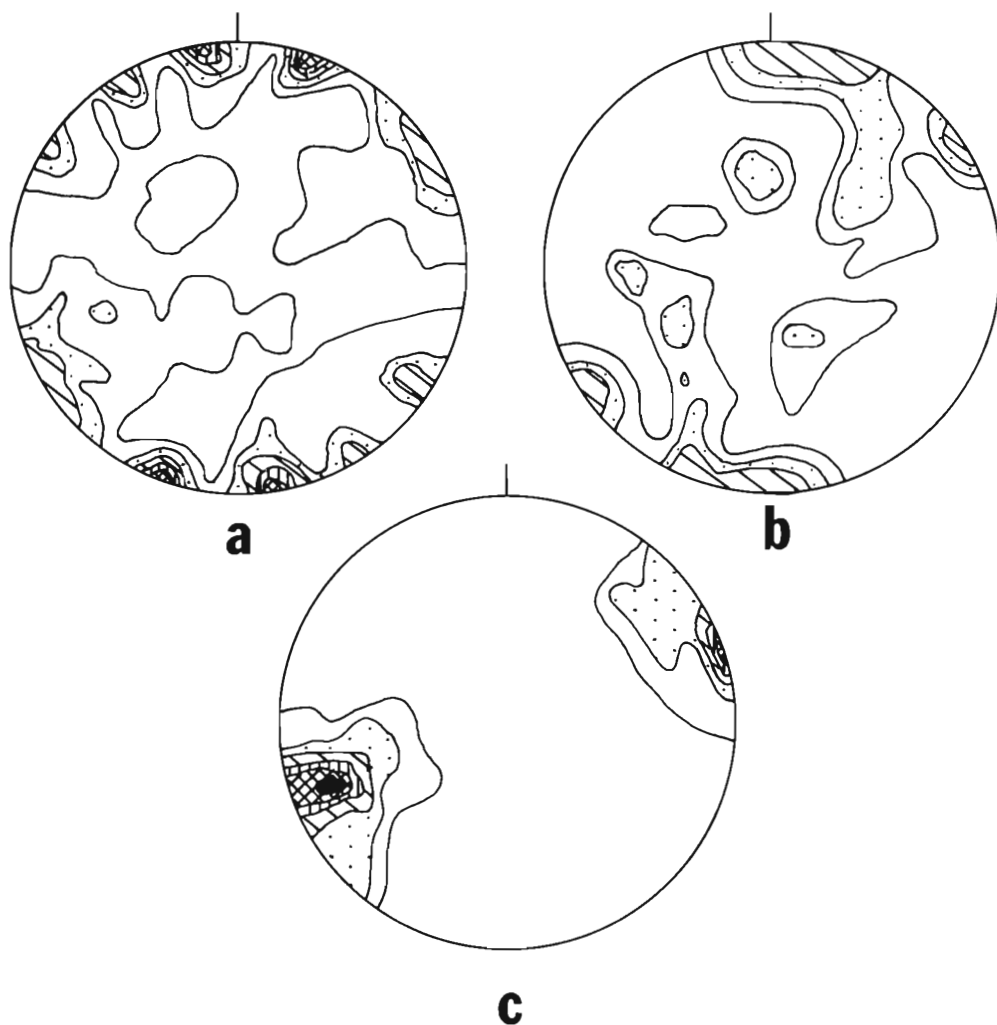
Figure 27. Stereograms showing orientation of joints, dykes and gneissosity.
(a) Stereographic projection of 87 poles to join planes, contours
drawn to represent concentrations of 2, 4, 6, 8, and 10 per cent
of poles per 1 per cent area of projection sphere. (b) Stereogra-
phic projection of 76 poles to planar dykes, contours same as (a).
(c) Stereographic projection of 197 poles to gneissosity, contours
at 4, 8, 12, 16, 20, 24 per cent.
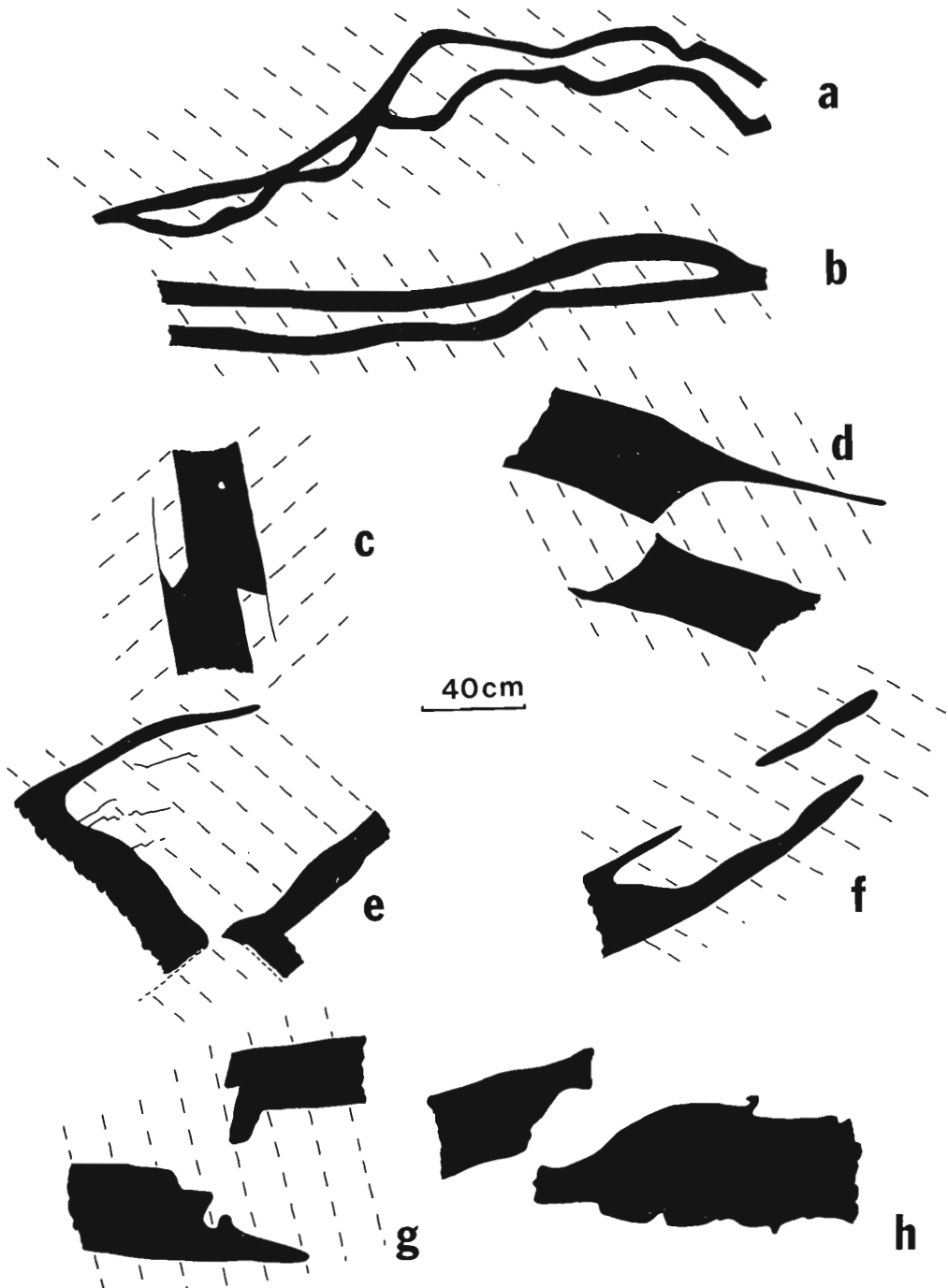
Figure 28. Geometric forms of lamprophyre dykes. All examples are traced from photographs. The dashed lines represent the trend of gneissosity in country rock. The host rock in 2 h. is massive.

Figure 29. Complexly anastamosing lamprophyre. Note the rounded character of the country rock screens. (G.S.C. photo 201305-C)

Figure 30. Rheomorphically veined lamprophyre. (G.S.C. photo 201305-K)
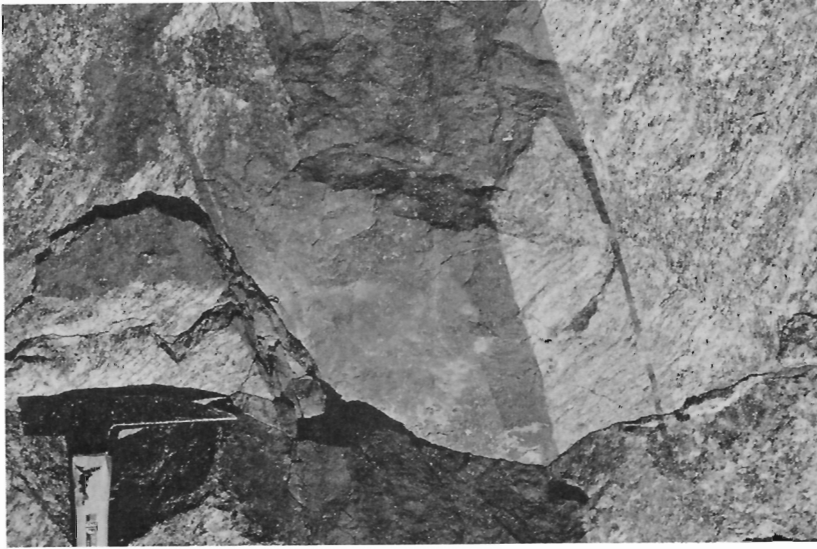
Figure 31. Typical 'horned' offset lamprophyre dyke. (G.S.C. photo 201305-A)

the margin in a 1 to 4-millimetre-wide zone where complete pseudomorphic replacement of the minerals has taken place. This alteration is not always confined to the marginal parts, but was also noted occurring as en echelon veins 0.3 to 0.5 centimetre wide, and as radiating veinlets at high angles to the margins of the lamprophyres. In the country rocks surrounding the dykes, alteration either chemical or thermal is minimal. Some of the dykes are accompanied by low-grade fenitization haloes producing a zone a few centimetres wide which is hematitized, and commonly contains aegerine. Other haloes are partially bleached. Very rarely, the largest dykes are rheomorphically veined by stringers of country rock 2-3 millimetres wide, and up to 15 centimetres long. No bending of the gneissosity of the country rocks against the dykes was observed. Many of the dykes cut cleanly across the country rocks, producing no detectable alteration, and no mechanical deformation; rarely small side rheomorphic back-veining is present (Fig. 30).

A study of the attitudes of the dykes shows that they follow the trend of regional joint sets (Fig. 27). Northwest-trending dykes, however, were not observed, although a prominent joint set trends in this direction. Whether this is an accident of exposure, or a real feature is unknown. Although the dykes appear to follow joints with some precision they do not have the planar appearance of joints and characteristically show a sinuosity, both in plan and section. A striking feature of the dykes is their variability in geometric form. Many of the larger dykes are almost planar in form, but even these commonly bifurcate abruptly, and send off many small apophyses. Smaller dykes show a great variety of forms (some of which are illustrated in Fig. 28) ranging from bifurcation with thin screens of undisturbed country rock separating the two parts (Fig. 28a, b) to complex anastamosing (Fig. 29). Small dykes are characteristically lenticular both in plan and section. Dykes pinch out entirely only to reappear further along the strike (Fig. 28f) forming a series of lenticular pods. Peculiar offsets occur in these dykes. Figure 31 shows a typical example. The dyke is apparently dextrally offset about 10 centimetres along

a plane almost perpendicular to the dyke. However, examination of the gneiss-
osity of the surrounding country rocks reveals no sign of a fracture of this
plane, nor does the dyke display any signs of fracturing. Further evidence
that the offset is not tectonic is provided by the thin "horns" projecting from
the outer edge of each part of the dyke across the line of offset. The internal
zoning of the dyke can be seen to continue into these projections which form
an extension of the marginal zone of the dyke. Other examples of this com-
mon type of offset are shown in Figure 28. In the latter case geniculate 'mini-
dykes', a fraction of a centimetre in width, have formed along conjugate joint
sets opened up in the embayment within the horns. On close examination we
were unable to find any connection between these small dykelets and the main
dykes.

Although offsets of the horn type are common, they are small, and
do not exceed the width of the dyke. A small screen of rock a few millime-
tres wide may separate the two parts but commonly the offset parts are in
contact. Larger offsets also occur, but the character of the ends of the dykes
is rather different. Examples are shown in Figure 28f and 28g. The ends of
the dyke are 'globby' and amoeboid, with many small, rounded lobate protru-
sions, and brownish, very fine grained margins. Such characters may extend
from the end of the dyke several dyke widths back along the dyke.

The mechanism of intrusion of lamprophyre dykes

The presence of offset dykes does not by itself indicate any par-
ticularly unusual conditions of emplacement. Many years ago Harker (1904)
figured such dykes and considered that they are the result of intrusion either
along a stepped fracture, or to the coalescence of dykes emplaced along sep-
arate, but close, parallel fractures. More recently Kaitaro (1953) has explained
how a single shear fracture could split up, causing a planar dyke to pass into
a stepped dyke. A consideration of the features of the dykes in question shows
that these explanations are inadequate.

Examination of the form of the dykes, together with the lack of
offset in the country rocks shows that room for intrusion of the dykes must
have been made by a slight movement perpendicular to the plane of the dyke
along a steeped fracture. In other words the dyke could not arrive at the plane
of the offset without some opening up of the rock as diagramed in Figure 32.
If this cross fracture is opened prior to the arrival of the magma, it is impos-
sible to intrude the horns, instead of pushing the magma down the open channel.

An understanding of the force of this objection is obtained by con-
sidering a simplified model of dyke intrusion. Consider any point along a
propagating dyke. The pressure head in the liquid must be sufficient to push
the magma along the fissure, and in some cases to generate the fissure itself.
The propagation of the dyke will cease either when the pressure head falls
below the value necessary for it to continue, or when the dyke solidified. If
we consider a fluid of viscosity z, the pressure head necessary for a plane
sheet to advance in laminar flow with velocity u is (Sommerfeld, 1950)

$$u = (a^2/12z)(dP/dl) \tag{1}$$

where a is the width of the sheet, and dP/dl the rate of pressure drop along
the dyke.

During intrusion the dyke is continuously losing heat to its walls,
causing solidification to proceed from the walls inward. This problem has
been considered by Jaeger (1957) who finds that, assuming the relevant
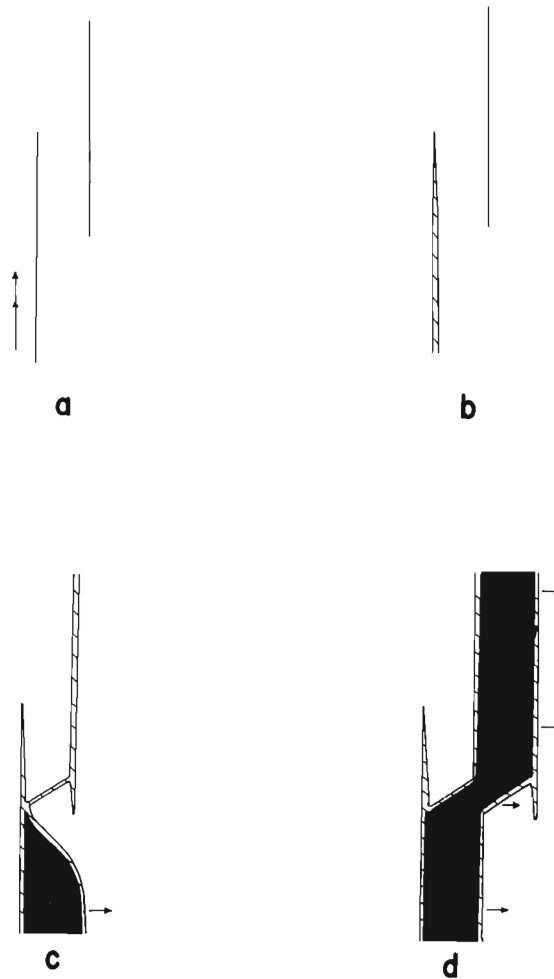
Figure 32. Schematic representation of the emplacement of an offset lampro-
phyre dyke. (a) Assumed initial configuration of two closed par-
allel fissures in the rock. The double headed arrow represents
the direction of advance of the magma. (b) Injection of low-viscosity,
high velocity, volatile-rich material boiled off the magma (hachured
pattern). (c) Emplacement of magma (solid black). Bending
strains have opened up a fissure joining the original fissure to a
parallel one. Volatile-rich material has escaped into this newly
opened fissure. The direction of dilation of the rock due to advance
of the magma is represented by the short arrow. (d) Final con-
figuration of offset after further advance of magma down the chan-
nel. The arrows show the direction of dilation of the wall-rocks
necessary for emplacement of magma.

thermal properties of the country rocks to be the same as those of the solidified dyke rocks

$$X = 2\lambda(Kt)^{1/2} \qquad (2)$$

where X is the distance in centimetres that complete crystallization has proceeded inward from the walls in time t, K is the thermal diffusivity, and λ a parameter derived from the latent heat of crystallization of the magma through a complex equation. Values of λ are tabulated by Jaeger (1957) for a wide range of conditions.

Noting that solidification of a dyke will be complete when X = a/2, substituting this value in (2), and rewriting

$$t = a^2/16\lambda^2 K \qquad (3)$$

where t is the time required for complete solidification of the dyke. Now if the magma advances with velocity u for time t, the length of the dyke will be u.t. In a real case the length would be less than this since viscosity increases rapidly as solidification proceeds, and the effective value of a decreases. The maximum length of a dyke is therefore

$$l = u.t. = \frac{a^4}{192\lambda^2 Kz} (dP/dl) \qquad (4)$$

and the length to width ratio of this dyke is

$$l/a = \frac{a^3}{192\lambda^2 Kz} (dP/dl) \qquad (4a)$$

Experimental data are available for the parameters of this equation. Jaeger tabulates values of λ for latent heat contents of 80 and 100 calories per gram. Tabulations by Robie and Waldbaum (1968) suggest the lamprophyric magma of composition 10 per cent olivine, 60 per cent clinopyroxene, and 30 per cent mica would have a latent heat of crystallization of about 65 calories per gram. We adopt the value of 80 calories per gram, noting that it is probably too high, giving minimum values to λ and maximum values to 1/a. The local presence of rheomorphic veining shows that where the magma directly contacted country rocks, the melting temperature of the latter was exceeded. From the data of Winkler (1967) this melting temperature can hardly have been less than 650°C. Examining the tables of Jaeger we find that this implies minimum magma temperature of 1,100°C, showing that the magma did not lie in the region of low temperature ultrabasic fluids discovered by Seifert and Schreyer (1966). These high magma temperatures also show that the magma cannot have been directly in contact with the wall-rocks for considerable periods otherwise more extensive rheomorphism would have resulted. Since textural evidence suggests the magma was crystallizing all its major minerals at the time of intrusion, it seems probable the crystallization interval was not unduly large. With these facts in mind we select a value of $\lambda = 0.40$, equivalent to a magma intruded at 1,100°C solidifying at 950°C.

For the thermal diffusivity K, we adopt Jaeger's (1957) value of 0.0071, corresponding to a rock density of 2.85, a thermal conductivity of 0.005 calories/centimetre^2-second, and a heat content of 0.25 calories per gram.

The visocity of natural rock melts ranges from 15- 37,900 poise (Clark, 1966). For natural lava flows, no values are less than 4,000 poise. Viscosity values are extremely dependent on temperature. However, for abyssal or hypabyssal conditions they may be appreciably lowered by high volatile content. We therefore adopt a value of 3,000 poise. Since the Reynolds number, $dua/2z$, for a planar flow of depth $a/2$ is about 330 (Sommerfeld, 1950, p. 121), it follows that for this viscosity, and an assumed magma density d, of 2.75 grams per cubic centimetre, the flow will be laminar, not turbulent, up to velocities of 2,000 centimetres/second for dykes 2 metres wide. It follows that all the observed dykes in the Callander Bay area were intruded in laminar flow, and equation (1) is justified.

Values of the pressure gradient around an intrusion are poorly known. If the surroundings are treated as elastic and the overpressure is P_o, then from elastic theory the value of the overpressure at a distance r from the centre of a cylindrical intrusion of radius r_i is

$$P_o = (r_i/r)^2 \, P$$

and the pressure gradient is $(-2P \, r_i^2/r^3)$. The radius of the Callander Bay intrusion is roughly 1 kilometre (0.6 mile), and the site of the observed offsets is about 2 kilometres (1.2 miles) from the centre. The maximum overpressure of the intrusion cannot exceed the cohesive strength of the rock, which is about 500 bars (Handin in Clark, 1966). It follows that the pressure gradient at the site of the horns cannot exceed about 125 bars per kilometre, or 12.5 dynes/centimetre^3. Adopting the values $\lambda = 0.40$, $K = 0.0071$, $z = 3,000$, $dP/dl = 12.53$, equation (4a) becomes

$$1/a = 0.0192 \, a^3 \tag{5}$$

for a dyke 1 metre in width, $1/a$ would be 19,200, and the possible length of the dyke 19.2 kilometres (11.9 miles). The authors know of no dyke of this width with such a length. Even with a pressure gradient of 12.5 bars per kilometre, this dyke could reach a length of 1.92 kilometres. From these estimates it is plain that the considerations of this section impose no serious limitation on the lengths of large dykes, which could be many kilometres, even with very low pressure gradients. For a dyke 10 centimetres wide, however, the maximum length according to (5) would be only 1,920 centimetres. A dyke 1 centimetre wide could hardly be intruded at all! No plausible selection of parameters can increase the length to width ratio of a 1 centimetre-wide dyke even to a value of 1. Since observed 1 centimetre-wide horns, have elongations of 30-40:1, they must therefore have formed by some other mechanism.

We have presented petrographic and chemical evidence showing the dykes to be remarkably rich in water and carbon dioxide. We have shown that a pressure head must exist along the length of an intruding dyke. If the magma is initially saturated with volatiles as suggested by bleaching and fenitization effects in the country rocks, and by carbonate margins along the dykes, such a drop in pressure at constant temperature must result in the boiling off of a volatile phase. This volatile phase would rush down the fissure until arrested by the end of the channel, resulting in abrupt adiabatic cooling, and chilling of any silicate liquid droplets entrained in the fluid as well as solidifying a thin, devolatilized layer on the front of the advancing

magma, which protects the fresh magma beneath. Behind this initial explosive burst the water-saturated magma would advance through a fissure partially opened and cleared of obstruction. As the magma advanced, if the fluid phase was unable to escape, it would be reheated and redissolved in the magma, producing a water-saturated magma at considerably higher water pressure than that remaining after the initial devolatilization. As we have noted from the offset shape of the dykes, the magma advanced to the end of the fissure without either causing, or taking advantage of a cross-fracture. When this occurs a further explosive degassing along the cross-fracture, and into the connecting fracture will take place. The whole process can obviously be repeated until sufficient water is lost to the wall-rocks so that explosive degassing no longer occurs, or until heat losses are sufficient that solidification occurs. The process is diagrammatically represented in Figure 32.

According to this hypothesis offsets are formed as follows. A water-saturated magma is introduced into a fissure. The pressure drop necessary for intrusion results in boiling off of a fluid phase at the leading edge of the magma, which fills the fissure to its farthest extremity. This fluid phase contains within it a small proportion of dissolved silicates, and if the boiling off is violent, droplets of silicate melt may be entrained during this process. The adiabatic quenching results in formation of a thin layer of chilled silicate material along the margin of the magma, and, if the gases are rich in CO_2, in the formation of carbonates in the fissure. Since the viscosities of H_2O-CO_2 mixtures are one millionth or less those of silicate melts, the boiled off gases may be expected to penetrate very small cracks for long distances. The further the phase spreads, the greater the pressure drop, and the lower the content of silicates it can hold in solution. The material precipitated, will presumably be deposited on the walls of the fissure. The tiny apophyses at the ends of the fissures might therefore be expected to be composed mainly of carbonates. After the rapid emplacement of the volatile phase, the magma, now reduced in volatile content, advances in accordance with equation (3). As we have seen the distance this magma can advance is strictly limited by its width. If the viscosity of the magma is one million times greater than that of the volatile phase, then from equation (3), the dyke must be one hundred times as wide as the fissure followed by the volatiles, if it is to advance the same distance. During this advance the dyke will trap the volatile phase in the fissure, if the fissure is gas tight, and will accumulate volatiles from the wall-rocks by the diffusion mechanism noted by Bradshaw and Sanchez (1969) if it is not. In either case the volatile pressure in the magma will rise as it approaches the end of the fissure. This rise together with the mechanical strains resulting from widening the fissure by a factor of 100, will produce fracturing. The rocks surrounding the advancing tip of the dyke are subjected to bending strains due to intrusion. Such strains must increase rapidly as the tip of the fissure is approached. If it is assumed that the tip of the fissure is welded, then fracturing will occur at a high angle to the dyke due to bending. If such a fracture intersects a fracture parallel to the original one, an offset may develop by repetition of the mechanism of intrusion outlined above. Since it is improbable that a cross-fracture will intersect another fracture precisely at its termination the initial inrush of volatiles will spread out in both directions in the new fissure. As we have noted, the dyke cannot propagate across the offset unless dilation along a geniculate fracture occurs. This dilation leaves one end of the new fissure as an inactive relict, preserving the 'horn' formed by the volatile emplacement while the magma advances in the other direction.

Finally we may note that the cross-fracture is of finite extent in the direction in the plane of the dyke, perpendicular to dyke propagation. Some parts of the original dyke may extend beyond the ends of the cross-fracture. At these points gas pressure will build up, and be only slowly (if at all) released by further intrusion. At moderate depths the temperature of the magma combined with high water pressure will eventually be sufficient to melt the wall-rocks, as shown by the local rheomorphic back-veining. If the lamprophyric melt and a melt of the syenitic wall-rocks are immiscible, as suggested by the presence of syenitic ocelli in the dyke, rheomorphic melting of this kind may be expected to give rise to lobate amoeboid dyke ends. We therefore explain the offsets of type of Figure 28, as extensions of offsets of ordinary type beyond the ends of the cross-fracture.

According to our analysis the presence of 'horned' offsets in dykes is due to a high content of volatiles in the magma which can be boiled off and redissolved due to pressure changes. Since carbon dioxide is very sparingly soluble in magmas, it probably plays little direct part, but it undoubtedly adds to the intrusive energy available, and to the efficiency of the adiabatic quenching part of the process. The key role of water in the process is attested by the universal high water content in dykes with observed offsets of this type (Watterson, 1968; Kaitaro, 1953; Hurlbut, 1939). The chemistry of the dykes varies greatly in other respects but water must be present. Its role is to create a low viscosity, high velocity precursor of the magma which opens a channel, and improves the thermal efficiency of intrusion by providing a marginal heat shield. This precursor can be partly recovered by the magma, but it leaves a relict in the horns of the offsets.

Age

Two samples of fine-grained lamprophyre dykes were used for K-Ar age determinations by M. Shafiqullah. They returned ages of 558 $\pm$ 14 m.y. These are identical to the age of 560 m.y. obtained by Lowdon et al. (1963) from the Manitou Island complex, 12 kilometres (7.5 miles) northwest of Callander, and the age of 566 m.y. obtained by Shafiqullah et al. (1968) from lamprophyre dykes in the Brent crater, 60 kilometres (37.2 miles) to the east. These ages demonstrate the existence of an extensive alkaline igneous province.

Origin of the ocelli

We shall consider the origin of the lamprophyre dykes in relation to the other parts of the alkaline complex in the following chapter. This relation depends critically on the view taken of the nature and origin of the ocelli.

We have shown that the ocelli are composed of the same minerals as the matrix of the rock (less olivine). They form bounded, coarse-grained aggregations, differentiated by their radically differing proportions of minerals. They are not found in chill zones but increase in size toward the centre of the dyke and with the size of the dyke. Minerals within the ocelli tend to be arranged in concentric zones, but large crystals may cross the boundary of the ocellus into the matrix. What process can produce a mineral segregation with these characteristics?

We shall discuss below other examples of ocelli, but here we merely summarize varying explanations which have been offered for their origin.

These may be summarized as (1) amygdales (Flett, 1935; Campbell and Shenk, 1950; Horne and Thompson, 1967; Watterson, 1968), (2) late-stage pegmatitic segregations (Dunham, 1933; Knopf, 1936; Simpson, 1954; Ramsay, 1955), (3) nucleation centres for leucocratic minerals (Evans, 1901; Smith, 1946), (4) immiscible liquid droplets (Flett, 1900; Tomkeieff, 1942, 1952; Drever, 1960; Upton, 1965; von Eckermann, 1966; Philpotts and Hodgson, 1968). We shall discuss these hypotheses in order.

The description of these objects as amygdales does not withstand examination. The minerals of the ocelli are almost identical to those of the matrix and show similar zoning. To suppose that these zoned pyroxenes and kaersutites grew from late-stage, relatively low temperature hydrous liquids after consolidation of the host rock is unreasonable. The identity of mineral composition between the ocelli and matrix show that the ocelli grew in equilibrium with the same liquid that produced the matrix. The amygdale 'explanation' does draw attention, however, to the volatile-rich character of the ocelli.

If the ocelli are late-stage pegmatitic segregations, it is difficult to understand the sharpness of their boundaries. Most late-stage segregations, unless they have been mobilized and intrude their host, have diffuse boundaries. However, a much more direct and decisive argument against this origin is the zoning present in both matrix and ocelli minerals. In many of the matrices, a nonpleochroic diopsidic pyroxene was the earliest pyroxene to crystallize. An identical pyroxene is present in apparent equilibrium in many of the ocelli. Similarly the core zones of kaersutite and biotite in the matrix are also present in the ocelli. From these considerations it is plain that crystallization of the ocelli, while post-dating that of olivine and the early pleochroic pyroxene of the matrix, was continuing through much of the crystallization interval of the matrix. They are clearly not late crystallization products.

The concept of nucleation centres apparently is based on the assumption that the leucocratic minerals of the ocelli have difficulty in nucleating from the melt. Hence when a nucleus is formed, leucocratic minerals will tend to grow on it, forming clumps of minerals, instead of being evenly distributed through the matrix. This idea is refuted by the evidence. Both calcite and potash feldspar occur as small well formed euhedra distributed throughout both matrix and ocelli, and in the former case there is no sign of a tendency of other leucocratic minerals to clump about them. Zeolites have a somewhat patchy distribution, but they occur in similar habit in both matrix and ocelli.

It has not been suggested in the literature that ocelli might be incompletely assimilated inclusions, but this idea is suggested by the appearance of some outcrops.

If the ocelli are supposed to be inclusions, the zonation of the minerals and the shape of the ocelli pose difficulties. In order for the zoned minerals to be present we must suppose that the inclusions were acquired at a very early stage, and softened sufficiently for the phenocrysts to grow into the plastic inclusions, and for some of the inclusions to coalesce with each other. Conversely the inclusions could not be so assimilated as to lose their sharp edges and disappear in the matrix. The only obvious way in which this can be accomplished is to have the inclusions resist assimilation, even after softening, in other words to be immiscible. The same point was made by Holgate (1954) with regard to certain xenoliths in basaltic rocks. Further, many undoubted inclusions of country rock can be seen in the lamprophyres

(Fig. 24). They are commonly angular, preserve the original gneissosity, and appear little altered, both in hand specimen and in thin section. Commonly they are surrounded by a pronounced brownish rim of carbonate material, which is never seen on ocelli.

Finally we may consider the hypothesis that the ocelli are immiscible droplets. According to this idea, an originally homogeneous magma splits up during cooling into two or more immiscible parts. During further crystallization the liquids will mutually change in composition, as minerals are crystallized until one of the liquids disappears after which the remaining portions continue to crystallize. An example of possible geological significance is provided by silicate-carbonate systems (Koster van Groos and Wyllie, 1966) and in the system fayalite-leucite-silica (Roedder, 1954).

In the latter case, if the crystallization path enters the two-liquid field from the fayalite side, fayalite will crystallize until one of the liquids is used up. Applying this concept to the Callander Bay dykes, one might suppose that after the crystallization of olivine and of an early pleochroic pyroxene was completed, immiscibility set in. When the liquid reached a critical composition droplets of a second immiscible liquid began to form in it. Minerals which were crystallizing in each liquid were necessarily in equilibrium with the other. Any changes of composition of minerals in one liquid were therefore faithfully reflected in the other liquid. When the more basic matrix had completely crystallized, liquid still remained in the ocelli, and continued to crystallize through some further temperature interval. In this interval the liquid in the ocelli was not in equilibrium with earlier formed crystals, either in the ocelli or in the matrix. If equilibrium is maintained reaction between this liquid and earlier formed crystals must occur. This may account for pseudomorphic replacement of one large prism of kaersutite by analcite in the central part of an analcite-rich ocellus, while the portion of the phenocrysts outside the ocellus is unaffected (Fig. 35).

Liquid immiscibility can explain the presence of sharply bounded ocelli of minerals identical to those in the matrix. The absence of ocelli in chilled margins, and their increase in size toward the centre of dykes can be explained by gradually increasing periods at temperatures high enough for nucleation and coalescence of liquid drops to take place.

The Callander Bay dykes contain two types of ocelli, carbonate-rich ocelli in olivine lamprophyre, and potash feldspar-zeolite-rich ocelli in kaersutite lamprophyre. This suggests two periods of liquid immiscibility. According to this hypothesis, the original magma was an olivine-rich lamprophyre. When olivine finished crystallizing, the magma became unstable and split into carbonate-rich and silicate-rich portions. Much of the magma was quenched at this point, forming olivine-lamprophyres with carbonate ocelli. The rest liquid expelled the carbonate fraction, and lost the phenocrystic olivine, perhaps by crystal settling. The residual liquid began to crystallize kaersutite. A second period of immiscibility caused division of the magma into a basic fraction and a feldspar-zeolite rich 'syenitic' fraction.

Experimental investigations

According to the above hypothesis, every lamprophyre dyke bearing ocelli represents the chilled remains of two immiscible liquids, from which has been subtracted a certain amount of volatile material lost to the wall-rocks. If this volatile material were added to the rock in correct

- 78 -

TABLE 23
Average Composition of Lamprophyres and Related Rock

	1	2	3	4	5	6	7	8	9	10	11	12	13
SiO_2	37.56	39.68	40.91	39.46	40.26	40.70	21.21	18.60	11.99	53.5	52.73	56.42	35.38
TiO_2	3.75	3.38	4.59	3.84	3.95	3.86	0.62	1.03	0.79	0.7	0.68	0.57	0.66
Al_2O_3	10.40	12.07	12.78	11.58	15.48	16.02	3.80	4.10	3.52	21.6	21.18	20.31	21.30
Fe_2O_3	4.86	6.81 }	11.45	4.80	6.23	5.43 }	5.55	1.15	3.09 }	4.1	2.63	1.84	2.42
FeO	7.24	7.04 }		7.39	6.56	7.84 }		4.90	3.74 }		2.00	1.48	2.00
MgO	9.56	9.70	7.01	8.56	5.29	5.43	3.52	8.96	5.59	2.2	2.41	2.15	0.57
CaO	12.42	13.60	9.79	12.19	10.28	9.36	25.91	25.00	34.80	1.3	2.39	1.52	1.98
MnO	0.20	0.24	0.24	0.18	0.23	0.16	0.09	0.89	0.60	n.d.	0.17	0.07	0.19
Na_2O	1.64	3.62	2.02	2.51	2.52	3.23	0.00	0.47	0.42	2.1	3.73	2.41	8.84
K_2O	3.64	1.75	4.47	3.82	3.69	1.76	4.38	3.49	1.48	10.2	8.16	9.80	5.34
H_2O	3.32	1.34	4.08	2.46	3.68	2.62	3.65	0.35	1.38		2.91	1.41	0.96
CO_2	4.70	nil	1.48	3.89	1.20	2.97	30.00	29.60	28.47 }	4.1	0.53	1.05	0.17
P_2O_5	0.96	0.77	1.18	0.96	0.63	0.62	1.27	1.82	2.04*		0.03	0.17	0.19
Total	100.25	100.00	100.00	100.64	100.00	100.00	100.00	100.36	97.91	99.8	99.55	99.20	100.00

n.d. = not determined
* - original analysis contains 2.09 per cent BaO + SrO + F + 5
1 - average olivine-bearing lamprophyre, Callander Bay (7 analyses)
2 - mean of Nockolds' average nephelinite and average olivine nephelinite (Nockolds, 1954)
3 - average olivine lamprophyre, less 8 per cent $CaCO_3$ and 10 per cent $Fe_{0.5}Mg_{1.5}SiO_4$
4 - olivine-free and ocellus-free lamprophyre Callander Bay (S. Courville, analyst)
5 - average kaersutite bearing lamprophyre, Callander Bay (3 analyses)
6 - average camptonite (Knopf, 1936)
7 - average carbonate ocellus, Callander Bay
8 - average carbonatite, Callander Bay
9 - average carbonatite (Gold, 1963)
10 - felsic ocellus (analysis 3b, Table 6)
11 - average nepheline syenite, Callander Bay (7 analyses)
12 - average potassium trachyte, Callander Bay (4 analyses)
13 - average nepheline syenite (Nockolds, 1954)

TABLE 24

Experimental Results of Heating Ocellar Lamporphyres

Olivine lamprophyre, BH1-553			Kaersutite lamprophyre, D57		
T(°C)	P(kb)	Products	T(°C)	P(kb)	Products
860	1	Ol + cpx + bio + ves	860	1	K + cpx + bio
880	1	Ol + cpx + bio + ves	880	1	g_1 + cpx + k ± bio
900	1	Ol + cpx + bio + ves	900	1	g_1 + cpx + k ± bio
920	1	Ol + cpx + bio + ves	920	1	g_1 + cpx + k
940	1	Ol ÷ cpx ± bio ÷ ves	940	1	g_1 + cpx + k
960	1	G + Ol + cpx ± bio + ves	960	1	g_1 + cpx ± k
980	1	G + Ol + cpx + ves	980	1	g_1 + g_2 + cpx ± k
1000	1	G + Ol + cpx + ves	1000	1	g_1 + g_2 + cpx
1020	1	G + Ol + cpx + ves	1020	1	g_2 + cpx
1040	1	G + Ol + cpx + ves	1040	1	g_2 + cpx
1050	4	G + Ol ± cpx	1060	1	g_2 + cpx
1060	1	G + Ol + cpx + ves	1080	1	g_2 ± cpx
1080	1	G + Ol ± cpx + ves	1100	1	g_2
1100	1	G + Ol ± cpx + ves			

Ol = olivine
cpx = clinopyroxene
bio = biotite
ves = carbonate filled vesicles

G = glass
K = kaersutite
g_1 = colourless to brownish glass
g_2 = greenish brown glass

proportions and the whole melted, two immiscible liquids should appear over some pressure-temperature interval. To test this hypothesis, melting experiments were carried out on crushed specimens of two ocellar lamprophyre dykes, one an olivine lamprophyre containing carbonate ocelli, and the other a kaersutite lamprophyre containing ocelli rich in potassium feldspar.

The specimens were crushed to -150 mesh in ceramic mortars, tumbled for 24 hours to ensure homogeneity, and 100 milligrams of the sample, together with 15 milligrams of distilled water were weighed into gold or platinum tubes having an inside diameter of 0.30 centimetre and a thickness of 0.3 millimetre. The tubes were sealed by electric arc welding and weighed to check for weight loss; those losing more than 5 milligrams during welding were rejected. The capsules were heated under 1 kilobar external pressure, a value based on observations suggesting that Callander Bay is a hypabyssal, or subvolcanic complex. Distilled water was chosen as a liquid phase, though the presence of fenitization around the dykes suggests that Na and K may have been significant components. The presence of Na- and K-rich fluid phases produced immiscible melting of camptonitic lamprophyres (Philpotts and Hodgson, 1968).

The capsules were heated to temperatures between 860° and 1,100°C. At temperatures below 980°C they were sealed in gold tubes and heated in René cold-seal bombs by a tube furnace using water buffered by oxalic acid as a pressure medium. Above this temperature they were sealed in platinum capsules and heated in an internally-heated pressure vessel of the type described by Goldsmith and Heard (1961) using a mixture of equal parts CO and CO_2 as a pressure medium. The capsules required about 16 minutes to come to temperature and were normally held at temperature for 3 hours. The cold-seal vessels were quenched by air-blast after removal from the furnace, while samples in the internally-heated apparatus were quenched by turning off the furnace. In both cases, pressure was maintained during the quench and the temperatures dropped below 300°C in 1 to 2 minutes. The products were examined by petrographic microscope with the aid of immersion oils. Most charges were recovered in a granulated condition so that crushing was not necessary.

The results of these experiments are compiled in Table 24. The olivine-bearing rock began to melt at about 950°C, forming a pale brown vesicular glass whose colour lightened with rising temperature. The vesicles were filled with minute dendrites of calcite, and rare, small spherules of glass of very low refractive index (Fig. 33). These vesicles were present down to the lowest temperatures investigated. In the absence of glass, they concentrated along the edge of the charge, particularly at the top. All of the capsules recovered from these experiments were distended upwards on extraction from the bomb and exuded liquid and gas on puncturing. No significant change in this behaviour was observed through the temperature interval considered except that the proportion of glass became larger. Biotite had disappeared below 1,000°C, and by 1,100°C the only remaining crystalline phases were olivine and a little clinopyroxene of very low birefringence. No calcite was seen in any of the residues except in the vesicles although calcite was common in the initial material. These results suggested that the carbonate fraction had melted at some temperature below the lowest experimental temperature and had remained immiscible in the silicate liquid when it formed. The vesicles could also be interpreted as bubbles of a CO_2-rich vapour phase, which had formed calcite on quenching. As we shall see the difference between these alternatives is one of terminology not substance.
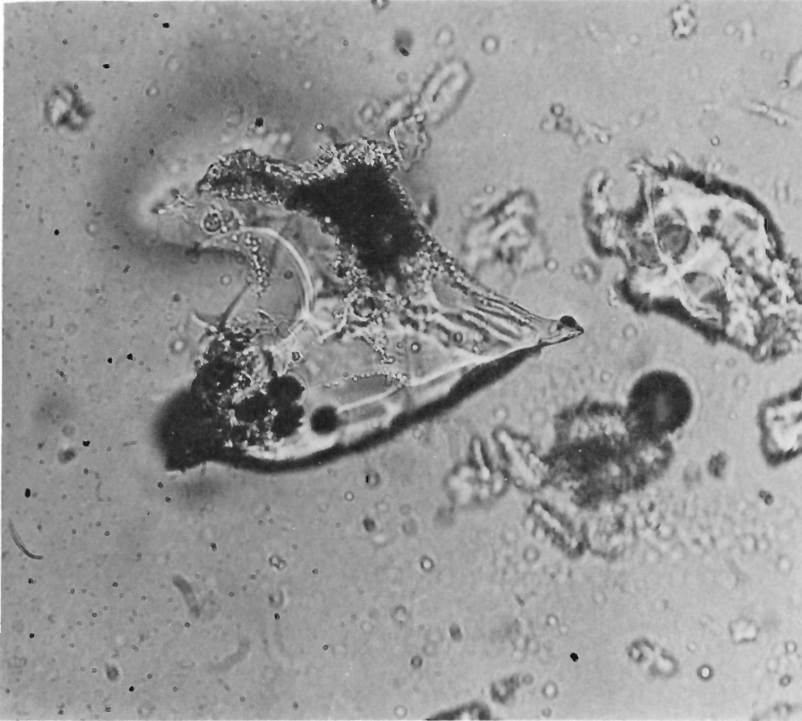
Figure 33. Fragment of olivine lamprophyre with carbonate ocelli
heated at 1,040°C 1 kilobar water pressure for 3 hours.
Clear = glass, large black angular fragment = olivine,
small rounded dots = opaque; note the outlines of globu-
lar vesicles in the large fragment and the smaller frag-
ment to the right. The minute beads crossing the top of
the fragment and rimming the vesicle are calcite. (Plane
polarized light, x100) (G.S.C. photo 201349-V)

        In order to test the behaviour of the carbonate ocelli at higher pres-
sure, one run was made at 1,050°C and 4 kilobars pressure. This run when
quenched gave a homogeneous pale yellow glass containing rounded grains of
olivine, a few corroded grains of clinopyroxene, and numerous minute ellip-
soidal vesicles a few which contained needles of a mineral too small to iden-
tify. The capsule collapsed during the run and only liquid exuded when it was
punctured.
        These data can be interpreted as indicating that the lamprophyre
melts to a homogeneous magma at pressures greater than 4 kilobars. As the
pressure is lowered, the volatile portion boils off, forming vesicles of a
water + carbon dioxide mixture (plus smaller amounts of CO, CH_4, H_2, etc.).
Since this phase is almost certainly at supercritical pressure (Greenwood and
Barnes, 1966), two fluid-like phases coexist with one another, a type of liquid
immiscibility which is surely very common and to which few petrologists
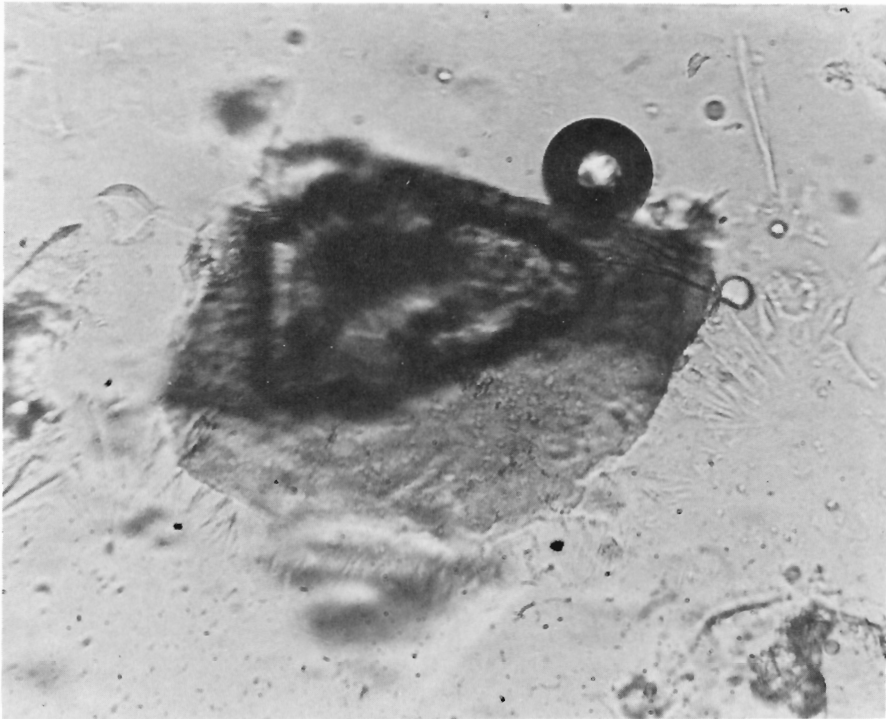
Figure 34. Fragment of kaersutite lamprophyre with felsic ocelli heated at 930°C and 1 kilobar water pressure for 3 hours. Pale grey-initial glass (very pale green in specimen). The large bubble on the dark glass is an artifact of the immersion oil (Cargille D.) (Plane polarized light, x100) (G.S.C. photo 201349-Y)

would object. As we have already pointed out any minerals growing in the silicate liquid must be in equilibrium with the aqueous liquid. If the droplets of the volatile-rich phase are trapped in the solidifying magma, crystallization will produce ocelli of volatile-rich minerals. In many cases, however, the early crystallizing phases and the volatile-rich phase will escape leaving a residual magma, still saturated in water. In the present case this magma is assumed to have the composition of a kaersutite lamprophyre.

The kaersutite-bearing lamprophyres began to melt at 870°C to a deep brown glass, apparently formed by breakdown of biotite and zeolites. The colour of this glass lightened to very pale yellow at 920°C, at which point a second glass of greenish brown shade suddenly appeared in the form of threads and filaments of glass (Fig. 34). At 1,000°C the situation was reversed, and rare threads of clear glass were present in the greenish brown glass. At these temperatures biotite and kaersutite had completely disappeared from the solid residue, and clinopyroxene was noticeably corroded. At temperatures above 1,000°C only one greenish glass was observed. The rock melted

completely at 1,080°C. The behaviour of this melt strongly suggests that the magma would form two immiscible liquids on melting under geologically plausible conditions. A definitive experiment would be the homogenization of the glass at or above the liquidus.

It also demonstrates a possible reason for the rarity of observed immiscibility in geological experiments. Immiscibility appears only over an interval of about 20 degrees in a cooling path of 200 degrees. If the range of composition in which immiscibility occurs is small, this range could very easily be missed by normal pressure-temperature-composition grids. Holgate (1954) has pointed out that the shape of many experimental systems suggests the presence of an immiscibility loop just below the solidus. Many of these same systems could be interpreted as having a small immiscibility field intersecting the solidus, but undiscovered due to coarseness of the experimental temperature interval, or composition interval, or both.

Application of experimental results

If the parent magma of the lamprophyres began as a homogeneous liquid, possibly containing some phenocrysts of olivine, then as it rose in the crust the pressure dropped and a CO_2-H_2O rich phase would boil off. This was the initial stage of fluid immiscibility. Since the Callander Bay complex contains a large amount of carbonatite it is tempting to see this volatile-rich phase as the source of these carbonatites. The degassed magma proceeded to crystallize, and when the residual liquid reached a certain composition, immiscibility again occurred, causing the liquid to split into 'syenitic' and basic fractions. The 'syenitic' fraction could be the source of the potassium trachyte dykes commonly associated with the lamprophyres, and of the nepheline syenites. According to this interpretation, a primitive lamprophyric magma could be the source of all the alkaline rocks in the complex by means of a process of successive immiscibility.

The plausibility of this hypothesis is supported by the similarity of the composition of the ocelli and matrices, with the respective rocks which they are assumed to produce.

Comparison with other similar complexes

Comparison of the olivine lamprophyres of Callander Bay with similar rocks elsewhere (Table 19) suggests that they are relatively normal monchiquites, but unusually high in potassium and relatively low in sodium. Analysis 1 of Table 19 also compares reasonably closely with the average nephelinite of Nockolds (1954) except for low sodium content. Despite the apparently relatively low soda content, the first pyroxene to crystallize in the Callander Bay rocks was an aegirine-augite, whereas later pyroxenes are augitic. This suggests that sodium was lost by the melt at some stage after the onset of crystallization. This could possibly be explained by loss of sodium in the boiled-off solutions which penetrated the wall rocks and produced fenitization aureoles. Alternately, the formation of immiscible droplets may have depleted the sodium content of the matrix by concentrating this element in the droplets.

The average kaersutite-bearing dyke, which could be produced by extraction of olivine and calcite from the olivine lamprophyres, is almost identical in composition to the average "camptonite" of Knopf (1936), but again

has unusually high potash content. Comparing the average nepheline from Callander Bay with Nockolds' (1954) average nepheline syenite we find the analyses to be very similar, except for potassium and sodium content, which are almost the reverse of Nockolds' values.

The association of relatively high potassium values with carbonatite is known at several other carbonatite occurrences, notably Tundulu, and Nothace Hill, Malawi. In all cases the carbonatite is associated with fine-grained to aphanitic, calcite-bearing rocks, commonly brecciated that consist essentially of potash feldspar (Garson, 1966).

Other occurrences of ocelli

Ocelli are so common in certain types of lamprophyre that according to Knopf (1936) early British petrologists regarded them as an important field aid in identifying lamprophyres. Ocelli appear to have been first mentioned by Brogger (1898) who found carbonate ocelli in monchiquites of the Oslo district. Flett (1900, 1935) describes felsic ocelli as very common in the camptonitic dykes of the Orkney Islands. Since that time the presence of ocelli and amygdules in lamprophyric and related rocks has been widely reported. Most occurrences are from monchiquitic rocks, but occurrences have also been described from picritic sheets (Drever, 1960), and kimberlite (von Eckermann, 1966). Unusual vesicular structures resembling ocelli have also been reported from volcanic rocks with similar chemistry, that is leucite basalt, trachybasalt and nephelinite. These have been described by Holmes and Harwood (1937), by Tomkeieff (1952) and by Dunham (1933). Minerals of both hydrous and anhydrous character are reported to project into the vesicles, and to form small pegmatoid patches around them.

From the many descriptions of ocelli it would seem that they are commonly distributed across the full width of the dykes, except in the chilled selvage. An exception occurs at Okonjeje (Simpson, 1954) where ocelli are only associated with coarse-grained patches of the groundmass. Ocelli have been found concentrated toward upper parts of sills (Philpotts and Hodgson, 1968), or toward the centre of the dykes (Ramsay, 1955; Upton, 1965; Horne and Thompson, 1967), or, rarely, toward the margins (Flett, 1935). The minerals of the ocelli are always coarser in grain size than those of the matrix, and commonly coarsen toward the centre of the intrusive. They generally show a parallelism or flattening parallel to the margin of the dyke. Campbell and Schenk (1950, p. 681) noted that both ocelli and phenocrysts coarsened in grain size toward the centre of camptonite dykes. The size of ocelli varies from "minute" (Tomkeieff, 1952), to flattened bodies 10 centimetres long (Philpotts and Hodgson, 1968, p. 178). The usual size range appears to be 0.05 to 3.00 centimetres, but coalescence of ocelli is a ubiquitous feature, making size measurement somewhat ambiguous. The volume ratio of ocelli to matrix varies greatly. Flett (1935, p. 176) reports ocelli constituting up to 50 per cent by volume of some captonites. Tomkeieff (1952, p. 365) reports ocelli to constitute 20 per cent of a trachybasalt. At Callander Bay the ocelli form 7 to 16 per cent of the volume of the rock. Estimates of the volume ratio of ocelli are commonly complicated by local concentrations and depletions of ocelli.

Minerals occurring in the ocelli are those occurring in the matrix with the exception of some accessories but they occur in differing proportions, with leucocratic and hydrous minerals concentrated in the ocelli. The most
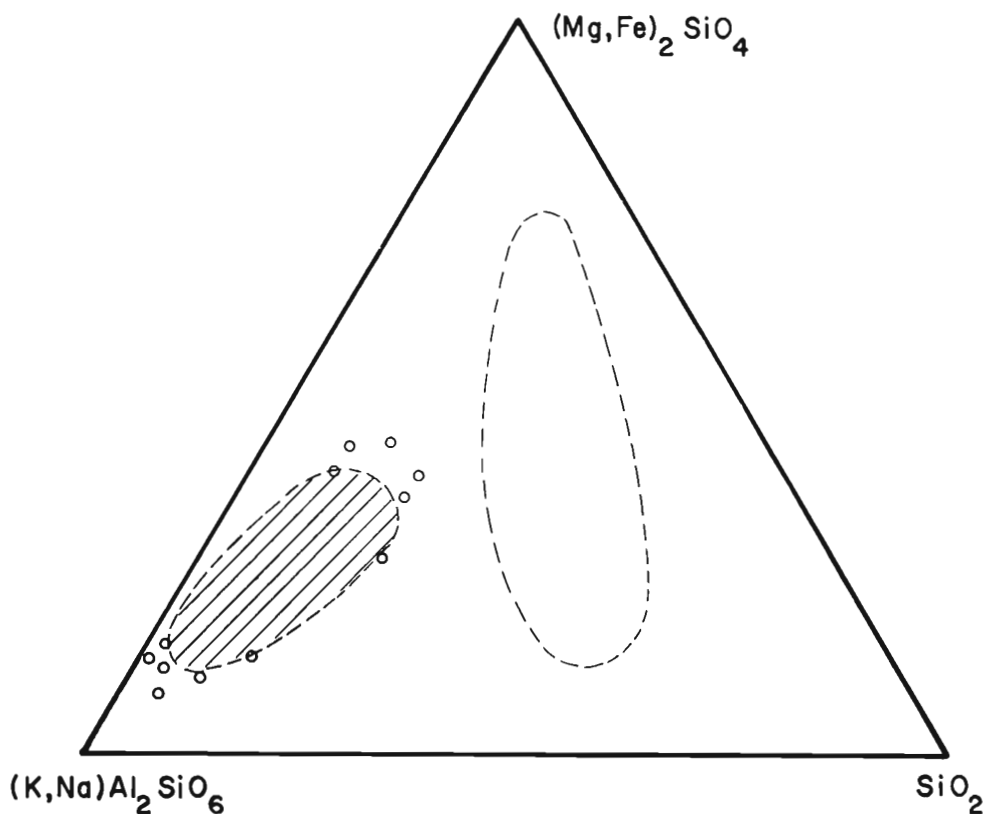
Figure 35.   Projection of the analyses of possibly immiscible alkaline rocks
into the generalized system feldspathoid-olivine-silica. The
immiscibility field discovered by Roedder (1954) is shown by a
dotted line, that apparently defined by ocellar rocks by a diagonal
hatching.

common ocelli minerals are zeolites, carbonates, feldspars, nepheline, bio-
tite, amphibole, pyroxene and opaques. Olivine is not found in ocelli, though
commonly present in the matrix (Drever, 1960, p. 50; Flett, 1935, p. 176).
Fractionation of minerals within the ocelli is common either forming density
layering (Drever, 1960; Philpotts and Hodgson, 1968), or concentric zones
(Flett, 1935; Tomkeieff, 1952; Ramsay, 1955; Upton, 1965; Horne and Thompson,
1967). The acicular minerals within the ocelli and the bordering matrix tend to
lie tangential to the boundary of the ocelli, but occasionally lie radially and may
project across the ocellus boundary (Evans, 1901; Tomkeieff, 1952; Simpson,
1954; Ramsay, 1955; Drever, 1960; Upton, 1965; Horne and Thompson, 1967;
Philpotts and Hodgson, 1968).
        Optical determinations suggest that coexisting minerals in ocellus
and matrix have similar compositions and similar zoning, even where zoning
is strong. Drever (1960) reported " ... pyroxene and feldspar both inside
and outside the globules show such slight differences that they could have been

precipitated under other circumstances from one and the same liquid ... ".
Philpotts and Hodgson (1968) find strongly zoned plagioclase showing identical
zoning in ocelli and matrix, and hastingsite, titanaugite and kaersutite to be
identical in both portions. Ramsay (1955) found good correlation between pla-
gioclases in the two environments but noted the outer rim of the ocelli plagio-
clase to be more sodic than the rims of the matrix plagioclase.

A rather common feature of many ocelli is a central cavity, now
often filled with carbonates (Ramsay, 1955; Philpotts and Hodgson, 1968).
This cavity presumably represents a gas bubble, and forms a transition to
the volcanic type of ocelli noted by Holmes and Harwood (1937) and by Dunham
(1933), where this cavity occupies a major part of the volume of the ocellus.

From these data we may conclude that ocelli identical in character
to the Callander Bay example are a ubiquitous feature of igneous rocks with
restricted chemical composition. The rocks are all ultrabasic alkaline hyp-
abyssal or extrusive varieties with high to extreme iron content, high iron to
magnesium ratios, and high to extreme volatile content. A high content of
CO_2 is a common but not universal accompanient, and an unusually large num-
ber of potassic types appear. An illuminating way of displaying these char-
acteristics is shown in Figure 35 a plot of $(K, Na)Al_2Si_2O_6 - (Mg, Fe)_2SiO_4 - SiO_2$
on which is superimposed the experimentally determined immiscibility field
in the system leucite-fayalite silica. The tendency for the compositions of
composite dykes and sills (compiled from Philpotts and Hodgson, 1968), and
of ocelli to avoid the region of a presumed immiscibility field and cluster around
its edges is clear, strongly suggesting that an immiscibility field, similar to
that discovered by Roedder in a simplified system, acts in natural systems
also. Luth (1967) found no immiscibility in the system leucite-forsterite-
silica, which suggests that if immiscibility is the cause of ocelli, they will
appear only in rocks of high iron to magnesium ratio.

Origin of Ocelli

Despite the general prejudice against liquid immiscibility as an
important petrologic process, the observational evidence has led a number of
workers to conclude that liquid immiscibility must be the cause of ocelli (Drever,
1960; Tomkeieff, 1952; Philpotts and Hodgson, 1968; von Eckermann, 1966).
We have already noted that ocelli have generally been passed off as amygdales
(Flett, 1953; Campbell and Schenk, 1950; Watterson, 1968; Horne and Thompson,
1967), despite the fact that the mineralogy of the ocelli makes this explana-
tion extremely implausible. Holmes and Harwood (1937, p. 155) decided
"There seems no escape from the conclusion that the biotite crystals (and
those of augite where present) crystallized from the gaseous contents of the
cavity in which they occur". The attitude of most petrologists is perhaps
neatly summed up by Knopf (1936, p. 1752) "The large spheroids and ellip-
soids are particularly impressive and readily suggest the idea of having formed
from immiscible globules of magma, but the explanation that they are ocelli
filled with late crystallizing pyrogenic minerals appears to be the more rea-
sonable". We believe that the explanation of ocelli as late crystallizing pyro-
genic minerals is completely unreasonable, and that liquid immiscibility is
not only powerfully suggested by field evidence, but supported by detailed
mineralogical studies, and by experiment.

Petrologic significance of liquid immiscibility

Olivine nephelinite has been suggested as the parental magma of many alkaline igneous complexes by a number of lines of evidence (King, 1965; Currie, 1970). Significantly evidence of liquid immiscibility is strongest in precisely this composition. If the magma is strongly carbonated, a carbonatitic magma will rise from it by immiscibility as it rises in the crust. The idea that at least some carbonatites arise by immiscibility of an alkaline ultrabasic parent is currently popular among some students of carbonatites (von Eckermann, 1966; Barth and Ramberg, 1966). Field observations of ocellar rocks and experiments on them strongly support this hypothesis. Numerous modifications of this fundamental idea can readily be envisaged by which the ultrabasic silicate rocks could become separated from, or appear in complex relations with the carbonatite fraction. The result of this period of immiscibility, together with removal of crystallized olivine, leads to formation of a camptonitic magma, which according to the evidence quoted may split into immiscible fractions of nepheline syenite and a more iron- and magnesium-rich camptonite. The association of camptonite dykes with nepheline syenite is well known and was used by Rosenbusch in his definition of camptonite (see Knopf, 1936, p. 1746). There are numerous examples of successful prediction of the presence of nepheline syenite on the basis of discovery of camptonite dyke swarms. This association receives a natural explanation from the idea of liquid immiscibility between a camptonite fraction and a nepheline syenite fraction. Of course this does not argue that all nepheline syenites have arisen in this way. Finally we may note that removal of the nepheline syenite fraction leaves a residue tending toward a strongly undersaturated alkaline rock of melteigite type. Such rocks have been suggested as parents for the ijolite-urtite series of alkaline rocks (King, 1965).

Liquid immiscibility acting on a parental carbonated nephelinitic magma could therefore produce three sharply differentiated series of rocks, namely carbonatite, nepheline syenite, and melteigite-ijolite-urtite. These three series are commonly seen in many alkaline complexes, in relations which have not hitherto been satisfactorily explained.

CHAPTER IV

ORIGIN AND DEVELOPMENT OF THE CALLANDER BAY COMPLEX

INTRODUCTION

We have discussed the origin of various components of the Callander Bay complex, and concluded that liquid immiscibility played a major role in fractionation of the magma and that metasomatism by strong brines produced the fenite aureole. It remains to unite these conclusions into a comprehensive scheme for the origin and development of the complex, and to relate them to some larger problems of alkali rock genesis.

ROLE OF IMMISCIBILITY

In discussion of the role of immiscibility in the formation of ocelli in lamprophyre dykes, we concluded that carbonatitic, then syenitic liquids separated from an ultrabasic alkaline magma by successive immiscibility. These three liquids seem so different from each other, that it might be supposed that there is little relation between their chemical compositions. However as shown in Figure 37, there are surprisingly close relations among apparently disparate rock types. On the most generalized projection (Si+Al)- (Fe+Mg)-(K+Na+Ca) the differentiation into three disparate groups is clear, the syenitic rocks being richer, and the carbonatites poorer, in Si+Al than the original magma. The carbonatites appear on this projection to be richer in alkalis than the other rocks, but as shown in the KCN projection this is due to their extreme content of calcium. The projection Si-Al-(Na+K) shows that immiscibility does not noticeably fractionate alkalis with respect to Si and Al. On a KCN diagram the enrichment of the syenitic rocks in alkalis with respect to calcium is clear. There is, however, no marked change in the K:Na ratio showing that the generally potassic character of the complex persists from the earliest ultrabasic magma through all phases. Finally, the classical AMF diagram once again shows a marked division into three groups. There is a tendency for the Fe:Mg ratio to remain approximately constant from the lamprophyres through the syenitic rocks. The carbonatites however show markedly lower Fe:Mg ratios, giving the diagram the somewhat 'hooked' appearance typical of series developed by fractional crystallization. Indeed one of the principal conclusions from the projections of Figure 37 is that immiscibility will lead to products very similar to those of fractional crystallization. The only clue from Figure 37 that immiscibility is involved is the very clear division into two, or three groups, depending on the projection. Similar divisions are seen in some fractional crystallization series. A particularly noteworthy point is the constancy of the ratios K:Na and Fe:Mg during immiscibility. From theoretical considerations, both of these would be expected to change during fractional crystallization, increasing in the residual liquids. This appears to offer a possibility of distinguishing rocks formed by immiscibility from those developed by fractional crystallization but examination of series of igneous rocks developed by fractional crystallization (Nockolds and Allen, 1954) suggested that these ratios are often constant, or near constant, over large parts of the crystallization path, so that in practical terms they offer limited possibilities of discrimination.

- 89 -

Figure 36. Kaersutite phenocryst straddling matrix-ocellus boundary,
            replaced in latter by calcite, analcite and opaques. The
            ocellus core is analcime (grey), the margin analcime,
            K-feldspar, calcite and opaques. Euhedral kaersutite
            phenocrysts (clear and grey) are set in a matrix of min-
            erals found in the ocellus. In upper left of photograph a
            vein of these minerals cuts the matrix of the lamprophyre.
            (x15, crossed nicols) (G.S.C. photo 201290-O)

       It therefore appears that immiscibility yields products chemically
similar to those of fractional crystallization. Only physical evidence of immis-
cibility is likely to be discovered, i.e. ocelli, or equivalent structures. Since
experiments on the Callander Bay rocks show that immiscibility appears only
over a limited range of pressure and temperature, and the evidence of immis-
cibility could easily be disguised by holding the rocks at unfavourable
pressure-temperature conditions, the determination of pressure-temperature
conditions of emplacement becomes a matter of significance.

PRESSURE-TEMPERATURE ENVIRONMENT

       The determination of these conditions is obviously difficult, since
rocks reflect best the conditions prevailing at the time of solidification, and
other conditions are evidenced only as relicts. The ocelli themselves form
such relicts. From experimental evidence, such ocelli would not exist at
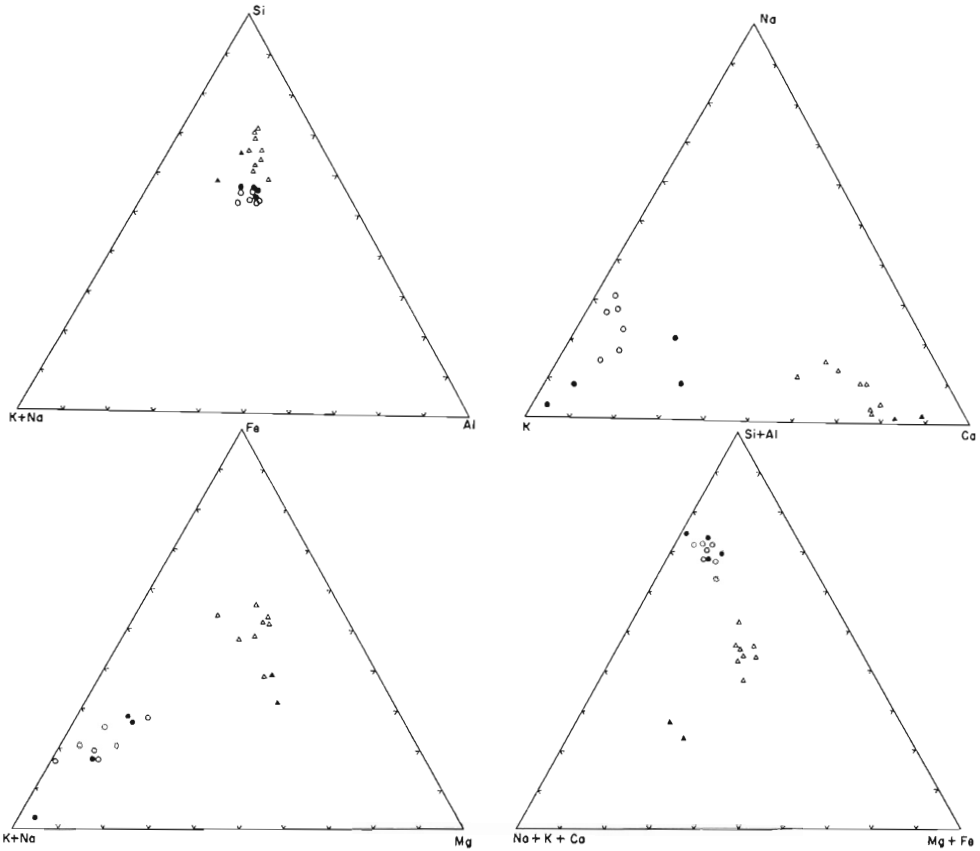
Figure 37. Ternary diagrams representing the chemistry of igneous rocks
from the Callander Bay complex, open circles-nepheline syenite,
closed circles-potassium trachyte, open triangles-lamprophyre,
closed triangles-carbonatite.

water pressures of 4 kilobars, and temperatures above the solidus (see Table 24).
The ubiquitous distribution of ocelli together with the homogeneity of the lam-
prophyres strongly suggests that the ocelli must have developed from an orig-
inally homogeneous magma, rather than being brought along as already seg-
regated droplets. In the latter case, strong segregation, and local absence
of ocelli would be expected. Furthermore, the well developed, but dispersed
character of the ocelli in the dykes shows that they were held in the immisci-
bility field long enough for efficient nucleation to take place, then quenched
before strong aggregation and segregation of immiscible liquids could occur.

Evidence on pressure-temperature conditions can be deduced from
the nepheline syenite and potassium trachyte dykes. The chemical data (Fig. 36)
show that these dykes are very similar to the coarse-grained nepheline syenite.
If the nepheline-potash feldspar intergrowth in one of the dykes is accepted
as being 'pseudo-analcite', then the dyke must have been held for a substan-
tial period at water pressures above 2.6 kilobars, rather than emplaced in a

lower pressure-temperature environment sufficiently rapidly that the pseudo-morphous character of the intergrowth was preserved, but sufficiently slowly that the analcite broke down completely to intergrowth. This chilling was also sufficiently rapid to cause the dykes to solidify as fine-grained rocks.

Finally, we note that the main body of nepheline syenite crystal-lized as a course grained rock, a feature generally accepted as evidence of relatively slow cooling. Furthermore, sufficient differentiation took place to distinguish leucocratic nepheline syenite from mesocratic nepheline syenite. These facts suggest a slow cooling under rather stable conditions. The composition of coexisting nepheline and alkali feldspar (Tables 10 and 11) strongly suggest equilibration under plutonic rather than volcanic conditions (Deer et al.; 1963, pp. 245-249, vol. IV).

These data may be correlated by supposing the parental lampro-phyric magma to rise slowly from its source to a level where the water pressure was sufficient to stabilize analcite, but low enough to permit boiling off the CO_2-rich phase that was parental to the carbonatite (i.e. greater than 2.6 but less than 4 kilobars). Assuming water pressure equal to total pressure, this would have been at a level of 8-12 kilometres below surface. The necessity for a magma chamber at this level follows from the physical separation of the carbonatite from the lamprophyre. Since dykes can rise to near surface levels with the carbonate fraction in the form of ocelli, it follows that for total separation to take place an extended period at favourable temperature and pressure is required. According to the experimental work these temperatures could have been as low as 960°C at 1 kilobar water pressure, and presumably lower at higher water pressures. After separation of the CO_2-rich phase, and presumed settling of olivine to the floor of the chamber, such conditions would also have been appropriate for the further development of immiscible syenitic liquid. At these temperatures and pressures both the syenitic and carbonatitic liquids could be expected to react vigorously with their surroundings. Since both are less dense than lamprophyre they would tend to rise to the top of the magma chamber and intrude its roof. The opportunity for intrusion of lamprophyre dykes with syenitic ocelli is restricted, since such dykes must leave the magma chamber after the initial separation of the CO_2-rich phase and before the total separation of the syenitic phase. This agrees well with the observed sparsity of such dykes compared to carbonate-bearing dykes, which could arise not only from injections from the magma chamber at the appropriate time, but also from injections of primitive magma at later times.

We thus arrive at a picture of an alkaline ultrabasic magma rising into the crust to a magma chamber at moderate depth and separating into contrasting fractions by immiscibility, the lighter of which continues to rise, driven by buoyant forces and gas pressures.

Mechanics of emplacement

This sequence suggests that the emplacement of the intrusion must have proceeded by the primitive magma rising into a magma chamber at moderate depth. Upon boiling off the CO_2-rich phase, this very penetrative, mobile material worked its way into the roof of the magma chamber. If the emplacement of this volatile phase proceeded by repeated fracturing of the roof and outrush of volatiles, then the higher the volatile phase advanced, the

more water-rich it became (Currie, 1970). This water-rich phase is appar-
ently the agent responsible for most of the fenitization effects (see Chapter III).

The fluid phase exerted pressure during its emplacement, which
presumably produced ring fractures (see detailed analysis by Anderson, 1935).
The form of the nepheline syenite may be conveniently explained by assuming
it to be a partial ring dyke. Since separation of the syenite did not take place
until after the separation of the CO_2-rich phase, the fracture was presumably
there, ready to be occupied, when the syenitic magma rose. If it is assumed
that this fracture did not intersect the surface, emplacement of the nepheline
syenite under a substantial water pressure is reasonable.

We have already noted that fenitization seems to have taken place
below a rather thin cover of rock. It is plausible to suppose that the Callander
Bay complex may be the roots of an alkaline carbonatitic volcano, such as
those seen in southern and eastern Africa although no direct evidence has been
found. If so, the onset of surface eruption would cause an immediate drop in
water pressure, which could explain the late-stage emplacement of fine-grained
nepheline syenite dykes. The general restriction of dykes to the fenite aure-
ole is also neatly explained by this assumption, since the edge of this aureole
marks the effective boundary of the fracturing caused by the volatile phase,
which fracturing is assumed to provide the channelways for the dykes. The
boundary of fracturing in turn is fixed by the loss of volatiles on eruption.
The generally late character of the dykes may be explained by the observa-
tion that emplacement of the complex apparently took place rather smoothly
until a late stage. The disturbances connected with activation of an eruptive
apparatus such as foundering of the roof may have been sufficient to cause
dyke injection.

In summary, considerations of the emplacement of the body sug-
gest that (1) a magma chamber exists at moderate depth below the complex,
(2) there is no necessity for a large mass of carbonatite below the central
part of the structure, but the observed melange of altered country rocks and
carbonatite may extend to depth, (3) the nepheline syenite forms a ring-dyke,
(4) the emplacement of the complex was quiet, rather than violent, except pos-
sibly at the late stages.

Generation of alkaline magma

We have shown that the Callander Bay complex can be understood
as originating from a primitive magma of nephelinite, or olivine nephelinite
composition. This leaves the problem of the origin of this magma. Green
(1969) has suggested that such magma can be generated by partial melting of
upper mantle 'pyrolite' under sufficiently high pressure conditions. This idea
is based on the assumption that such liquids can crystallize orthopyroxenes
greatly in excess of olivine at high pressure, thus enabling the residual liquid
to become progressively more undersaturated. This assumption, though it
has some experimental support, has been severely criticized on both exper-
imental and theoretical grounds by Kushiro (1969) and others. Even if correct,
it is difficult to see how the idea can explain the observed confinement of
Callander Bay and the related alkaline rocks of this igneous province to a
contemporary rift system, that is a zone of crustal, and possibly upper man-
tle tension. One would expect that such tension would tend to lower the pres-
sure in the subjacent upper mantle, and hence tend to generate tholeiitic

magmas according to the scheme of Green. A completely different idea has
been outlined by Currie (1970), who supposed nephelinite magma to arise by
desilication of alkali basaltic magma, a generally accepted primitive magma,
by flux of water through it. This idea depends on the assumption that an aqueous
fluid phase can exist at upper mantle depths. From the work of Burnham
(1967) other workers suggest that this phase cannot be pure water, but must
contain large amounts of CO_2, which is essentially insoluble in silicate melts,
even at pressures as high as 10 kilobars (Holloway and Burnham, 1969). The
data of Hill and Boettcher (1970) show a strong inflection in the P-T projec-
tion of the beginning of melting curves of the systems basalt-water, and basalt-
water-carbon dioxide. The slope of the melting curve reverses at this inflec-
tion, and at higher pressures the melting behaviour is qualitatively similar
to that of dry melting with increasing pressure. Thermodynamic plausibility
arguments strongly suggest that this reversal in slope indicates a sharp
decrease in solubility of water in the melt. Consider a solid in equilibrium
with a melt. As physical conditions change along the melting curve,

$$dF_s = dF_l \tag{1}$$

where F_s is the free energy of the solid and F_l that of the coexisting liquid.
Now assuming the free energy change to depend on temperature, pressure
and composition, we may write

$$dF_s = (\partial F_s/\partial P) \, dP + (\partial F_s/\partial T) \, dT + \sum_i (\partial F_s/\partial n_i) \, dn_i)$$

$$= V_s dP + (H_s/T)dT + \sum_i \overline{F}_s^i \, dn_i \tag{2}$$

where v_s is the mol volume of the solid, H_s the 'ideal heat of vaporization',
or the heat required to infinitely disperse the solid, and $\overline{F}_i$ the partial molar
free energy of component i, and dn_i the increment in mols of component n_i.
A precisely analogous equation may be written for the liquid, using the sub-
script 'l' instead of 's'. Substituting these two equations in (1) we obtain,

$$(v_s - v_l)dP + (H_m/T)dT + \sum_i (\overline{F}_s^i - \overline{F}_l^i)dn_i = 0 \tag{3}$$

where H_m is the heat of melting (the difference in heat required to vaporize
a solid and the melt in equilibrium with it is the heat of melting). For any
component present in both solid and liquid whose fugacity is controlled by the
solid-melt equilibrium, the last term must be zero, since by definition the
partial molar free energy of any component is the same in coexisting phases
at equilibrium and material removed from the solid goes into the melt. In
the absence of other factors, equation (3) then reduces to the Clapeyron equation.
Now consider the melt saturated with water, that is the fugacity of
water to be controlled by factors external to the equilibrium between the solid
and its melt. The appropriate terms in equation (3) do not cancel. Suppose
for simplicity the water is insoluble in the solid phase (i.e. $dn_s^w = 0$), and no
free water phase is present. Equation (3) may then be written

$$(v_s - v_l)dP + (H_m/T)dT + \overline{F}_l^w dn_w = 0 \tag{4}$$

where $\overline{F}_l^w$ is the partial molar free energy of water in the liquid. Since on the
saturated melting curve, the melt is theoretically in equilibrium with a pure

water phase, this partial molar free energy is the same as the free energy of pure water at equivalent P, T. Equation (4) may be rearranged to yield

$$dT/dP = (T/H_m)\left[(v_1-v_s) + F_w(dn_w/dP)\right] \qquad (5)$$

Experimentally we know that dT/dP is negative for moderate water pressures. Now if solubility continues to increase with increasing water pressure dn_w/dP is always greater than zero, though it may become very small. Hence dT/dP must always be less than that for the dry system since $F_w < 0$, and hence $F_w(dn_w/dP) < 0$. If the slope becomes greater than that for the dry system, then (dn_w/dP) must be negative, that is the solubility decreases with further increase in pressure. These comments apply regardless of phase changes. A phase change may result in an abrupt increase in (v_1-v_s) and hence reverse the sign of dT/dP, but the magnitude of dT/dP in the wet system must always be less than that in the dry system if solubility increases with pressure. Note these comments apply mutatis mutandis to any volatile, including CO_2. Now consider the work of Hill and Boettcher (1970). In the high pressure region, above 20 kilobars the slopes of the melting curves are virtually identical for hydrous and anhydrous systems. Between 15 and 20 kilobars the positive slope of the wet system is very markedly greater than that of the dry system. Further, above 20 kilobars there is no difference in the melting temperatures of systems with varying amounts of CO_2 in the vapour phase, although below 15 kilobars there is a marked difference, with the melting point rising with increasing CO_2 content. These data cannot be explained by a phase change for the reasons pointed out above. They can only be explained by assuming a change in sign of (dn_w/dP), that is a decrease in solubility with pressure above 15 kilobars. This decrease continues to around 20 kilobars, at which point the solubility has declined to a very low value, so that H_2O and CO_2 act only as a dry pressure medium, and the slopes of the melting curves above these pressures are parallel to that of the dry system, but the position of the curve is lower due to the slight residual solubility. From these considerations it seems probable that, in so far as basaltic liquids represent the low melting fraction of the upper mantle, at the depths where basalt generation takes place water is but slightly soluble in the melt, and a free aqueous vapour phase is not improbable. Since there is evidence that CO_2 is essentially insoluble in basalt melts likely to be in equilibrium with the upper mantle, this leads to an interesting conclusion, that at pressures different from the inflection point in the melting curve, the vapour phase in CO_2-H_2O saturated rocks is likely to grow richer in H_2O with increasing depth, and also with decreasing depth (i.e. the solubility has a maximum). Therefore carbonatitic fluids are most likely to be separated at a relatively constant depth, which according to Hill and Boettcher (1970) would be equivalent to about 15 kilobars, or say 45 kilo- metres (about 28 miles). This would place carbonatite separation at deepest crustal, or top of upper mantle levels, a conclusion reached on other grounds by several students of these rocks. Since we have concluded that separation of the carbonatitic phase of the Callander Bay complex took place at much shallower levels (8-12 kilometres or 5-7.4 miles) this may explain the lack of massive carbonatite in the Callander Bay complex.

During the rise of a water-saturated magma into the crust, it will boil off water. Since the aqueous phase in equilibrium with a silicate melt has a higher Na:K ratio than the melt (Luth and Tuttle, 1970) the boiling off of water will produce a sodic aqueous vapour phase and tend to make the melt

potassic. Conversely the water-poor vapour phase (i.e. CO_2-rich) will be richest in potash, and the (later) aqueous fluids will be richest in soda.

The geometry of the upper mantle under some present day rift systems and up-bulged welt of anomalous material, is compatible with the hypothesis that they are the sites of mantle degassing (Currie, 1970). According to the key role of water in the hypothesis of alkaline magma generation just outlined, this would explain the widespread evidence of high water activity in nephelinitic magma (fenitization, biotitic lamprophyres, associated carbonatite, explosive volcanism, etc.). According to the conventional views of fractional crystallization, such high water activity in material assumed to come from deep in the upper mantle (that is very water-poor regions) is a distinct embarrassment.

We have assumed the syenitic portion of the Callander Bay complex to arise mainly by immiscibility from nephelinitic magma. Since the immiscible ocelli occupy 8-16 per cent of the volume, this requires a volume of 'de-syenited' magma 6-12 times that of the syenite. At Callander Bay the volume of the syenite is relatively small, and with the assumption of a magma chamber at depth, the disposition of this volume of ultrabasic alkaline rocks offers no problem. For some large syenitic complexes which contain minor amounts of ocellar dykes (for example the Port Coldwell complex) the disposition of a volume of ultrabasic rocks sufficient to generate the observed syenite by immiscibility offers an almost insuperable problem. If the parent nephelinite is saturated with an aqueous vapour phase, as assumed above, this problem can be avoided by supposing the crustal rocks around the rising intrusion to be desilicated by the vapour flux, and then melted by the magma. Since the melting temperatures derived from the experimental work on the lamprophyre are of the order of 1,000°C, it follows that they are capable of melting significant amounts of syenitic compositions. The anatectic magma will be immiscible with the nephelinite, and because of its lower specific gravity, may be expected to rise more rapidly in the crust. Immiscibility may be a major factor in the generation of syenitic melts.

CHAPTER V

SUMMARY AND CONCLUSIONS

(1)   The Callander Bay alkaline complex comprises a central core of fenitized Precambrian crystalline rocks roughly 3 kilometres in diameter shot through with many screens and dykes of carbonatite. This central core is surrounded by a crescentic screen of nepheline syenite up to 100 metres thick, which is in turn surrounded by a fenite aureole of variable thickness. All of these rocks are cut by dykes of lamprophyre, nepheline syenite, potassium trachyte, and carbonatite.

(2)   The fenite aureole was developed by circulation through fractures of roughly 1 molal alkali chloride brines at temperatures between 450-600 °C, F_{O_2} near 10^{-17} and F_{S_2} near 10^{-3} bars. Minor sulphide mineralization compatible with these conditions is present. Fluid pressure equalled total pressure, and was probably a few hundred bars.

(3)   Nepheline-potash feldspar intergrowths, which have the shape of pseudoleucite, are richer in soda than the coexisting matrix, and are therefore not pseudoleucite, but could be 'pseudo-analcite'. If so, water pressure during crystallization of part of the nepheline syenite was greater than 2.6 kilobars.

(4)   Lamprophyre dykes displaying nontectonic offsets, with thin 'horns' crossing the line of off-set are emplaced with the aid of a water-rich volatile phase which alternately boils off the magma, enlarging and heating the region to be intruded, and is then partly resorbed by the advancing magma.

(5)   The ocelli characterizing lamprophyre dykes of nephelinitic composition appear to represent droplets of immiscible liquid. Two types of immiscibility are displayed, one a boiling off of a volatile fluid phase, the other a separation into two silicate liquids.

(6)   The magma parental to the Callander Bay complex came from the mantle, most probably derived by disilication of alkali basalt magma. It rose in the crust to a level of 8-12 kilometres deep, where a period of quiescence permitted the formation and growth of immiscible droplets. At a late stage more violent igneous activity, possibly connected with volcanic eruption at surface, caused intrusion of dykes into relatively cool and dry rocks.

(7)   The temperatures deduced for the parental magma suggest that substantial amounts of syenite may be generated by anatexis and immiscibility around nephelinite magmas in the crust. No direct evidence of this process is apparent at Callander Bay.

(8)   The similarity of the Callander Bay complex to other complexes containing nephelinite, carbonatitic and nepheline syenitic rocks (Table 23), suggests that mechanisms similar to those deduced for the Callander Bay complex may be of major importance in the generation and emplacement of alkaline igneous rocks.

REFERENCES

Ahrens, L.H., Pinson, W.H., and Kearns, M.
   1952: Association of rubidium and potassium and their abundance in common igneous rocks and meteorites; Geochim. Cosmochim. Acta, vol. 2, pp. 229-242.

Anderson, E.M.
   1935: The dynamics of the formation of cone-sheets, ring dykes, and cauldron subsidences; Proc. Roy. Soc. Edinburgh, vol. 56, pp. 128-157.

Barlow, A.E.
   1897: Geology and natural resources of the area included by the Nipissing and Temiscaming map-sheets; Geol. Surv. Can., Ann. Rept., vol. x, Pt. I.

Barrer, R.M., and Baynham, J.W.
   1956: The hydrothermal chemistry of the silicates; Pt. VII, Synthetic potassium aluminosilicates; J. Chem. Soc., pp. 2882-2901.

Barth, T.F.W., and Ramberg, I.B.
   1966: The Fen circular complex, pp. 225-260; in Carbonatites, eds. O.F. Tuttle and J. Gittins, 591 pp., Interscience, New York.

Borodin, L.S. (editor)
   1967: Rare metal metasomatites of alkaline massives; Isdatel'stvo Nauka, Moscow, 192 pp. (in Russian).

Bradshaw, R.L., and Sanchez, F.
   1969: Migration of brine cavities in rock salt; J. Geophys. Res., vol. 74, pp. 4209-4213.

Brogger, W.C.
   1898: Das Ganggefolge des Laurdalits; Videnskabs-Selskabets, Skrifter, Math.-Naturv. Klasse, No. 6.

   1921: Die Eruptivgesteine des Kristiana Gebietes IV; Das Fengebiet in Telemarken, Videnskabs-Selskabets, Skrifter, Math.-Naturv. Klasse, No. 9.

Burnham, C.W.
   1967: Hydrothermal fluids at the magmatic stage, pp. 36-74; in Geochemistry of hydrothermal ore deposits, ed. H.L. Barnes, Holt, Rinehart, Winston, New York.

Campbell, I., and Schenk, E.T.
   1950: Camptonite dikes near Boulder Dam, Arizona; Am. Mineralogist, vol. 35, pp. 671-692.

Clark, S.P. (editor)
   1966: Handbook of physical constants; Geol. Soc. Am., Mem. 97, 587 pp.

Colqhoun, D. J.
    1958:   Stratigraphy and paleontology of the Nipissing and Deux Rivieres
            outliers; Geol. Assoc. Can. Proc., vol. 10, pp. 83-93.

Currie, K. L.
    1970:   An hypothesis on the origin of alkaline rocks suggested by the tec-
            tonic setting of the Monteregian Hills; Can. Mineralogist, vol. 10,
            Pt. 3, pp. 411-420.

Davidenko, I. V.
    1966:   Contribution to the practical use of Barth's method for deter-
            mining the paleotemperatures of granitoids; Geokhimiya, (5),
            pp. 546-555.

Deer, W. A. , Howie, R. A. , and Zussman, J.
    1963:   Rock-forming minerals (5 vols.); Longmans, Green and Co. ,
            London.

Drever, H. I.
    1960:   Immiscibility in the picritic intrusion at Igdlorssuit, West
            Greenland; XXI Intern. Geol. Congr. , Pt. XIII, pp. 47-58.

Dunham, K. C.
    1933:   Crystal cavities in lavas from the Hawaiian Islands; Am.
            Mineralogist, vol. 18, pp. 369-385.

Ermanovics, I. F. , Edgar, A. D. , and Currie, K. L.
    1967:   Evidence bearing on the origin of the Belleoram stock, southern
            Newfoundland; Can. J. Earth Sci., vol. 4, pp. 413-431.

Evans, J. W.
    1901:   A monchiquite from Mt. Gronias, Juragarh (Kathiawar); Quart.
            J. Geol. Soc. , London, LVII, pp. 38-54.

Ferguson, John
    1970:   The significance of the kakortikite in the evolution of the Illimausaq
            Intrusion, south Greenland; Medd. om Grønland, Bd. 186, tlf. 5,
            193 pp.

Flett, J. S.
    1900:   The trap dykes of the Orkneys; Trans. Roy. Soc. Edinburgh,
            vol. 34, pp. 883-926.

    1935:   The geology of the Orkneys; Geol. Surv. Scotland, Mem. , 205 pp.

Fudali, R. E.
    1963:   Experimental studies bearing on the origin of pseudoleucite and
            associated problems of alkalic rock systems; Geol. Soc. Am.,
            Bull. 74, pp. 1101-1126.

Garson, M. S.
    1966:   Carbonatites in Malawi; in Carbonatites, eds. O. F. Tuttle and
            J. Gittins, 591 pp., Interscience, New York.

Gerasimovskii, V.I., and Lebedev, V.I.
    1958:   Proportions of strontium and calcium in rocks of the Lovozero
            massif; Geokhimiya, 6, pp. 699-705 (translation).

Gold, D.P.
    1963:   Average chemical composition of carbonatites; Econ. Geol.,
            vol. 58, pp. 988-991.

Green, D.H.
    1969:   Origin of basaltic and nephelinitic magmas in the earth's mantle;
            Tectonophysics, vol. 7, pp. 409-422.

Goldsmith, J.R., and Heard, H.C.
    1961:   Subsolidus phase relations in the system $CaCO_3$-$MgCO_3$; J. Geol.,
            vol. 69, pp. 43-61.

Greenwood, H.J., and Barnes, H.L.
    1966:   Binary mixtures of volatile components; in Handbook of physical
            constants, ed. S.P. Clark; Geol. Soc. Am., Mem. 97,
            pp. 385-400.

Harker, A.
    1904:   The Tertiary igneous rocks of Skye; Geol. Surv. United Kingdom
            Mem.

Hill, R.E.T., and Boettcher, A.L.
    1970:   Water in the earth's mantle; melting curves of basalt-water, and
            basalt-water-CO_2; Science, vol. 167, pp. 980-981.

Holland, H.D.
    1959:   Some applications of thermochemical data to problems of ore
            deposits I; Econ. Geol., vol. 54, pp. 184-233.

    1965:   Some applications of thermochemical data to problems of ore
            deposits II; Econ. Geol., vol. 60, pp. 1101-1166.

Holgate, N.
    1954:   The role of liquid immiscibility in igneous petrogeneses; J. Geol.,
            vol. 62, pp. 439-480.

Holloway, J.R., and Burnham, C.W.
    1969:   Phase relations and composition in basalt-H_2O-CO_2 under the
            Ni-NiO buffer at high temperatures and pressures; Geol. Soc.
            Am., Abstracts, 1969, p. 104.

Holmes, A., and Harwood, H.F.
    1937:   The petrology of the volcanic area of Bufumbira; Geol. Surv.
            Uganda, Mem. III, Pt. 2, 300 pp.

Horne, R.R., and Thomson, M.R.A.
    1967:   Post-Aptian camptonite dikes in southeast Alexander Island; Bull.
            Brit. Antarctic Surv., vol. 14, pp. 15-24.

Hurlbut, C.S.
    1939:   Igneous rocks of the Highwood Mountains, Montana; Bull. Geol.
             Soc. Am., vol. 50, pp. 1043-1112.

Jaeger, J.C.
    1957:   Temperatures in the neighbourhood of a cooling intrusive sheet;
             Am. J. Sci., vol. 255, pp. 306-318.

Joint Army, Navy, Air Force
    1966:   Thermochemical tables (JANAF), ed. D.R. Stull, Dow Chemical
             Co., Midland, Michigan.

Kaitaro, S.
    1953:   Geologic structure of the Late Precambrian intrusives in the Ava
             area, Aland Island; Bull. Comm. Geol. Finland, No. 162, 71 pp.

King, B.C.
    1965:   Petrogenesis of the alkaline igneous rock suites of the volcanic
             and intrusive centres of eastern Uganda; J. Petrol., vol. 6,
             pp. 67-100.

Knopf, A.
    1936:   Igneous geology of the Spanish Peaks region, Colorado; Bull.
             Geol. Soc. Am., vol. 47, pp. 1727-1784.

Koster van Groos, A.F., and Wyllie, P.J.
    1966:   Liquid immiscibility in the system $Na_2O-Al_2O_3-SiO_2-CO_2$ at
             pressures up to 1 kilobar; Am. J. Sci., vol. 264, pp. 234-255.

Krogh, T.E., and Davis, G.L.
    1969:   Isotopic ages along the Grenville front in Ontario; Carnegie Inst.
             Wash., Year Book 68, pp. 308-313.

Kumarapeli, V.S., and Saull, V.A.
    1966:   The St. Lawrence valley rift system; a North American equiva-
             lent of the East African rift valley system; Can. J. Earth Sci.,
             vol. 3, pp. 639-659.

Kushiro, I.
    1969:   Discussion of the paper "Origin of basaltic and nephelinitic mag-
             mas in the earth's mantle"; Tectonophysics, vol. 7, pp. 427-436.

Lowdon, J.A., Stockwell, C.H., Tipper, H.W., and Wanless, R.K.
    1963:   Age determinations and geological studies; Geol. Surv. Can.,
             Paper 62-17.

Lumbers, S.B.
    1968:   North Bay; Ont. Dept. Mines, Prelim. Map 381.

Luth, W.C.
    1967:   The system $KAlSiO_4-Mg_2-SiO_4-SiO_2-H_2O$; J. Petrol., vol. 8,
             pp. 372-429.

Luth, W. C., and Tuttle, O. F.
    1970:   The hydrous phase in equilibrium with granite and granitic mag-
            mas; Geol. Soc. Am., Mem. 115, pp. 513-548.

MacKenzie, W.S.
    1954:   The orthoclase-microcline inversion; Mineral. Mag., vol. 30,
            pp. 354-366.

McKie, D.
    1966:   Fenitization, pp. 261-294; in Carbonatites, eds. O. F. Tuttle and
            J. Gittins, Interscience, New York.

Meyer, C., and Hemley, J. J.
    1967:   Wall rock alteration, pp. 166-234; in Geochemistry of hydrother-
            mal ore deposits, ed. H. L. Barnes, Holt, Rinehart, Winston,
            New York.

Nockolds, S. R.
    1954:   Average chemical composition of some igneous rocks; Bull. Geol.
            Soc. Am., vol. 65, pp. 1007-1032.

Nockolds, S. R., and Allen, R.
    1959:   The geochemistry of some igneous rock series, Part II; Geochim.
            et Cosmochim. Acta, vol. 5, pp. 246-276.

Orville, P. M.
    1963:   Alkali ion exchange between vapour and feldspar phases; Am. J.
            Sci., vol. 261, pp. 201-237.

Pearce, T.
    1967:   The analcite bearing volcanic rocks of the Crowsnest formation;
            unpbl. Ph. D. thesis, Queens Univ., Kingston, Ont.

Peters, T., Luth, W.C., and Tuttle, O.F.
    1966:   The melting of analcite solid solutions in the system $NaAlSiO_4$-
            $NaAlSi_3O_8$-H_2O; Am. Mineralogist, vol. 51, pp. 736-754.

Philpotts, A.R., and Hodgson, C.J.
    1968:   Role of liquid immiscibility in alkaline rock genesis; XXIII Intern.
            Geol. Congr., vol. 2, pp. 175-188.

Ramsay, J. C.
    1955:   A camptonite dyke suite at Mona, Ross-shire and Inverness-shire;
            Geol. Mag., vol. 92, pp. 297-309.

Roedder, E.
    1954:   Low temperature liquid immiscibility in the system K_2O-FeO-
            Al_2O_3-SiO_2; Am. Mineralogist, vol. 36, pp. 282-287.

Robie, R.A., and Waldbaum, D.R.
    1968:   Thermodynamic properties of minerals and related substances at
            298.15°K(25°C) and one atmosphere (1.013 Bars) pressure and
            at higher temperatures; U.S. Geol. Surv., Bull. 1259, 256 pp.

Seifert, F., and Schreyer, W.
  1966:   Fluide Phasen in System K_2O-MgO-SiO_2-H_2O und ihre Bedeutung
           fur die Entstehung ultrabasischer Gesteine; Ber. Bunsengesell.,
           70, pp. 1045-1050.

Shafiqullah, M., Tupper, W.M., and Cole, T.J.S.
  1968:   K-Ar ages on rocks from the crater at Brent, Ontario; Earth.
           Planet. Sci. Letters, vol. 5, pp. 148-152.

Sieber, T.C., and Tiemann, T.D.
  1968:   Formation of artificial acmite above 500°; Trans. Soc. Mining
           Engr. (AIME), vol. 241, pp. 190-194.

Siedner, G.
  1965:   Geochemical features of a strongly fractionated alkali igneous suite;
           Geochim. et Cosmochim Acta, vol. 29, No. 2, pp. 113-138.

Simpson, E.S.W.
  1954:   The Okonjeje igneous complex, southwest Africa; Trans. Geol.
           Soc. South Africa, vol. 57, pp. 125-172.

Smith, H.G.
  1946:   The lamprophyre problem; Geol. Mag., vol. 86, pp. 165-171.

Sommerfeld, A.
  1950:   Mechanics of deformable bodies; Academic Press Inc., Publishers,
           New York, 396 pp.

Tomkeieff, S.I.
  1942:   The Tertiary lavas of Rum; Geol. Mag., vol. LXXIX, pp. 1-13.

  1952:   Analcite trachybasalt inclusions in the phonolite of Traproin Law;
           Trans. Geol. Soc. Edinburgh, vol. 15, pp. 360-373.

Upton, B.J.G.
  1965:   The petrology of a camptonite sill in south Greenland; Medd. om
           Grønland, Bd. 169, tlf. 11, pp. 1-19.

Verwoerd, W.J.
  1966:   Fenitization of basic igneous rocks, pp. 295-308; in Carbonatites,
           eds. O.F. Tuttle and J. Gittins, 591 pp., Interscience, New York.

von Eckermann, H.
  1948:   The genesis of the Alno alkaline rocks; 18th Intern. Geol. Congr.,
           Pt. 3, pp. 94-101.

  1966:   Progress of research on the Alno carbonatite, pp. 3-32; in
           Carbonatites, eds. O.F. Tuttle and J. Gittins, 591 pp.,
           Interscience, New York.

Watterson, J.
  1968:   Plutonic development of the Ilordleq area, south Greenland; 2,
          Late-kinematic basic dykes; Grǿnlands. Geol. Undersogelse,
          Bull. 70, 104 pp.

Winkler, H. G. F.
  1967:   Petrogenesis of metamorphic rocks, 2nd ed. Springer-Ver lag,
          New York, 237 pp.

Wright, T. L.
  1968:   X-ray and optical study of alkali feldspar: II, An X-ray method
          for determining the composition and structural state from mea-
          surement of 210 values for three reflections; Am. Mineralogist,
          vol. 53, pp. 88-104.

Wyllie, P. J.
  1966:   Experimental studies of carbonatite problems; the origin and dif-
          ferentiation of carbonatite magmas, pp. 311-352; in Carbonatites,
          eds. O. F. Tuttle and J. Gittins, 591 pp., Interscience, New
          York.

Yoder, H. S., and Sahama, T. G.
  1957:   Olivine X-ray determinative curve; Am. Mineralogist, vol. 42,
          p. 475.

BULLETINS

Geological Survey of Canada

Bulletins present the results of detailed scientific studies on geological or related subjects. Some recent titles are listed below (Information Canada No. in brackets):

185 Barremian Textulariina, Foraminiferida from Lower Cretaceous beds, Mount Goodenough section, Aklavik Range, District of Mackenzie, *by* T. P. Chamney, $2.50 (M42-185)

186 Devonian stratigraphy of northeastern British Columbia, *by* G. C. Taylor and W. S. MacKenzie, $1.50 (M42-186).

187 Contributions to Canadian paleontology, *by* M. J. Copeland, *et al.*, $6.00 (M42-187)

188 Ammonoids of the Lower Cretaceous Sandstone Member of the Haida Formation, Skidegate Inlet, Queen Charlotte Islands, western British Columbia, *by* F. H. McLearn, $5.00 (M42-188)

189 Precambrian fossils, pseudofossils, and problematica in Canada, *by* H. J. Hofmann, $3.00 (42-189)

190 Surficial geology of Rosetown map-area, Sask., *by* J. S. Scott, $2.00 (M42-190)

191 Precambrian geology of northwestern Baffin Island, District of Franklin, *by* R. G. Blackadar, $2.00 (M42-191)

192 Contributions to Canadian paleontology, *by* A. E. H. Pedder, *et al.*, $6.00 (M42-192)

194 Triassic petrology of Athabasca-Smoky River region, Alberta, *by* D. W. Gibson, $2.00 (M42-194)

195 Petrology and structure of Thor-Odin gneiss dome, Shuswap metamorphic complex, B. C., *by* J. E. Reesor and J. M. Moore, Jr., $2.50 (M42-195)

196 Glacial geomorphology and Pleistocene history of central British Columbia, *by* H. W. Tipper, $4.00 (M42-196)

197 Contributions to Canadian paleontology, *by* B. S. Norford, *et al.*, $6.00 (M42-197)

198 Geology and petrology of the Manicouagan resurgent caldera, Quebec, *by* K. L. Currie, $3.00 (M42-198)

199 The geology of the Loughborough Lake region, Ontario, with special emphasis on the origin of the granitoid rocks—A contribution to the syenite problem (31 C/7, C/8), *by* K. L. Currie and I. F. Ermanovics, $3.00 (M42-199)

200 Part I: Biostratigraphy of some early Middle Silurian Ostracoda, eastern Canada; Part II: Additional Silurian Arthropoda from arctic and eastern Canada, *by* M. J. Copeland, $1.50 (M42-200)

201 Archaeocyatha from the Mackenzie and Cassiar Mountains, Northwest Territories, *by* R. C. Handfield, $2.00 (M42-201)

202 Faunas of the Ordovician Red River Formation, Manitoba, *by* D. C. McGregor, *et al.*, $2.00 (M42-202)

203 Geology of lower Paleozoic formations, Hazen Plateau and southern Grant Land Mountains, Ellesmere Island, *by* H. P. Trettin, $3.00 (M42-203)

204 Brachiopods of the Detroit River Group (Devonian) from southwestern Ontario and adjacent areas of Michigan and Ohio, *by* J. A. Fagerstrom, $2.00 (M42-204)

205 Comparative study of the Castle River and other folds in the Eastern Cordillera of Canada, *by* D. K. Norris, $2.00 (M42-205)

206 Geomorphology and multiple glaciation in the Banff area, *by* N. W. Rutter, $2.00 (M42-206)

207 Geology of the resurgent cryptoexplosion crater at Mistastin Lake, Labrador, *by* K. L. Currie, $2.00 (M42-207)

208 The geology and origin of the Faro, Vangorda and Swim concordant zinc–lead deposits, Central Yukon Territory, *by* D. J. Tempelman-Kluit, $3.00 (M42-208)

209 Redescription of *Marrella splendens* (Trilobitoidea) from the Burgess Shale, Middle Cambrian, British Columbia, *by* H. B. Whittington, $3.00 (M42-209)

210 Ordovician trilobites from the central volcanic mobile belt at New World Island, northeastern Newfoundland, *by* W. T. Dean, $2.00 (M42-210)

211 A Middle Ordovician fauna from Braeside, Ottawa Valley, Ontario, *by* H. Miriam Steele and G. Winston Sinclair, $2.00 (M42-211)

212 Lower Cambrian trilobites from the Sekwi Formation type section, Mackenzie Mountains, northwestern Canada, *by* W. H. Fritz, $4.00 (M42-212)

214 Classification and description of copper deposits, Coppermine River area, District of Mackenzie, *by* E. D. Kindle, $4.00 (M42-214)

215 Brachiopods of the Arisaig Group (Silurian–Lower Devonian) of Nova Scotia, *by* Charles W. Harper, Jr., $5.00 (M42-215)

217 The geology and petrology of the alkaline carbonatite complex at Callander Bay, Ontario, *by* John Ferguson and K. L. Currie, $2.00 (M42-217)